Analysis of Multibeam Sonar Data for the Characterization of Seafloor Habitats

by

José Vicente Martínez Díaz

B.Sc., Universidad Autónoma de Baja California, 1991

A Report Submitted in Partial Fulfillment of
the Requirements for the Degree of

Master of Engineering

in the Graduate Academic Unit of Geodesy and Geomatics Engineering

Supervisor: Larry A. Mayer, Ph.D., Geodesy and Geomatics Engineering

Examining Board: Y.C. Lee, Ph.D., Geodesy and Geomatics Engineering, Chair
J.E. Hughes Clarke, Ph.D., Geodesy and Geomatics Engineering
D.E. Wells, Ph.D., Geodesy and Geomatics Engineering
D.J. Coleman, Ph.D., Geodesy and Geomatics Engineering

This Report is accepted.

_____
Dean of Graduate Studies

THE UNIVERSITY OF NEW BRUNSWICK

November, 1999

…a Daleth y Aitana

ABSTRACT

Multibeam sonar products, including bathymetric DEMs and acoustic backscatter maps, provide descriptions of the seafloor's spatial distribution of relief, terrain derivatives, and estimates of bottom composition. These seafloor properties are considered important physical variables governing the distribution of seafloor habitats. This project investigates the potential of using multibeam sonar data for the characterization of the seafloor in terms of benthic habitats. Map products were created from multibeam data trying to depict seafloor features at the level of resolution of the sonar system. Quantitative measures for depth, topographic roughness, and backscatter strength were derived and presented as thematic layers. Spatial modeling of attributes from each thematic layer is proposed as a means of identifying suitable bottom habitats. The thematic layers were also compared with fisheries data to explore relationships.

Knowing that map resolution is dependent on the geometry of the multibeam measurement, the results of this investigation revealed no statistical difference for topographic variability at two different map resolutions. Also, it was found that mean backscatter strength can be used as a good predictor of bottom types even though it is often difficult to relate it to individual sediment properties. In the area explored here, backscatter strength showed a moderate correlation to grain size.

Conclusive evidence of the associations between seafloor properties and fisheries parameters was elusive, as correlation analyses were moderate to low. However, highly descriptive multibeam maps addressed potential uses like improvements in sampling design and oceanographic modeling for fisheries research.

RESUMEN

Los mapas digitales producidos con sonar multihaz, incluyendo modelos digitales de elevación (MDE) batimétricos e imágenes de retrodispersión acústica, proporcionan descripciones de la distribución espacial de relieve, derivados de terreno y estimaciones de la composición del fondo. Estas características son consideradas como variables importantes en la distribución de habitats en el lecho marino. Este proyecto investiga el uso de datos de sonar multihaz para la caracterización del fondo marino en términos relevantes de habitats bénticos. Mapas describiendo las características del fondo fueron producidos con datos de sonar multihaz a la resolución del sistema empleado. Medidas cuantitativas de profundidad, relieve topográfico, e intensidad de retrodispersión acústica fueron derivadas y presentadas como capas temáticas. El uso de éstas capas temáticas es propuesto como medio de identificación de habitats submarinos, a través del modelaje espacial de sus atributos. A su vez, las capas temáticas fueron comparadas con datos de captura pesquera para investigar posibles interrelaciones entre propiedades del fondo y parámetros biológicos.

Aun sabiendo que la resolución de los mapas de datos multihaz es dependiente de la geometría de medición, los resultados de esta investigación no revelaron ninguna diferencia estadística de variabilidad topográfica para dos diferentes resoluciones. De la misma forma, la intensidad de retrodispersión acústica puede ser utilizada como indicador del tipo de fondo marino a pesar de que a menudo es difícil relacionarla con propiedades sedimentológicas. En el área aquí explorada, la intensidad de retro-dispersión mostró una correlación moderada al tamaño de grano.

Evidencia concluyente de la asociación entre las características del fondo marino y los parámetros de captura pesquera fue evasiva, pues los resultados de correlación fueron de moderados a bajos. Sin embargo, la alta capacidad descriptiva del sonar multihaz demostró tener aplicaciones potenciales en el monitoreo de recursos e investigación pesquera, tales como mejoras en el diseño de muestreos y en el modelaje oceanográfico.

ACKNOWLEDGEMENTS

TABLE OF CONTENTS

LIST OF TABLES

LIST OF PLATES

Chapter 1

INTRODUCTION

This report summarizes an investigation dealing with the analysis of multibeam sonar data and its potential as a research tool in fisheries and related marine environmental studies. It involves the characterization and classification of the seafloor in terms relevant to the distribution of benthic habitats. For this goal, two main issues are reviewed. The first deals with the production of digital maps from multibeam sonar data. The second is related to the examination of these digital products in order to derive new information relevant to fisheries studies. This information is presented as thematic layers of a series of synoptic maps in which the spatial distribution of attributes is related to observations of benthic or ground fish.

Multibeam sonar systems (MBSS) have been successfully used for gathering high-resolution seafloor bathymetric data and acoustic imagery in shallow- and deep-water regions [Renard and Allenou, 1979; Farr, 1980; de Moustier, 1988; Hammerstad et al., 1991; Mills and Perry, 1992]. With modern shallow-water MBSS detailed geomorphology and geology can be described at spatial resolutions of as little as a few centimetres [Hughes Clarke et al., 1996]. For that reason multibeam sonar data is considered to be a primary source of information for marine geologic research.

In many ways, geologic research has contributed to the identification of bottom features that could be associated with the quality and distribution of benthic habitats. Interdisciplinary approaches combining marine geology, biology, physical

oceanography, ocean engineering, and others have been taken by many investigators in order to understand the spatial and temporal distribution of marine environments [Valentine, 1992; Yoklavich et al., 1997; Baker et al., 1998; Fader et al., 1998; Collins and McConnaughey, 1998; Scanlon et al., 1998].

In this report, the problem being investigated is the relationship between the spatial variability of seafloor variables depicted with multibeam sonar and the occurrence of ground fish and other benthic fauna. A methodology is presented to process multibeam raster data products for the creation of synoptic maps describing some properties defining seafloor environments. The seafloor properties used are related to the geomorphology (terrain relief) and the geology (sediment type). It is important to state that these are not the only variables affecting the distribution of benthic biota but they are some of the most important. According to some researchers [Scott, 1982; Perry et al., 1994] sediment type and water depth play an important role in the distribution of fish assemblages. Other contributions relate the abundance of certain fish species to geomorphologic features, such as rock outcrops and other rough bottoms, which serve as natural shelters from predators and ocean dynamics [Carr, 1991; McCormick, 1994; Yoklavich et al., 1997].

1.1 Motivation for This Work

The use of multibeam sonar systems by research and academic institutions, as well as by specialized companies offering multibeam surveying services, is rapidly growing.

The highly descriptive seafloor maps obtained with such systems are contributing to the accumulation of high-quality bathymetry and imagery data in recipient geo-spatial databases. Additionally, concurrent developments in computer capability and software tools are allowing researchers from diverse fields to explore and manipulate large databases and perform complex analyses in a geographic context. These issues, along with the increased concern of the public for the management and protection of marine resources, are driving institutional researchers to examine new methods and tools for providing a better and more accurate description of marine environmental processes and associated marine resources, particularly biological. Accordingly, the factors motivating this research are based on two principal components. First, the excellent mapping capabilities of multibeam sonar systems for seafloor charting, and second, the potential uses of derived data products in a wide variety of applications benefiting marine sciences.

Multibeam sonar high-resolution maps of the seafloor are possible because millions of measurements are made by the acoustic swath over large areas of seafloor. However, it is only after the creation of digital map products involving the handling and processing of enormous data sets that the user is aware of its real descriptive potential, including three-dimensional (3-D) visualization and spatial modeling. The production of high-density soundings on a regular grid is a significant process that has received a great deal of attention in the research conducted within the Ocean Mapping Group (OMG) of the Department of Geodesy and Geomatics Engineering at the University of New Brunswick, Fredericton, Canada. One of the aims of this project is to take advantage of

the tools derived from that research effort and transfer that capability to other potential applications.

The advantage of creating digital map products is that they can be moved with reasonable transparency to other analytical platforms such as geographic information systems (GIS) and image processing packages. Current tools available in these environments permit the application of elaborate spatial modeling techniques, most of them developed for more traditional land applications. These methods can be imported, adapted, and applied to multibeam data to derive new thematic layers of seafloor features varying continuously over large areas.

Considering the above factors, the specific objectives pursued in this investigation are given in the following list:

a) Describe the principles behind the creation of multibeam sonar data products to understand their strengths and limitations.

b) Derive a feasible methodology to analyze bathymetric digital elevation models (DEM)[1] and backscatter imagery to meet the descriptions of specific physical variables characterizing seafloor habitats (depth, surface relief, bottom type).

c) Generate synoptic base maps depicting the spatial distribution of thematic information derived from the analysis of multibeam data.

d) Search for relationships between the thematic layers and the response of benthic fish in a test region.

---

[1] Some authors prefer the term digital terrain model (DTM) to describe sampling networks of hypsometric surfaces representing variations of land or, in this case, seafloor.

1.2 Report Outline

This report is presented in the following parts. Chapter 2 introduces the principles of multibeam sonar. Sections are dedicated to the basics of multibeam sonar acoustics including the concepts of spatial resolution, acoustic backscatter measurement, and geometry of measurements.

Chapter 3 presents a background on the characterization of benthic habitats. It also addresses research regarding acoustic remote sensing techniques that have been used in the description of these environments. The chapter finishes with some general remarks about the utilization of multibeam sonar for the description of benthic habitats.

Chapter 4 describes the methods and procedures used in this study. First is a description of the principles and practical implementation regarding the creation of multibeam sonar data products with the OMG suite of programs. Second is the proposed spatial analysis techniques for raster products. This chapter also mentions the source of multibeam data and the area of study.

Chapter 5 presents the outcomes of the procedures described in Chapter 4 including patterns, quality, and reliability of the results. Chapter 6 discusses the meaning of observed results and their significance as well as the approaches for modeling map attributes. Chapter 7 develops the relationships between biological observations and the multibeam map products. Sources and descriptions of biological data used are presented. Finally, Chapter 8 summarizes the conclusions and discusses some directions for future work.

Chapter 2

MULTIBEAM SONAR PRINCIPLES

This chapter presents an overview of the principles behind the use of multibeam sonar to measure depth and backscatter strength. It emphasizes issues dealing with the spatial resolution of the acoustic ensonification because this is directly related to the resolution of the final data products.

2.1 Technological Background

Since the introduction in 1977 of the first commercially-available MBSS for deep-sea research —the General Instruments' *SeaBeam* [Farr, 1980]— the use of MBSS has steadily increased through the years to its present status as a proven and reliable survey instrument. Improvements in sonar technology, computer performance, and ancillary instrumentation made possible the implementation of multibeam technology in the more demanding shallow-water environment. The main differences between deep- and shallow-water MBSS are that the latter utilizes higher frequencies, shorter pulse lengths, and faster repetition rates. This translates into resolving seafloor features with higher resolution at higher vessel's speed, while still keeping near one hundred percent bottom coverage with a narrower swath width. However, the trade off for the above is the massive data acquisition, management, and storage requirements, as well as the greater demands on the platform's attitude compensation system.

6

Today users have the opportunity to select an MBSS from a variety of manufacturers including such systems as *EM-100x* and *EM-3000* (Kongsberg Simrad, Norway), *Fansweep 20* (STN ATLAS Marine Electronics, Germany), *SeaBeam 1185* (L-3 Communications ELAC Nautik, Germany)[2], *Seabat 900x* and *81xx* series (RESON, Denmark), *Echoscan* (Odom Hydrographic Systems, U.S.), and *ISIS* interferometric side scan sonar (Submetrix, U.K.).

2.2 Generation of Acoustic Beams

Most shallow-water MBSS use two arrays of piezo-electric ceramics fitted in one transducer head that can be hull-mounted (fixed) or pole-mounted (portable). One array forms the transmitting acoustic signal, while the other creates a receiving one. The product of both arrays results in a fan-shaped beam set with 48 to 1440 beams in angular sectors from 90° (Seabat 9001) to 180° (Fansweep 20) [Mayer et al., 1997a]. The operating acoustic frequencies range from 95 kHz (EM-1000) to 455 kHz (Seabat 9001). In general, shallow-water MBSS transmit acoustic energy in a beam-formed lobe narrow in the along-track direction (usually 1.5° to 5°) and wide across-track (between 100° to 180°). The receiving array is formed by a number of lobes shaped narrowly athwartships (1.5° to 3.3°), and usually somewhat broader in the fore-aft direction (between 3.3° to 30°). The intersection product of both beam patterns creates individual narrow beams

---

[2] Previously known as BottomChart MkII. After the acquisition of ELAK Nautik and SeaBeam Instruments by L-3 Communications, all the multibeam products carry the name *SeaBeam.*

normally spaced at 0.9° to 2.5° intervals. A typical model of a transmit-receive beam

array can be seen in Figure 2.1.
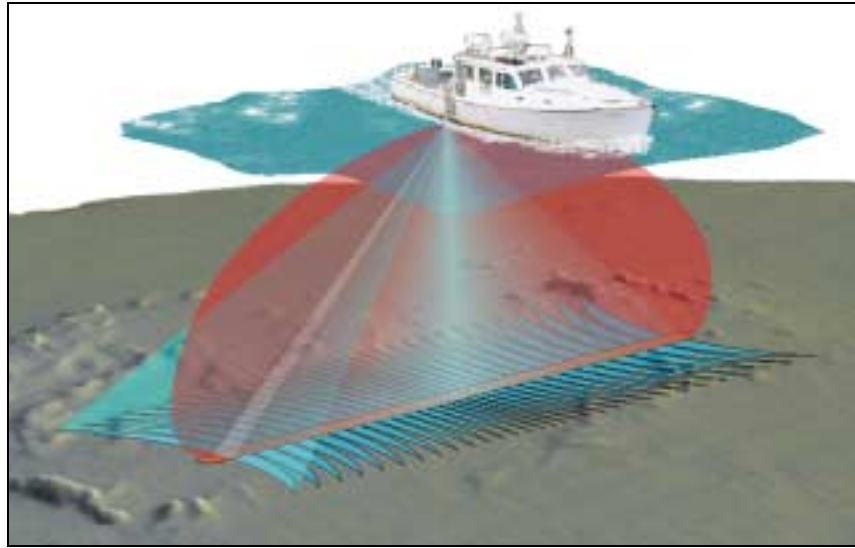
Figure 2.1. Conceptual model illustrating the beam pattern geometry of multibeam sonar.

2.3 Concepts of Acoustic Ensonification

The area ensonified by the individual beams refers to the energy from within the "main" beam product which has reached part of the seafloor [Hughes Clarke, 1997]. In technical terms the main part of a beam pattern is defined by the value of one half the source power expressed in decibels, that is: $10\log(1/2) = -3$ dB (Figure 2.2). Thus, it is the -3 dB limit product of the transmit and receive beam patterns which defines the ensonified patch.

The area ensonified by each beam takes the shape of an ellipse. The dimension of this ellipse varies principally as a function of depth, individual beam pointing angle, and

8

the true angle of incidence. Knowing that each formed beam has limited dimensions we can estimate the smallest feature in the seafloor that can be resolved within the ensonification region.
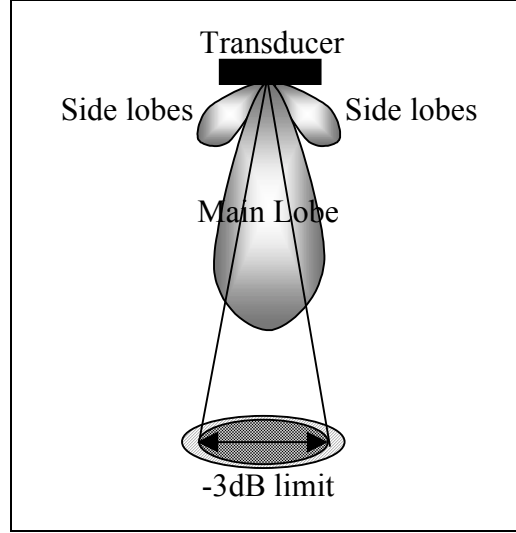
Figure 2.2. Illustration of the –3 dB limit from a hypothetical acoustic beam (from Wells [1997]).

2.3.1 Spatial Resolution: The Acoustic Parameters

The spatial resolution of a sonar system is determined in terms of beamwidth and bandwidth of a transmitted pulse. The bandwidth of the transducer is the dominant factor conditioning the *range resolution* ΔR [de Moustier, 1998a]:

$$\Delta R = \frac{C}{2W},$$

where C is the speed of sound and W is the bandwidth of the signal. The larger the bandwidth the higher the range resolution, which is the ability to discriminate returning signals from particular adjacent targets. The bandwidth of a typical transducer is usually

9

about 10% of the operational frequency, thus the association of higher range resolution with higher frequencies. In the same sense, the *angle resolution* $R\theta$ is proportional to the frequency,

$$R\theta = \frac{C}{F\,L},$$

where F is the centre frequency and L is the length of the aperture[3]. The angle resolution is the ability to discriminate the direction from where an echo is returning to the transducer. It is related to the beamwidth θ_{bw} of the transducer, expressed in the form,

$$R\theta \approx \theta_{bw} = 0.88\frac{\lambda}{L},$$

where λ is the acoustic wavelength and the constant term 0.88 is a rough approximation when aperture lengths L are greater than 4λ (narrow beamwidth at high frequencies). The area A ensonified by a pulse within a beam is the product of the range resolution ΔR projected on the horizontal by the extent of the angle resolution $R\theta$ in the same plane, at the grazing angle ϕ (Figure 2.3)

$$A = \frac{\Delta R}{\cos\phi} \cdot R\theta = \frac{C}{2W\cos\phi} \cdot \frac{R\,C}{F\,L}.$$

This equation denotes that the instantaneous area of ensonification by the pulse within the beam is proportional to the slant range R but inversely proportional to the operational frequency F for a given aperture L, thus higher frequency leads to potentially higher spatial resolution in the along-track dimension. Additionally, because the

---

[3] Aperture refers to the physical extent of the transducer through which sound waves are allowed in or out, basically to limit the spatial propagation of sound radiation.

frequency dependent term bandwidth *W*, is also in the denominator, the higher the bandwidth the higher the across-track resolution.
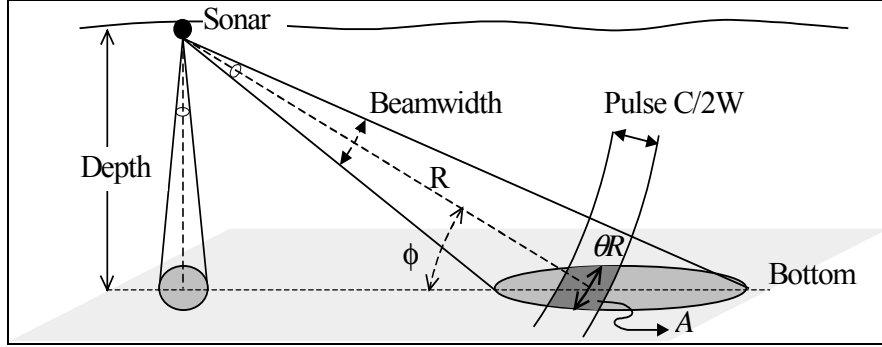
Figure 2.3. Incident pulse on the seafloor within different beam geometry; for a beam at normal incidence and for low grazing angles (after de Moustier [1998b]).

2.3.2 Spatial Resolution: The Footprint Dimension

Spatial resolution of an acoustic beam differs to some extent to that described in section 2.3.1 in terms of the footprint dimension. Each beam in an MBSS produces a bathymetric sounding solution. Bottom detection within a beam is determined by the finite area of ensonification or footprint as a function of beamwidth, beam angle of incidence, and depth. The footprint dimension in the athwartship direction f_a is estimated by

$$f_a = \frac{2d}{cos^2\theta} \cdot tan\frac{\varphi}{2},$$

where *d* is the measured depth, θ is the angle of incidence, and φ is the receiving beamwidth in the across-track direction. From the above one can see that, assuming a flat surface and constant depth, the footprint increases its dimensions with increasing

angle of incidence. Therefore, the resolution is expected to be maximum in the nadir region and to gradually decrease toward the outer part of the swath.

2.4 Acoustic Backscatter from MBSS

The backscatter strength of the seafloor is the incoherent returning energy of an acoustic pulse transmitted in the water column at a certain range and angle over a finite area of seafloor. The spatial variability of backscatter strength can be determined with MBSS as a result of the interaction between the seafloor physical properties and acoustic energy. Acoustic backscatter is dependent on several variables:

- A reflection coefficient caused by the difference of acoustic impedance between sea water and bottom materials.

- The surface roughness as a function of the acoustic wavelength.

- The volume reverberation that must also be expressed in terms of acoustic wavelength.

In theory, different seafloor types return a characteristic response signature, which makes viable the implementation of sea bottom classification systems. In practice, this is far from being achieved since the three phenomena mentioned above are individually complex and the combined effect is almost unmanageable [Novarini and Caruthers, 1998]. The backscatter intensity also varies as a function of the angle of incidence of the acoustic pulse. The angular variations of intensity normally behave in a Lambertian pattern assuming a flat surface; in practice, the Lambertian assumption is not totally

12

appropriate as the bottom surface is ordinarily not flat. This is one of the advantages of MBSS where instantaneous across-track sections could be used to estimate the actual profile in order to compute the real angle of incidence and the footprint area ensonified. Additionally, short swath series can be used to correct real angle of incidence in the fore-aft direction where slope variations also contribute to an angular dependency.

A useful implementation for backscatter map generation is to use the geographic variations of mean backscatter intensity where bottom types with different backscatter strength can be resolved. Assumptions made in this approach include correction to all automatic gains, calibration of Tx/Rx beam patterns, actual across-track profile correction (eliminating a Lambertian assumption), and no refraction. In qualitative terms, high contrast sediment types can be discernible (rock outcrops/boulders, coarse sand, fine sand, mud) without some of these assumptions, especially in flat seafloor surfaces, however, these premises should be considered if quantitative estimations are desired. Moreover, with the collection of seafloor physical properties like grain size, surface roughness, impedance, etc., one can relate the measured acoustic responses of discrete locations to specific bottom types and generate surfaces of corresponding attributes. Research has been conducted [Hughes Clarke et al., 1997a] to extract the most from the backscatter strength and to develop seafloor classification tools that make use of backscatter angular dependency functions, which should describe different bottom types with higher accuracy. In the following section, basic concepts of acoustic backscatter are described in order to provide a better understanding of the meaning of the measurements.

2.5 Acoustic Backscatter Principles

The intensity of a backscatter echo is the incoherently returned energy from an acoustic pulse transmitted in the water column at a certain range and angle over a patch of seafloor. The intensities of backscatter echoes depend on the scattering strength of the seafloor, distribution of scatters, bottom penetration, and sub-bottom volume scattering [Nishimura, 1997]. The proper quantification of acoustic backscatter strength requires an understanding of several topics. Some are presented in subsequent sections but not in exhaustive detail.

2.5.1 Reflection at the Bottom Interface

For an idealized smooth surface, and at an incident angle different from zero, the backscatter energy is non-existent since all the energy is reflected away from the source. Being more realistic, the seafloor surface never behaves with a perfectly coherent response; there is always a certain amount of energy that is scattered back to the source. Knowing that just a fraction of the source level is returning, the acoustic intensity must account for spherical spreading and water column attenuation as the pulse travels a two-way path from the source to target and back.

The magnitude of reverberation at the water/bottom interface is usually known as the backscatter coefficient. A simplistic formula for backscatter coefficient [de Moustier, 1998b] can be expressed as:

$$I_s = I_0 \frac{A \cdot s(\theta_i)}{R^2},$$

14

where I_s is the intensity of the backscattered pulse measured at a reference distance of 1 m from the surface; I_0 is the intensity of the acoustic pulse transmitted by a sonar system in the water column; A is the area of ensonified seafloor; θ_i is the pulse's angle of incidence; and R^2 is twice the range traveled in the water column. The term $s(\theta_i)$ is the backscatter coefficient that can be defined as:

$$s(\theta_i) = s_r + s_\mu + s_v,$$

where s_r represents the scattering contribution from bottom roughness (geomorphology), s_μ is the contribution from microscale roughness (grain size and shape), and s_v is the contribution from sediment volume inhomogeneities (sub-bottom lithology) [Novarini and Caruthers, 1998]. The backscatter strength S_b is measured in decibels and expressed as

$$S_b = 10\log(s(\theta_i)).$$

The physical properties of the seafloor have a direct influence in the attenuation and scattering processes. Main constituents in these processes are: (1) grain size, density, and velocity; and (2) seafloor roughness.

2.5.1.1 Grain size and density

The particle size of sediments acts like irregular surfaces working at different scales. At a certain acoustic wavelength, clays and silts are smooth compared to sands and gravel, however, differences are less noticeable between closer sediment classes like sandy clays and fine sands. Grain size also affects the porosity and interstitial water content that in turn control compressional-wave velocity. The product of compressional-

wave velocity v and saturated bulk density ρ of sediment gives a measure of a material's resistance to an acoustic wave; this is called acoustic impedance. Differences in impedance between two media determine, in part, the behavior of an acoustic pulse. This relationship is represented in the following expression (only for normal incidence):

$$R_0 = \frac{\rho_1 v_1 - \rho_2 v_2}{\rho_1 v_1 + \rho_2 v_2},$$

where R_0 is the reflection coefficient for two media (1 and 2) with velocities v_1 and v_2 and densities ρ_1 and ρ_2, respectively. For non-normal incidence and rough surfaces the reflection coefficient is extended by additional parameters described in the following sub-section, 2.5.1.2.

2.5.1.2 Seafloor roughness

Surface elevation differences impart phase shifts on the reflected acoustic wave (Figure 2.4). When the elevations tend to zero (smooth) the reflection coefficient R_0 remains governed by the impedance contrast. When the elevation differences are significant, the phase shifts are in direct proportion to averaged returned estimates given by:

$$R = R_0 \exp(-2k^2 \sigma^2 \cos^2 \theta_i),$$

where σ is the standard deviation of the assumed normal distribution of returned values, k is the acoustic wavenumber defined as $2\pi/\lambda$, accounting for the frequency dependence of surface roughness, and θ_i is the angle of incidence.
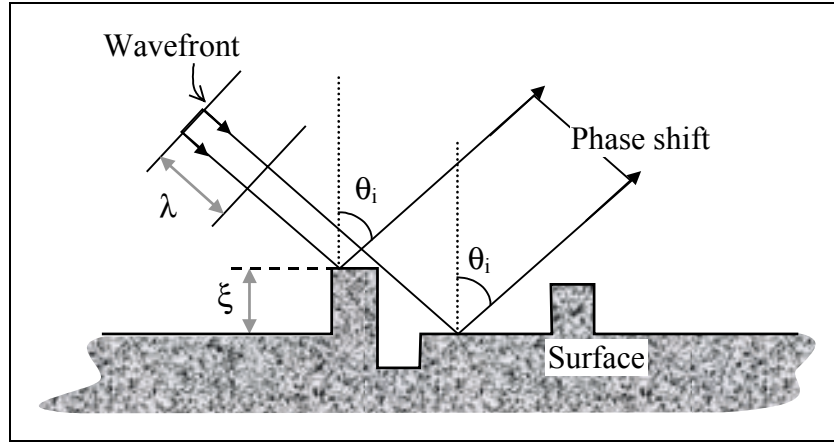
Figure 2.4. Wavefront phase shift due to surface roughness at non-normal incidence (from de Moustier [1998b]).

The scale of the interface roughness is described in terms of the acoustic wavelength λ. A certain surface may appear rough to a small λ since the elevation differences impart phase shifts to the reflected wave causing interference between the wavefronts returning from the surface. On the other hand, the same surface may appear smooth to a larger λ because the wavefronts are reflected with phase shifts that are now very small with respect to λ.

Qualitatively, the relationship between surface roughness and surface scattering can be illustrated through the examples shown in Figure 2.5. The angular distribution consists in two constituents: a reflected component (coherent, anisotropic, specular) and a scattered component (incoherent, isotropic, diffuse). For a smooth seafloor, relative to the acoustic wavelength, the reflected component is larger than the scattered, resulting in a backscatter time series response with relative low intensity. As the surface becomes rougher, the scattered component is larger than the coherent component, thus the response approaches that of a Lambertian surface (varying as $\cos^2\theta$).
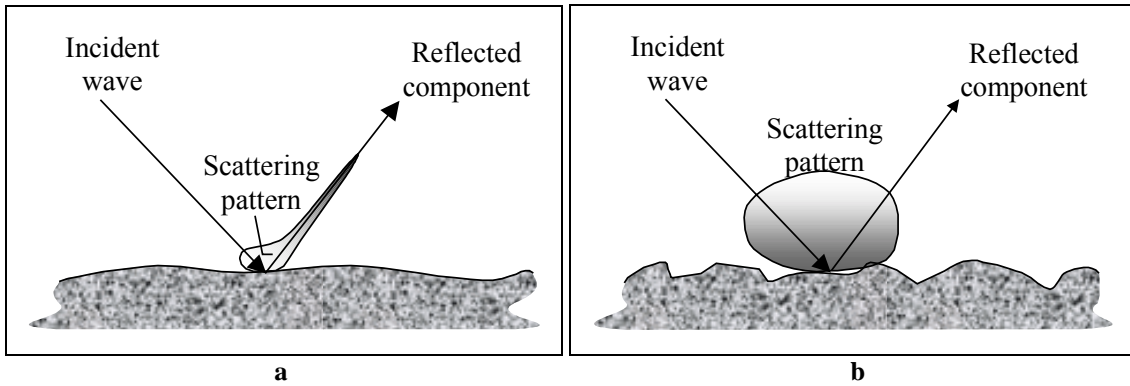
Figure 2.5. Examples of surface-scatter patterns at oblique incidence. (a) A smooth surface reflecting coherently the incidence wave; (b) a rough surface with a large fraction of acoustic energy scattered incoherently.

2.6 Angular Dependence of Acoustic Backscatter

In order to understand the angular dependence of seafloor acoustic backscatter, it is necessary to describe the geometry associated with multibeam measurements. The area ensonified by a pulse intersecting the seafloor varies with the angle of incidence. At normal incidence the pulse travelling towards the bottom expands in a spherical wavefront which approaches a plane parallel to the bottom. The bottom contact results in a disc with dimensions defined by the pulse length, which expands through the limits of the main lobe (−3 dB) ensonification. On the other hand, away from normal incidence the pulse expansion is no longer parallel to the bottom so the disc becomes a ring sector that narrows as the incident angle moves away from nadir. A pulse length geometry for normal and off-nadir incidence is shown in Figure 2.6.
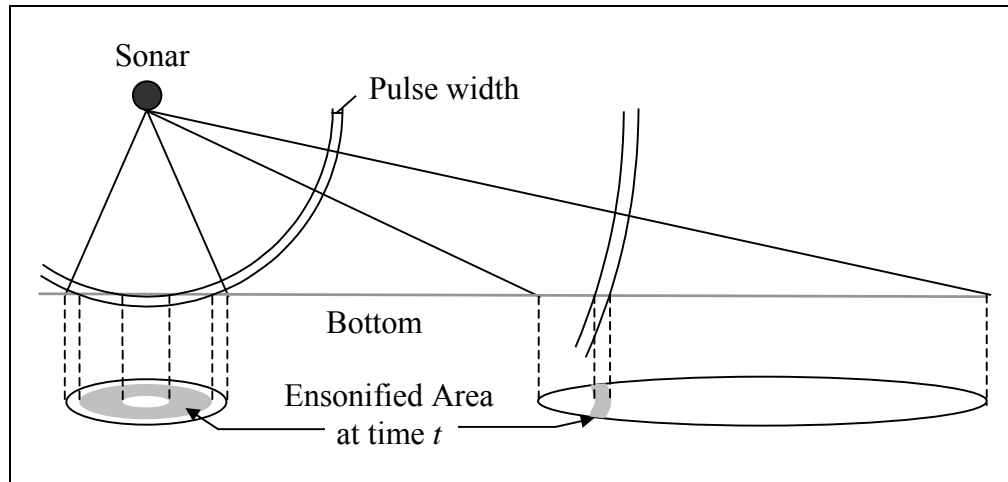
Figure 2.6. Geometry of incident pulse length on the seafloor for beams at normal and oblique incidence. Note the different dimensions of pulse imprint for both cases and the proportions to the beam footprints (after de Moustier [1998a]).

The backscatter strength is measured by the contributions of a sample defined by the instantaneous area given by the pulse length imprint at a certain incident angle and the across-track beam footprint dimension. As mentioned in a previous paragraph, the backscatter angular dependency requires that the angles of arrival of the bottom echoes be converted to angles of incidence or grazing angles. For that, it is necessary to account for roll compensation, refraction, and bottom slope corrections. Assuming that roll compensation is applied from the ancillary motion compensation unit and that the refraction problems are correctly eliminated with appropriate modeling, the bottom slope corrections can be inferred from the across-track instantaneous bathymetric measurements (Figure 2.7) and from a few consecutive swaths along-track (Figure 2.8).
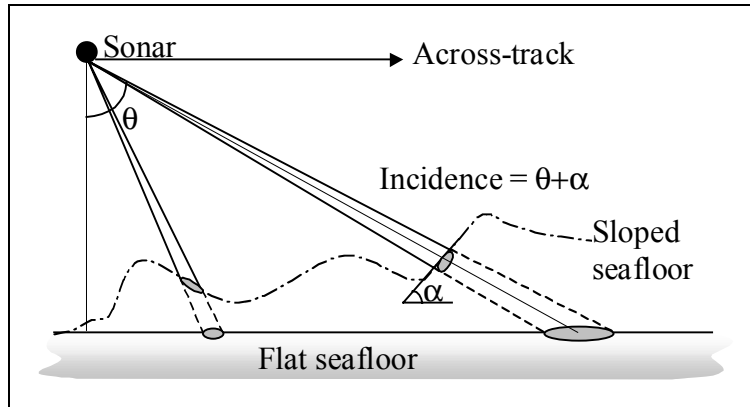
Figure 2.7. Across-track slope is corrected to the angle of incidence with the instantaneous swath profile.
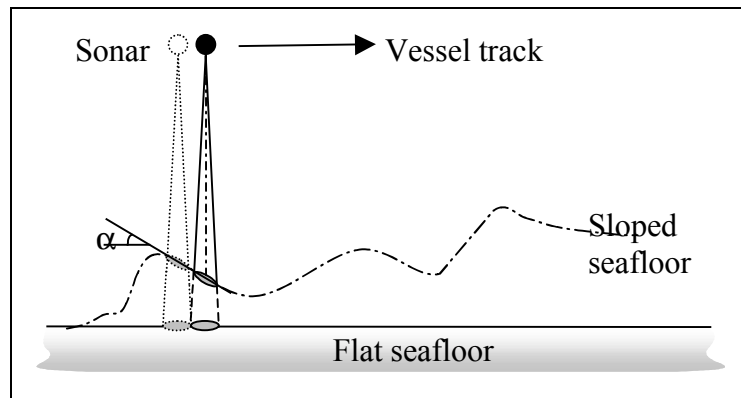
Figure 2.8. Correction to the angle of incidence using a swath series to determine the along-track slope.

The across-track bottom slopes are calculated with the bathymetric profile measured at each ping interval. The angles of incidence are computed by adding the slope of the appropriate swath segment to the angles of arrival, producing the angular dependence function of acoustic backscatter for each ping. Nevertheless, it is necessary to average several pings before a confident angular dependence function can be derived [de Moustier and Matsumoto, 1993]. This also requires that the data be recorded over a seafloor that is homogeneous within a swath width.

Chapter 3

CHARACTERIZATION OF BENTHIC HABITATS

3.1 Definition of Seafloor Habitat

A particular habitat —and specifically a benthic habitat— is defined by a series of physical variables extending from substrate type to surrounding water mass quality. Variable types include depth, bottom composition, relief, temperature, salinity, RedOx chemical balance, and nutrient concentrations, among others. The ability to define a particular habitat for certain species depends on having comprehensive databases for each of those variables. Some variables might have a larger component than others in the distribution of species, in particular those showing no seasonal changes or relative invariance. For example, depth and topographic relief have little or no temporal variation compared to the seasonal variability of temperature or salinity. Some authors have identified the strong link between invariant parameters and the occurrence of fish [Perry et al., 1994] and have stated the necessity to understand these relationships as one of the first steps towards incorporating habitat information in abundance indices for fisheries management. Therefore, it is not rare that depth is described by several authors as one of the most important determinants in the distribution of ground fish and benthic fauna [Scott, 1982; Stein et al., 1992; McCormick, 1994; Perry et al., 1994; Coleman et al., 1997]. This is not only related to a water column pressure-driven factor, but to the fact that there are associations between depth and other variables such as bottom type

and food availability [Scott, 1982], temperature and dissolved oxygen [Bonsdorff et al., 1996].

Bottom type and fish assemblages are the primary focus of fish-habitat associations studies. Stein et al. [1992] found unique fish assemblages on a whole range of bottom types (mud, boulders, rock ridges, mud and cobble, mud and boulders) on a large continental shelf reef. Bottom selectivity can be highly specific in both shallow- and deep-water [Scott, 1982]. After storm events, time series observations of diversity and abundance of benthic fauna have been related to modifications of sediment composition [Grémare et al., 1998].

Similarly, surface relief or topographic variability have an important role on benthic communities. Surface variability influences the abundance and distribution of organisms by creating a refuge against ocean currents, wave action, predators, and in general by providing a more exposed surface area [Guichard and Bourget, 1998]. Even for apparent low relief environments, small surface variations modify community characteristics in soft-bottom types [Cusson and Bourget, 1997]. Methods quantifying surface topography and measuring height differences have shown a high correlation with fish abundance and diversity [McCormick, 1994].

As the characterization of bottom relief and sediment/lithology composition are in the domain of marine geologic research, it is not surprising that this discipline has made important contributions to the understanding of ground fisheries and other related environmental concerns, such as disposal dumping, pollutant dispersal, and the impact of marine exploration. The elaboration and subsequent study of geologic maps providing

knowledge of the sedimentary environment are a basis for the implementation of resource management plans for fisheries and other human-derived coastal activities [Valentine, 1992]. Along with extensive core sampling, submersible observations and geophysical methods, acoustic remote sensing using side scan sonar, sub-bottom profiling and multibeam sonar has become a primary source of information for the creation of comprehensive maps of sedimentary environments.

The link between geology and benthic habitats is of intense interest to marine biologists and fisheries managers who have approached the geologic initiatives to characterize habitats and to assess natural and human-induced habitat change or disturbance [United States Geological Survey (USGS), 1998]. At the same time, geologic research has traditionally used acoustic remote sensing to map the underlying geologic character of the seafloor. Some examples of acoustic methods and the interrelationships between the two areas of marine research (biology and geology) are presented in the following section.

3.2 Acoustic Remote Sensing and Habitat Characterization

A wide range of remote sensing methods has been proposed and used to characterize benthic habitats. Traditionally, remote sensing is perceived as satellite or airborne measuring. In a broader sense, however, remote sensing is becoming a platform independent concept embracing a whole range of marine measurements from vessels, towed platforms, and other deployed sensors. Numerous acoustic and electro-magnetic

sensors and techniques have been reviewed for assessing seafloor environments [Rhoads et al., 1996]. However, without a doubt, acoustic methods are the most commonly used due to technological maturity and a developmental background of several decades. There are several examples addressing the identification of the seafloor environment based on the statistical analysis of vertically incident acoustic returns [Collins et al., 1996; Greenstreet et al., 1997; Davies et al., 1998]; the interpretation of side scan sonar records [Yoklavich et al., 1995; Greene et al., 1995; Yoklavich et al., 1997]; and with less research conducted but probably with larger potential, the bathymetric and imaging capability of multibeam sonar [Hughes Clarke et al., 1997b; Mayer et al., 1997b; Baker et al., 1998; Mayer et al., 1999].

3.2.1 Vertical-Incidence Sonar Approach

Vertically incident acoustic seafloor classification has been documented through the years by several authors [Chivers et al., 1990; Collins et al., 1996] including some research by the OMG [Mayer et al., 1997b]. The fundamental concept behind these classification systems is the analysis of the acoustic waveform return for amplitude, rise-time, spectral characteristics, returned pulse length, among other features, that may be indicative of discrete seafloor types. There are commercially available seafloor classification systems (SCS) based on the analysis of returning acoustic waveforms.

The best-known SCS are *RoxAnn* (Stenmar Microsystems, Scotland) and *QTC VIEW* (Quester Tangent, Canada), the latter with an important collaborative input from OMG research. Both systems are essentially coupled to vertical-beam echosounders where the amplitude and shape of the acoustic bottom returns are analyzed by a set of statistical

24

algorithms. The seafloor type is determined by the acoustic response of the bottom, which is assumed to be a function of the physical properties (e.g., grain size, porosity, density) as well as seafloor roughness (ripple marks, gravel-cobble fields, seaweed, etc.). These classification systems have been used for many applications including the identification of fish habitat and in the mapping of biological communities [Collins et al., 1996; Greenstreet, et al., 1997; Collins and McConnaughey, 1998; Davies et al., 1998] and environmental concerns [Rukavina, 1998]. For example, fish species exhibit preferences for few types of benthic habitats that may vary seasonally and as fish grow. Identifying such preferences is an important goal for effective conservation and management [Collins et al., 1996]. Another example is the acoustic mapping of sediment types as some pollutants tend to be concentrated in finer sediments; knowing their distribution may help to optimize sampling and to plan remedial action [Rukavina, 1998].

3.2.2 Side Scan Sonar Approach

Swath sonar systems have also been used as bottom type classification tools. Side scan sonar has been used to characterize the quality of marine habitats through the differentiation of hard bottoms from contrasting soft sediments (backscatter strength) [Yoklavich et al., 1995; Greene et al., 1995; Poppel et al., 1995; Yoklavich et al., 1997; Scanlon et al., 1998]. The low grazing angles of side scan ensonification allow the recording of characteristic shadows delineating seafloor geomorphology, a significant contributor to habitat definitions. High-resolution side scan records have been used to map the effects of trawling fishing gear. The acoustic imaging not only has provided

proof of the scale of the damage caused in the benthic structure by trawling fishing gear [Collie et al., 1997], but studies have shown a correlation between habitat destruction and the reduction of fishing resources [Auster et al., 1996]. Remote sensing monitoring of the extension of trawling damage may help to evaluate and promote adequate policies for the management of marine resources.

Most of the time the discrimination of bottom types and roughness features from side scan records has been performed only in a qualitative sense. This procedure works to some extent for certain applications, for instance, when identifying regions of large backscatter contrast and texture, (e.g., rock outcrops) from sediments, cobble fields from sands, and so on. This has often been a constraint in such efforts as it is known that slight sediment variations contribute to the habitat selection of some species [Stein et al., 1992]. Therefore, acoustic research into benthic environments would be largely improved with approaches that could discriminate sediment types with closer grain size and/or mixtures of sediment classes; such discrimination can only be made with quantitative methods.

Quantitative acoustic seafloor classification methods based on backscatter measurements have been proposed. Many are supported by models describing the backscatter process based on the interaction of water/sediment interface roughness, volume scattering in the sub-surface, and sediment physical properties (density, sound absorption, impedance contrast, volume parameter, etc.) [Jackson et al., 1986; Mourad and Jackson, 1989; Matsumoto et al., 1993]. Others are based on the angular response of backscatter strength characteristic shapes, which may provide discrimination of sediment type [de Moustier and Alexandrou, 1991; Hughes Clarke et al., 1997a]. Image

26

processing techniques have also been reviewed for backscatter imagery segmentation and classification [Reed and Hussong, 1989]. The implementation of some of the above methods could assist to differentiate bottom types in the discussed research.

Other unconventional uses of sonar devices for remote sensing of benthic activities have been actively pursued and documented, like that described by Jumars et al., [1996] at the University of Washington. In this case, time-series of backscatter intensity and phase were analyzed to assess patterns of benthic activity and other biogenic modifications in the seafloor. Extensive sampling of physical property data and statistical measurements were employed to separate backscatter contributions leaving a benthic biota component to be spatially analyzed. The method described by Jumars et al. [1996] is another example of the potential use of information contained in the returns of acoustic sensors, which could be particularly useful for understanding natural benthic activity patterns.

3.2.3 Multibeam Sonar Approach

More recently, and due to the advent of reliable measurements and data management, multibeam sonar data have been used as an aid to characterize seafloor environments for several applications. The potential applications of MBSS for fisheries research were proposed by Mayer et al. [1997a]; they enlist a range of applications where MBSS are appropriate:

- Real-time use in planning sampling programs.

- Analysis of multi-temporal data sets for monitoring changes in habitat conditions.

27

- Improvement of circulation models with accurate boundary descriptions.

- Assessment of the impact of human activity on benthic habitats (trawling, dredging, dumping).

Some of these applications have already been reviewed by several investigators and organizations. The evaluation and understanding of the disturbance of benthic habitats by trawling, dredging, and natural disturbances have been addressed by Baker et al. [1998]. Current conditions and future development of aquaculture sites were examined with the high-resolution shallow-water EM-3000 MBSS capable of generating a bathymetric DEM at a spatial resolution of 1.5 m and backscatter mosaics at 0.5 m [Hughes Clarke et al., 1997c].

Other applications of multibeam sonar go beyond the original principle of seafloor classification to target midwater schooling fish. Research is being conducting within the OMG among others to explore the potential of multibeam sonar for school classification, internal school structure, spatial distribution of schools, fish behavior, and biomass estimates [Mayer et al., 1997b; Mayer et al., 1998; Gerlotto et al., 1999].

3.3 Analysis of Sonar Data

Despite the fact that several research and other programs have focused on the practical implementation of multibeam sonars and other high-resolution sonar systems, few discussions exist regarding suitable methodologies to analyze digital map products in the context of an objective approach needing minimal interpretation. These methods

represent alternatives to quantifying seafloor backscatter imagery unambiguously, which could lead to systematic efforts to characterize bottom habitats.

Statistical analysis and classification techniques have been used to describe biological communities from acoustic ground discrimination data obtained with vertical-beam echosounding [Greenstreet, et al., 1997]. In addition, spatial analysis and image processing techniques have facilitated the analysis of SCS as they were treated as spectral components in a *n*-dimensional space [Davies et al., 1998]. In Baker et al. [1998], GIS software has been used to recognize different thematic layers depicting seafloor environments; the main data input of this system was a multibeam bathymetric DEM and backscatter imagery along with other data such as core samples, videography and photography.

From the geologic and geomorphologic perspectives several studies have addressed the classification of the seafloor using sonar data either side scan imagery [Chavez and Karl, 1995] or multibeam data [Mitchell and Hughes Clarke, 1994]. Most acoustic data products are represented in a raster data model. This provides the convenience of having access to fully developed regular grid processing techniques. In general terms it is easier to work with regular grids because of the simplicity of the calculations. Standardized spatial analysis methods have been fully implemented in raster-based geographic information systems and image processing packages. The spatial analysis of continuous surfaces allows the users to work with a diverse number of spatial operations: spatial filtering, first and higher order derivatives, and clustering classification. In Chapter 4, this report will explore some of these methodologies.

Chapter 4

ANALYTICAL PROCEDURES

This chapter describes the analytical steps involved in addressing the objectives stated in Chapter 1. The steps are divided into the following types of analyses:

1. Production of regional map sheets from multibeam data, both bathymetric DEM and backscatter imagery.

2. Spatial analysis of bathymetric DEM including spatial filtering and terrain derivatives.

3. Classification of backscatter strength through textural and angular response (AR) analyses.

The descriptions of each of these groups of procedures are extended in the next sections, but first the multibeam data set is described with respect to its source and initial processing.

4.1 Source of Multibeam Data

The University of New Brunswick's Ocean Mapping Group has been working under a cooperative agreement with the U.S. Geological Survey (USGS) to map portions of the southern California continental margin as part of a systematic mapping program [Gardner and Mayer, 1998]. In 1996 the USGS surveyed the shelf and slope of the Santa

Monica Bay from the 20 to 800-metre isobaths using an EM-1000 multibeam sonar system (Figure 4.1). This investigation makes use of the data collected during this cruise campaign. General bathymetric DEM and backscatter imagery maps produced by the USGS were employed for initial analysis tests. Afterwards, processed (merged) data from edited survey lines were employed to create customized regional base maps for both bathymetric DEM and backscatter mosaics, which in turn were brought into a GIS package for spatial analysis. The following sub-sections give a description of the EM-1000 system, the details of the surveying operations, and the standard processing of raw data.
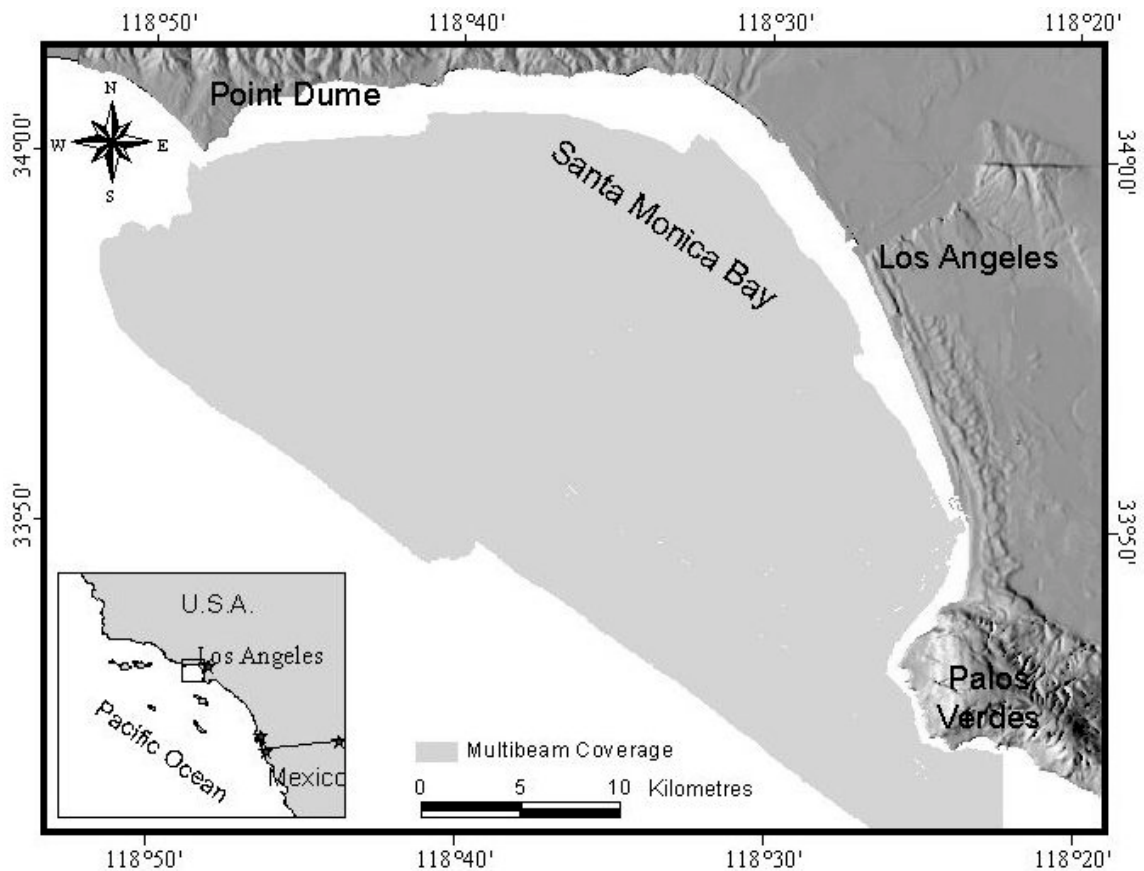
Figure 4.1. Area covered by the 1996 USGS/OMG Santa Monica Bay multibeam sonar survey.

4.1.1 EM-1000 MBSS Characteristics

The EM-1000 MBSS operates at a frequency of 95 kHz and is designed to work in several modes through depth ranges from 5 to 900 metres. It employs a semi-circular transducer array producing beamwidths 3.3° across-track and 3.3° in the along-track directions. The main operational modes depend on the type of acoustic pulse put in the water (Table 4.1). In a shallow mode the system distributes the output power in a large number of beams and shorter pulse width; this characterizes the maximum angular sector. On the other hand, deeper modes reduce the number of beams and increase pulse widths to compensate for power loss as a function of spherical spreading and attenuation; as a result the coverage swath width becomes narrower.

Table 4.1. Operational modes of the EM-1000 multibeam system.

Mode	Max. depth (m)	No. of beams	Beam spacing	Swath width	Coverage (times water depth)	Pulse width
Shallow	200	60	2.5°	150°	7.4	0.2 ms
Intermediate	600	48	2.5°	120°	3.4	1.0 ms
Deep	900	48	1.25°	60°	1.1	2.0 ms

4.1.2 Santa Monica Survey Operations

The EM-1000 system was installed in a pole-mounted configuration on the 12.8-m survey vessel *Coastal Surveyor* (Figure 4.2) owned and operated by C & C Technologies (Lafayette, U.S.). Navigation and positioning were determined with Trimble 4000 GPS units and redundant differential corrections provided by SATLOC and RACAL SkyFix signals. An S.G. Brown 1000-A gyro-compass output heading

readings. Vessel attitude compensation was achieved with an Applied Analytics POS-MV motion sensor measuring roll, pitch, and yaw. Speed of sound casts were made with a Sea-Bird CTD and Sippican XBTs. All depths were corrected to mean lower low water (MLLW) using a predicted tide model and tide staff at the Santa Monica pier.

Figure 4.2. The *Coastal Surveyor* showing the pole-mounted configuration of the EM-1000 sonar's head on the vessel's bow.

The survey was completed in twenty-eight days in October 1996 including a *patch test* to calibrate sonar misalignments and time offsets between sensors. EM-1000 raw data were logged with C & C Technologies proprietary acquisition and processing software, while data reformatting, editing, merging, gridding, and mosaicing were accomplished with the OMG suite of software tools. Data acquisition/processing were achieved at a 1 to 1 rate including the gridding and mosaicing of regional map products as soon as data were cleaned. The ultimate goal for the USGS/OMG survey team has been to process all the data in the field in near real-time [Gardner, 1996].

4.1.3 Processing of Multibeam Raw Data

Although the survey raw data were processed in near-real time during the acquisition and no further reprocessing was performed for the completion of this report, a brief summary of the important steps is given to illustrate the standard data processing methodology.

OMG's *SwathEd* is a collection of programs specifically oriented to process a variety of data formats from swath sonar systems [Hughes Clarke, 1998b]. A real time tool (RT) is implemented for data acquisition monitoring with an assortment of display functions for quality control and acquisition. RT reads the sonar's manufacturer-specific data telegrams and converts them into a suitable OMG-format for further data processing. Once a line is completed, navigation data are edited through an interactive display called *jview* where bad fixes and blunders may be flagged for subsequent rejection when merged with sounding data. Once the navigation has been checked the next step is the inspection of soundings using the Swath Editing tool, which is the core of the OMG multibeam data processing.

SwathEd allows the users to visualize stacks of consecutive swath series from across-track and along-track views, including a window with the imaging geometry. Data may be flagged or unflagged either interactively or through user-controlled filters. Tide level corrections are applied at this stage as well as a graphical refraction correction if necessary. The backscatter data is retrievable at any time to aid in data cleaning. Once the soundings are edited, the backscatter intensity information is used to create the corresponding imagery strips (side scan) equivalent to the swath coverage.

Bathymetric soundings and backscatter imagery can be gridded and mosaiced into raster DEMs at various scales, map dimensions, resolutions, reference datum, projections, and rotations. These processes are reviewed more extensively in the following sections as they have a direct implication in the quality of regional base maps.

4.2 Creation of MBSS Digital Data Products

MBSS main data products are bathymetric DEMs and backscatter imagery mosaics. These map types are produced after a thorough cleaning and editing process to remove spurious data and artifacts. The editing process briefly described in section 4.1.3 creates bathymetric and imagery data formats that are ready for the next processing stage, where data from each survey line are gridded and mosaiced into regional map sheets.

The basic principle of gridding and mosaicing is that variable density point values distributed in irregular patterns are forged into regular orthogonal matrices using an averaging procedure. Although, in essence, both bathymetry and imagery are sampled in similar predefined base maps, a different rationale is applied in their creation. The two processes are explained in the following sections. The procedures and methods used to grid and mosaic multibeam sonar data have been developed within the OMG.

4.2.1 Creating Regular Grid DEM

Considering the ease of their manipulation by raster-based computer packages, regular grids or altitude matrices are the most common form to represent DEMs. They are simple models depicting the spatial variation of an elevation value z (nodes) in an

35

orthogonal plane. Node values in a regular grid DEM generated from multibeam data are derived from a detailed sampling strategy because the density of soundings per unit area varies as a function of several factors:

1. The footprint dimension of a projected beam on the seafloor, dependent on depth, beamwidth, and angle of incidence.

2. The inter-beam and inter-swath spacing as a function of across-track beam spacing and pulse repetition (sonar design), and vessel speed and beam motion stabilization (survey design).

The selection of the node spacing or cell size to produce a DEM should represent a conservative value considering the factors mentioned above.

The first consideration is that the cell size should be close to or larger than the footprint dimension. This is because bottom features smaller than the footprint cannot be resolved. As seen in section 2.3.2, the footprint will vary as a function of beamwidth, incident angle, and depth. Thus, it is not advisable to use a cell size that is based on the single observation of nadir beams at the shallowest depth, which is the highest resolution scenario. Even if a cell size reflecting the largest scale footprint dimension is chosen, an averaging process is still required to minimize the errors related to uncorrelated noise present in the bottom detection process [Hughes Clarke, 1998b]. Therefore, node values are determined by the contribution of soundings within a radius of certain dimension. The approach taken by the OMG for gridding high density soundings into a DEM is presented in section 4.2.1.1.

4.2.1.1 OMG's weighted gridding method

Several methods exist to average values of neighboring soundings to regularly spaced cells. The method used in OMG's software is a variation of weighted filtering [Ware et al., 1991]. OMG's *weigh_grid* calculates the depth of a cell by a sum of weighted soundings within a given search radius. The method is preferred over other techniques like spline and kriging because it can be used iteratively —data can be gridded progressively— and it is less computationally restrictive [Hughes Clarke, 1998b].

Special considerations are taken in *weigh_grid* for sparse soundings at the outer parts of the swath where the spacing might be larger than the search radius. A scaled interpolation radius w_r is used to reflect the footprint spacing varying with angle of incidence. At the same time, the w_r considers the change in footprint size as a function of depth where beam footprints scale linearly. If this consideration is not taken into account grid singularities may be generated due to cell spacing being greater than the search radius. It is important to note that a w_r optimized to higher resolution close-to-nadir beams will oversample the information of outer soundings. On the contrary, a w_r enhanced to lower-resolution outer beams might miss the truly resolved features in the nadir region. A practical implementation is to scale w_r to a mean beam resolution [Hughes Clarke, 1998b].

With respect to inter-swath overlap, *weigh_grid* uses a predefined array of beam weights which gradually reduces the contribution of soundings off nadir to deal with the dilemma to which soundings will contribute in the cell value assignment. This is

significant from the point of view of sounding solution confidence within the swath. Several reasons contribute to consider outer beams as lower priority: bottom amplitude detection techniques decrease in accuracy, errors in vessel attitude compensation may be larger, and errors due to inappropriate water sound speed knowledge are also larger. An additional weighted filter w_b is used to assess the confidence of soundings as a function incident angle. In practice the user defines the array of weights per beam angle with values decreasing toward the outer beams linearly or with another function (Figure 4.3).
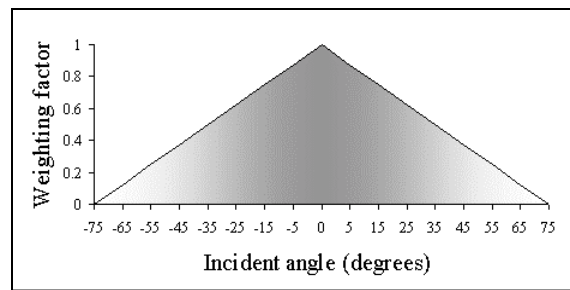
Figure 4.3. Linear weighting array applied to soundings for inter-line swath overlap.

4.2.2 Creating Backscatter Imagery

The spatial resolution of an MBSS in terms of bandwidth of the acoustic system were reviewed in sections 2.3.1 and 2.3.2. From that discussion it should be clear that the resolution of a backscatter image is different from the resolution achieved with bathymetric soundings and thus requires a different processing procedure. The basic difference is that bathymetric measurements are obtained by determining the slant range from twice the travel time of each individual beam. On the other hand, backscatter imagery measurements are extracted from the time series traces contained within a beam. For instance, the beam footprint in the outer swath section might contain several

38

backscatter traces as a function of the pulse length and across-track ellipse dimension (Figure 4.4). Joining the beam footprints within a swath, a continuous time series trace is created along the line of the transmitting beam pattern axis where the resolution is given by the pulse length of the system. However, other considerations are required to choose the minimum cell size for backscatter imagery resolution.
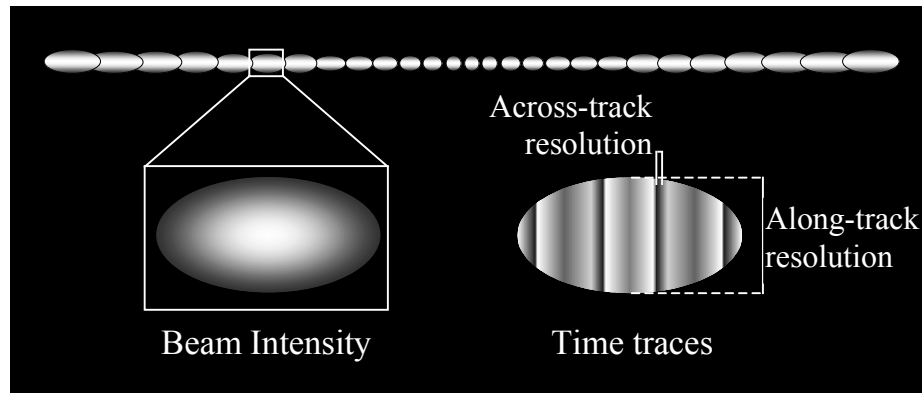
Figure 4.4. Ensonification of a hypothetical multibeam pattern. The ellipse at left shows the intensity within a beam (grey level); at right the ellipse shows the time series traces for the same beam assuming a certain pulse length (bands) (from Hughes Clarke [1998a]).

As can be seen in Figure 4.4, there is a large difference between the along-track and across track resolution. The difference between both can be from a few centimetres in the across-track to a couple of metres in the along-track direction. The practical solution for selecting a cell resolution is to average the across-track resolution to an along-track equivalent. This approach will minimize the speckle component and reduce the computational load in the pixel creation. At this point, backscatter traces within a swath have been converted to pixels values (0 dB→255, −128 dB→0). The next issue is the inter-swath pixel spacing that is required to avoid gaps in the imagery.

It is very difficult to achieve full-bottom ensonification at the −3 dB limit during data acquisition because of a number of factors including the repetition rate, vessel speed,

leverage of outer beams at heading changes, and effects of roll and pitch. This leaves voids in the backscatter imagery that need to be filled. The method used by the OMG software fills gaps by linear interpolation using pairs of sequential pixels in a swath and the equivalent pair in the following swath. However, some criteria are implemented in the software to prevent gap filling of areas that are too large. These settings include:

- A maximum azimuth change from swath to swath to prevent bluring in sharp turns.

- A maximum time interval from swath to swath possibly caused by interruption of navigation or changing sonar parameters.

Gap filling produces a continuous strip of backscatter imagery equivalent to the angular sector covered along the survey track. Similar to regular grid DEM generation the processing now deals with inter-line mosaicing.

The issue at this stage is the pixel overlap of adjacent lines. Because backscatter magnitude is highly dependent on the angle of incidence one cannot use a weighted filter as in bathymetric soundings. Averaging of pixel values is not an option because the information in the outer parts of overlapping swaths is significantly different based on the geometry of ensonification. Thus, the method is reduced to a decision process where priority is assigned to pixels with the best ensonification geometry, for instance, the weighting factor decreases with increasing beam angle. Nadir beams are also assigned with low weighting because of common troubles of backscatter acquisition in this angular sector (Figure 4.5).
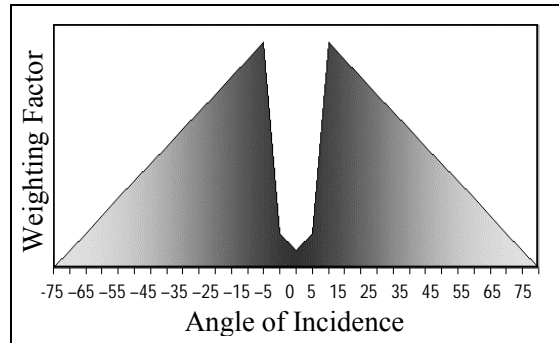
Figure 4.5. Common weighting function applied to pixels in the process of registering overlapping backscatter imagery strips. Note the low weight assigned to the nadir beams (from Hughes Clarke [1998b]).

4.2.3 Production of Regional Map Sheets

The OMG's *weigh_grid* and mosaic programs take data from each survey line to fill up a predefined blank base map. Base maps are created with map parameters specified by users such as: cell size, map projection, reference ellipsoid, and geographic bounding limits. The regular procedure is to create regional maps of similar depth range where the cell size can be selected based on the mean average depth.

Mean average depth works better than the extreme options. A cell size value optimized for the shallowest depth is not appropriate for areas of greater depth because feature resolution will not be improved and it will result in raster images of inefficient and unmanageable size. Conversely, choosing a cell size representing the greater depths will eliminate the fine details achieved by a smaller footprint in the shallow areas.

Normally for the EM-1000 system, bathymetric DEM maps are created using a cell size value of 5 to 10 percent of mean water depth, and backscatter mosaic maps are generated at a slightly higher resolution of 3 to 5 percent of water depth. The difference

41

is because of the number of backscatter time series traces as compared to the single sounding present in a single beam footprint.

The approach to creating regional map sheets is intended to preserve bottom features at the maximum resolution allowable. The choice of geographic extension, projection, and cell size is, in most cases, decided by the user based on the knowledge of the area of study and the aim of the regional maps; however, the user must be conscious of the disk storage requirements to avoid management problems (files becoming too large for efficient handling).

At this point regional maps are suitable for visualization, processing of derivatives, and transfer to GIS and image processing packages. The data format of maps produced with the OMG software can be used by only a few software packages because the software tools are intended to be a research tool rather than fully developed packages. Nevertheless, regional maps can be exported to other software platforms in generic ASCII files where the 3-D coordinates (xyz) are extracted for each node of the grid array. Usually, the z value in bathymetric grids is given in float precision while backscatter values are integers.

4.3 Spatial Analysis of Map Products

The advantages of the raster model allow for the analysis of multibeam sonar data products using numerous procedures implemented in mature GIS and image processing packages. Many studies have been done using spatial analysis and image processing

techniques to extract information from modern swath sonar systems, such as side scan sonar imagery [Reed and Hussong, 1989; Chavez and Gardner, 1994; Chavez and Karl, 1995], and MBSS bathymetry and backscatter [Mitchell and Hughes Clarke, 1994].

Many spatial analysis operations can be performed on continuous raster surfaces. The main characteristic of these spatial operations is that new attributes for a given cell can be calculated as a function of the attributes of neighboring cells. The main spatial operations include [Borrough and McDonnell, 1998]:

1. Spatial filtering, involving passing a rectangular window or kernel over the surface and computing a new value of the cell values covered by the window. The most commonly used window functions are high- and low-pass filters.

2. First- and higher-order derivatives, which are approximated by calculating differences within a square filter or by fitting a polynomial to the data within the filter. Slope and aspect are first-order derivatives.

3. Interpolation, which is used to create continuous surfaces from point data distributed at regular or irregular intervals; also used for resampling to a different grid size or to a different rotational coordinate plane.

Some spatial analysis operations are employed in this report. Descriptions of the procedures are presented in the following sub-sections.

4.3.1 Analysis Using Spatial Filtering

Spatial filtering allows for the extraction of attributes from multi- and single-layer maps. This is especially important for data sets with only one layer, where data need to

be analyzed in extended detail, like backscatter imagery and bathymetry. The most common family of methods for filtering are those where a window of variable cell dimension or map units moves along on every cell of the grid defining the local neighborhood for such cell. Typically for local scale filtering, the window is of size 3x3, 5x5, 7x7, and so on; however larger windows (e.g. 65x65) are used to derive regional information [Chavez and Gardner, 1994].

The two main types of filters likely to be considered are high-pass and low-pass filters (HPF and LPF, respectively) (Figure 4.6). HPFs enhance the high frequency information (short range spatial properties) of an image or raster surface, amplifying the attributes of areas of high complexity. The HPF shows how much a pixel differs from the neighborhood at the scale of the window size. On the other hand, the LPF has the effect of removing extremes from the data. The usual perception of an LPF is that images appear smoother than the original. LPFs are used to extract low frequency information (long range spatial variations) of a raster surface.

a   b   c
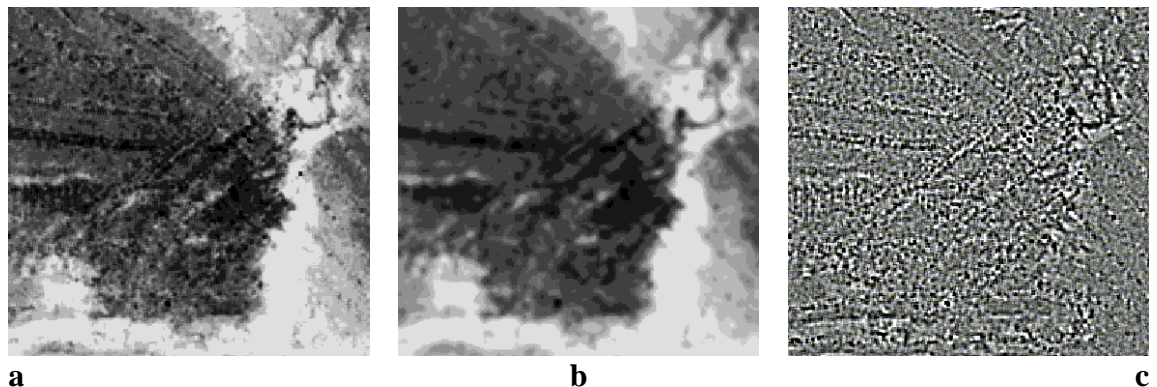
Figure 4.6. Images illustrating the respective effects of an LPF (b) and HPF (c) on a gridded data set (a).

44

A proven spatial filtering method for seafloor classification is adopted in the analysis of multibeam data presented in this report. The procedure was originally used to extract spatial amplitude and variability information from digital side scan imagery [Chavez and Gardner, 1994]; it has also been used to show topographic variability of digital bathymetric data [Chavez and Karl, 1995]. Basically, the method computes an HPF to extract spatial amplitude and variability information, which are called, Spatial Amplitude Index (SAI) and Spatial Variability Index (SVI), respectively. In this report SAI and SVI will be used to analyze the topographic surface of the seafloor. Therefore, these terms are conveniently renamed as Topographic Amplitude Index (TAI) and Topographic Variability Index (TVI). The generic filtering calculations are described as,

$$LPF = \text{filter}(I_O, N),$$

$$HPF = I_O - LPF,$$

where I_O is the original image, N is the number of cells forming the sides of the moving window; most common operations used in filtering are average or modal. *TAI* is then obtained as the absolute value of *HPF* because only the amount of surface change is what is desired,

$$TAI = \text{abs}(HPF).$$

The TAI explains how much an elevation within a given cell differs from the average of cell elevations within a given neighborhood (vertical range) (Figure 4.7b). It is a measure of the amount of height change over the seafloor without considering the direction of change. Although the TAI is directly associated to bottom relief, it does not show how variable a cell is within the neighborhood. This is offered by the TVI.

45

a b c
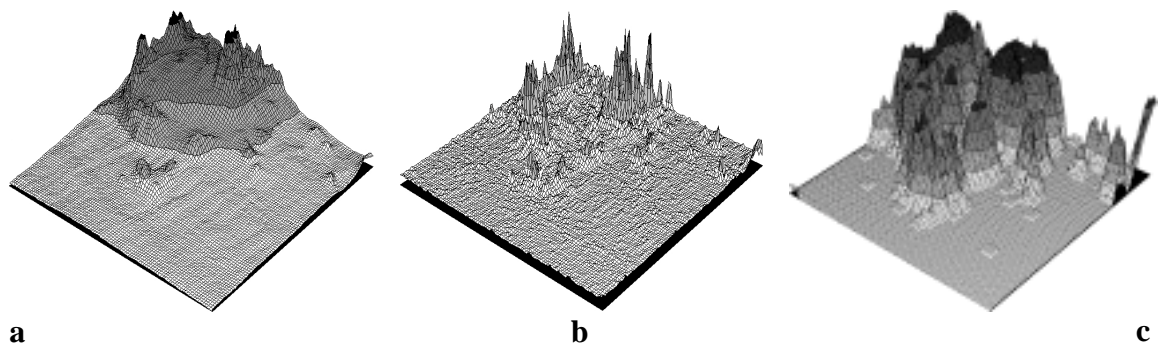
Figure 4.7. Three-dimensional comparisons between the original raster surface (a) with TAI (b), and TVI (c).

The TVI is generated from a filter that separates those pixels showing amplitude differences from its neighborhood from those that show no difference (Figure 4.7c). The limits for deciding which pixel values are in each category can be selected from the frequency histogram of the HPF, for example, the 15% low and high pixel values. Another way to select the threshold is to take an *n* measure of the standard deviation at both sides of the normal distribution curve for instance, at the steepest point on the curve; a graphical method can be used to facilitate this selection (Figure 4.8).
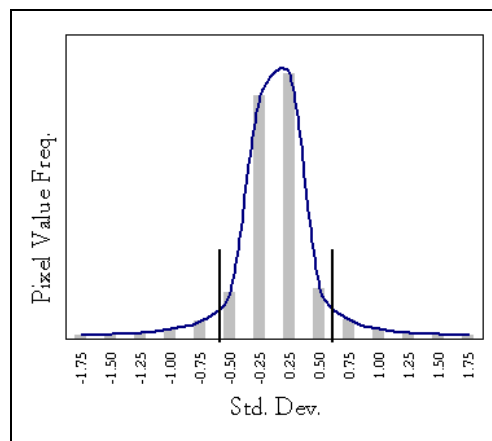
Figure 4.8. Selecting threshold limits for TVI generation. Limits separate the data showing spatial variability (extremes).

Pixel values outside the limits are considered already to have large enough amplitude differences to be considered spatially variable with their neighborhoods. Pixels with values inside the limits are considered not spatially variable. Pixels outside and inside the limits are reclassified with a value of 100 and 0 respectively. A LPF is applied to the reclassified layer where the resultant pixel values represent the percent of pixels with large amplitude differences (Figure 4.9). In other words, an individual pixel would have information regarding the variability of its neighborhood.
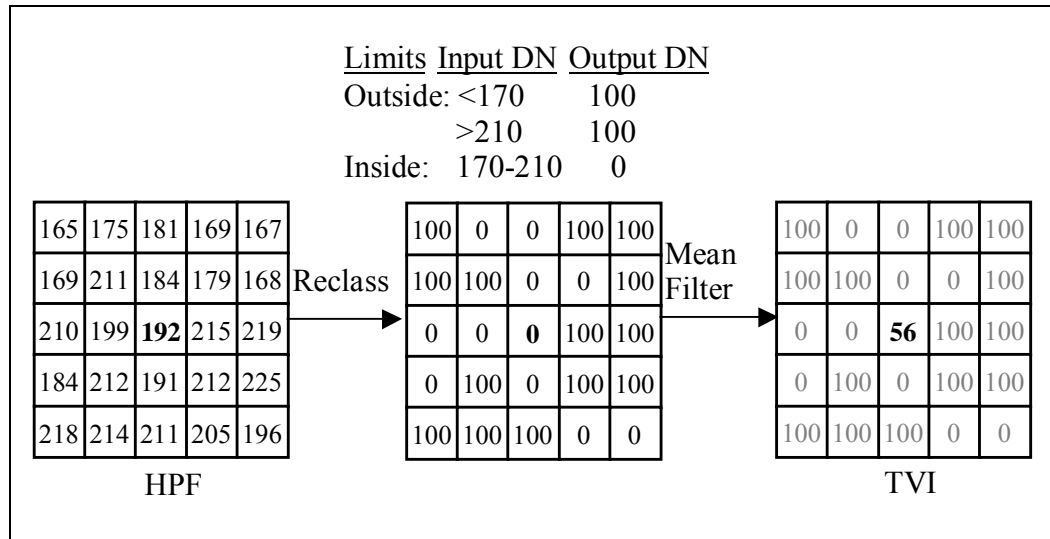
Figure 4.9. Process for the generation of the TVI from the HPF of an image and subsequent reclassification and filtering.

4.3.2 DEM Derivatives

Derivatives of continuous surfaces are common analysis tools widely used in terrain analysis. First-order derivatives are the slope and aspect of the surface. Second-order derivatives are the rate of change of slope expressed as plan and profile convexity. There

are a variety of methods for calculating slope, aspect, and other derivatives. This report is not intended to discuss which is best but to use those already implemented in spatial analysis software packages such as the Spatial Analyst extension of ArcView GIS (ESRI, California, U.S.) and the terrain analysis tools in EASI/PACE (PCI, Ontario, Canada).

Slope is derived from the general bathymetric DEM. This layer is used along with the TAI, TVI, and depth layers in map modeling to classify the topographic surface of Santa Monica Bay in terms of these properties.

4.4 Classification of Backscatter Imagery

As mentioned on Chapter 2, backscatter imagery is the result of a complex combination of physical phenomena between acoustic energy and the properties of the scattering interface. Undoubtedly, the variations of gray scale in a backscatter image reflect the variations of seafloor properties. The issue is to what degree of precision is it possible to classify those variations. The simplest assumption is to assign variations of grey level to discrete sediment types, for example, rock outcrops, boulder fields, sand, mud, and so on. However, bottom sampling has not only shown that the correlation of sediment type and backscatter intensity is weak if not negligible [Gardner et al., 1991], but other properties inherent to bottom nature contribute to that variability, for instance, acoustic impedance, local slope, short wavelength roughness, and so forth.

For these reasons, various approaches have been pursued to improve the understanding of backscatter response. The most common is texture analysis that tries to classify the pixel variability through the extraction of statistical features. Texture analysis has been utilized to classify side scan imagery [Reed and Hussong, 1989]. A second approach looks at the bottom response signatures of homogeneous seafloor types through the complete range of incidence angles (angular response *AR*). Because the low aspect ratio (low grazing angles) of ensonification achieved with sidescan sonar, variations caused by angular response are normally resolved with the Lambertian model. With multibeam backscatter, the Lambertian model is applied to remove the attenuation of the acoustic intensity as a function of grazing angle; the model is applied in the EM-1000 system and other Kongsberg Simrad MBSS. In geologic mapping, the model can separate bottom types with fairly different backscatter strengths (gravel/rock from mud), but it is unable to discriminate the broader range of sands and silts and their combinations.

In this report, both approaches, texture and angular response, are used in an attempt to classify sea-bottom types at the highest precision and clarity possible. The exercise is not only beneficial for fisheries applications but for other applications requiring seafloor classification.

4.4.1 Texture Analysis of Backscatter Images

The extraction of information from MBSS backscatter imagery is analogous to that from radar remote sensing imagery, and particularly to image processing techniques used for texture analysis and clustering. Texture in a digital image is closely related to

the measure of roughness in morphological terms. Wood [1996] provides a definition of statistical texture as the highest frequency of variation within an image. Texture is one of the important characteristics used to identify changes in regions of interest in an image. Unlike multi-layered images, texture may contain information about the spatial distribution of tonal variation within a single-layer image.

Projects related to the processing of digital images are quite extensive in the remote sensing literature; some methods have permeated the field of synoptic seafloor imagery, specifically for side scan imagery. A technique used by Reed and Hussong [1989] to enhance and classify SeaMARC II side scan sonar imagery evaluates the textural features based upon grey-level co-occurrence matrices (GLCM). Summary statistics calculated from GLCM measure distinctive textural properties from an acoustic image showing the relationships between a given pixel and a specific neighbor.

The GLCM is a useful image analysis technique for the extraction of information from side scan imagery because its results do not depend on the absolute backscatter strength (non-calibrated data) but rather on individual sonar characteristics such as pulse length, beamwidth, and the image transformations used in sonar data processing. Additionally some ground-truthing is required to identify the seafloor type and relate the relative variations of textural characteristics [de Moustier, 1998c].

In this report, backscatter imagery maps were analyzed with the Texture (TEX) analysis tool available in EASI/PACE ver. 6.2.2 in an effort to identify the contributors to the total backscatter response from the seafloor. The TEX utility uses a regular window of dimension N where the entries are expressed as the number of times a pixel

of value *i* neighbors a pixel of value *j* in direction θ, at distance *d*. A simple case with a matrix N=3, θ=0° (horizontal) is shown in Figure 4.10.

Window of imagery				Resulting GLCM				
1	1	2				PxValue		

Window of imagery

1	1	2
2	3	4
3	4	2

Resulting GLCM

PxValue

Px Value		1	2	3	4
	1	1	1	0	0
	2	0	0	1	0
	3	0	0	0	2
	4	0	1	0	0

Figure 4.10. Example showing a GLCM produced from a 3x3 pixel window with θ=0°.

The direction θ is usually tested for 0°, 45°, 90°, and 135°; alternatively the four estimations can be averaged for invariant directionality. In TEX, feature statistics supported are homogeneity, dissimilarity, correlation, variance, mean, entropy, contrast, angular second moment, gray-level difference vector (GLDV) contrast, GLDV mean, GLDV angular second moment, and GLDV entropy. Each statistical feature creates a new band (layer) in the EASI/PACE database file, however, it is impractical to treat every statistical measure as a dimension in the feature vector space.

The number of dimensions can be reduced because some of the features are strongly correlated with each other. Reed and Hussong [1989] suggest that principal component analysis (PCA) be used to detect these associations and reduce the dimensionality of the data set. The same process was applied for the multibeam backscatter imagery. Once the statistical measures were determined, PCA was used to separate the dimensions with

51

larger components in the data and then a clustering classification method was used to find texture classes defined by the *n*-feature vector.

4.4.1.1 Classification of texture features

The objective of classifying the *n*-dimensions resulting from the GLCM analysis is to separate clusters of feature vectors into discrete thematic groups. Unsupervised and supervised classification methods are used to group feature vectors. Unsupervised algorithms, also described as clustering procedures, determine the natural groupings of the data. The most common unsupervised algorithm is the K-means and extensions like ISODATA and fuzzy K-means. The ISODATA algorithm within EASI/PACE was used to classify the eigenchannels created in the PCA analysis of the feature measures extracted from the GLCM. Basically, the procedure is initialized with the selection of *K* number of classes specified by the user. Each pixel in the image is assigned to the cluster whose mean vector is closest to the pixel vector. A new mean vector is calculated from the previous assignment, and the pixels are reassigned to a new *K* cluster vector. After each iteration, statistical parameters examine each cluster following three criteria:

1. Clusters with a too large standard deviation (threshold defined by user) are split to form two smaller clusters.

2. Clusters statistically too close (close averages, small standard deviation) are merged into a single cluster.

3. Clusters with a very small number of pixels are discarded.

The procedure continues until there is no significant change in pixel assignments from one iteration to another or after the maximum number of iterations (defined by

user) has been reached. Although a desired number of clusters is set at the beginning of the processing it is unlikely that the statistical cluster number estimate would agree.

4.4.2 Angular Response Analysis of Backscatter Strength

As reviewed in Chapter 2, the backscatter strength (BS) varies as a function of grazing angle. This is called the angular response (AR) of the seafloor for a given frequency. A methodology developed by Hughes Clarke et al. [1997a] was used to differentiate bottom types that normally cannot be separated by standard backscatter imagery. Hughes Clarke's tool is based on the inversion of Jackson's model [Jackson et al., 1986], which estimates the scattering response based on sediment parameters like bulk density, compressional-wave velocity, loss tangent, volume parameter, and other statistical properties of sediments.

Traditionally, BS is normalized assuming a Lambertian response that removes the mean variation in backscatter with grazing angle. The Lambertian compensation accordingly separates bottom types with high backscatter contrast, e.g., rock and gravel fields (high) from mud ponds (low), however, the analysis of the angular response shapes of intermediate sediments types showed that similar mean BS can be discriminated by analyzing the BS values at different incident angles (domains) [Hughes Clarke et al., 1997a].

AR curves can be derived from the EM-1000 sonar records using a tool developed within the OMG. The AR tool extracts the angular response curves for subsets of consecutive pings sampled over a homogeneous area of seafloor. The AR method

requires that beam pattern, sound refraction, and seafloor slope corrections have already been applied to the backscatter measurements.

In theory, beam patterns are calibrated by sonar manufacturer and compensated within the sonar processor, however, small variations persist after all. To correct this problem an empirical approach is applied. The technique employs finding a region with a very rough and isotropic surface (ideally a very coarse boulder field), which should have a Lambertian response, and calculating the differences between the observed response and that modeled for all angles. Data from the remaining areas are then subtracted from this empirical beam pattern estimate. Sound refraction problems are corrected during the cleaning and editing of raw data (SwathEd), and therefore no further corrections are applied. Currently, slope corrections are not applied thus the tool would be useful for a relatively flat seafloor, which corresponds to large areas in Santa Monica Bay above 200 m in depth.

The estimation of AR curves was performed by averaging the backscatter measurements taken from a stack of consecutive swaths. Fifty to one-hundred swaths can give good estimates of the AR shape. The averaging must be calculated over regions of homogeneous backscatter type. Naturally, there will be stacks where sediment boundaries occur. In that case, AR curves become impractical and are rejected when the across-track variance exceeds a predetermined threshold.

Three main domains can be identified from the AR curves as well as their boundaries (Figure 4.11). Domains and boundaries can be separated and analyzed reducing to a few parameters the potential sediment classification.

Mean BS of each domain (*a, e, i*) were gridded separately as part of a multi-dimensional space. Assuming that the relationships of BS for each domain could result in the identification of sediment classes, typical BS curves were used as training signatures in supervised classification. Typical BS curves were obtained plotting selected 50-ping stacks over the backscatter imagery as background. These curves were compared against ground-truth data to associate them with sediment properties.
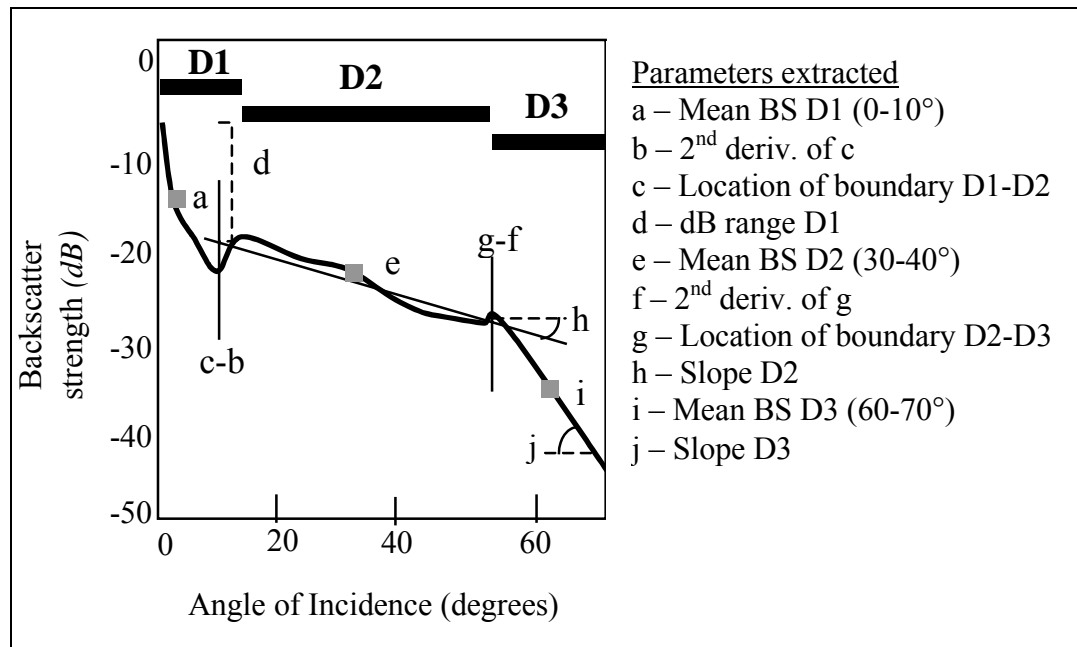
Figure 4.11. The three main domains (D1, D2, D3) of angular response curves and the parameters extracted to describe each domain (*a* to *j*) (from Hughes Clarke et al. [1997a]).

4.4.3 Ground Truth Data

To validate any backscatter classification method, either GLCM textural analysis or AR curves, a data set containing sediment core information was used. The data were

provided by the USGS [Lee et al., 1998] from two separate cruises conducted in 1997 and 1998 in the area of study. Core descriptions include estimations of saturated bulk density, compressional-wave velocity, and grain size analysis.

4.5 Map Modeling

The layers produced by spatial filtering, DEM derivative analysis, and backscatter imagery classification are brought to a common spatial extent to exercise the application of spatial map modeling. Because all individual multibeam map sheets have been produced in a homogeneous coordinate reference frame with the same geographical extent and cell size, arithmetic and Boolean operations are performed cell to cell, facilitating calculations. This means that overlapping operations can derive more attributes for the same cell in a new thematic layer. Another advantage of the raster model is that these kinds of operations are computationally very easy to perform.

Chapter 5

MAP GENERATION AND ANALYSIS

5.1 Bathymetric DEM Compilation

The bathymetric DEM was mapped on a series of customized base maps at three grid resolutions distributed along the area of multibeam coverage. Map resolution for the shallow areas (20 to 60 m) was set to 4-metre cell-size; intermediate areas (60 to 160 m) to 8 m; and deeper areas (more than 160 m) to 16 m. These map resolutions were selected specifically to depict detailed bottom topography considering that the spatial resolution of soundings varies with water depth. The orthogonal base map design allowed box overlapping to minimize areas where the gridded depth ranges were out of the desired map resolution. Figure 5.1 shows the distribution of map boxes.

The bathymetry was gridded at resolutions of 5 to 10 percent of water depth for areas up to 200 metres. This assured a good bottom relief depiction especially in areas with rough relief. Nevertheless, below the 200-m isobath, the ratio of cell-spacing to water depth becomes smaller resulting in beam footprints larger than the map resolution. For example, compared with a 16-m cell size, the footprint's across-track dimension for nadir beams at 300-m water depth is approximately 17 metres; at 500-m water depth the footprint is around 28 metres.
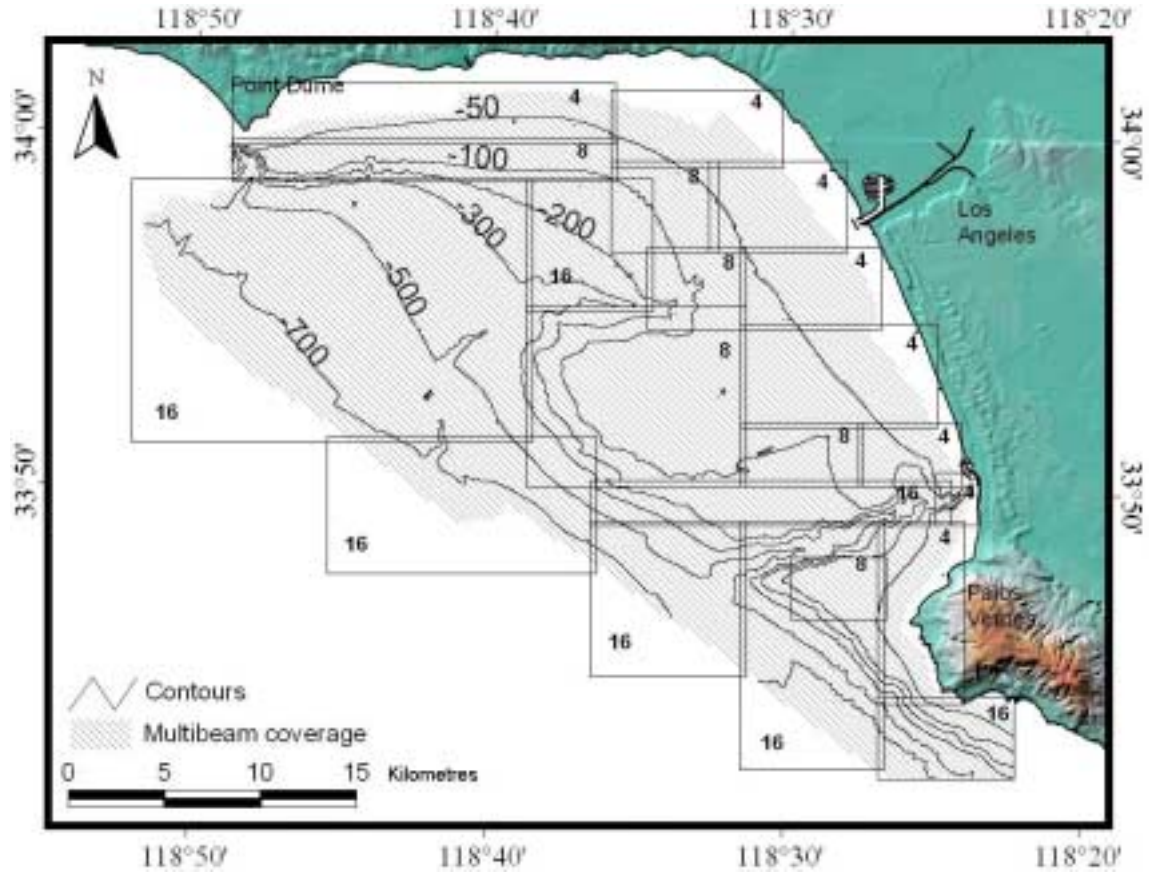
Figure 5.1. Partition of the surveyed area in map boxes according to the desired map resolution. Numbers indicate the grid spacing.

For those cases, the weighted filter w_r implemented in the program *weigh_grid* provided an efficient solution to preserve the cell-size without extrapolation. Cell values using w_r are estimated by increasing the search radius in direct proportion to water depth. The side effect of the scaled search radius is the appearance of grid artifacts when the soundings become very sparse. Fortunately, this was not the case and no serious artifacts or aliasing effects were observed. Visualization methods, mainly sun-shading at different elevation and azimuth angles, were used to assess probable spurious effects. A

general bathymetric map for Santa Monica Bay is shown in Figure 5.2 and Plate A-1 (Appendix A).
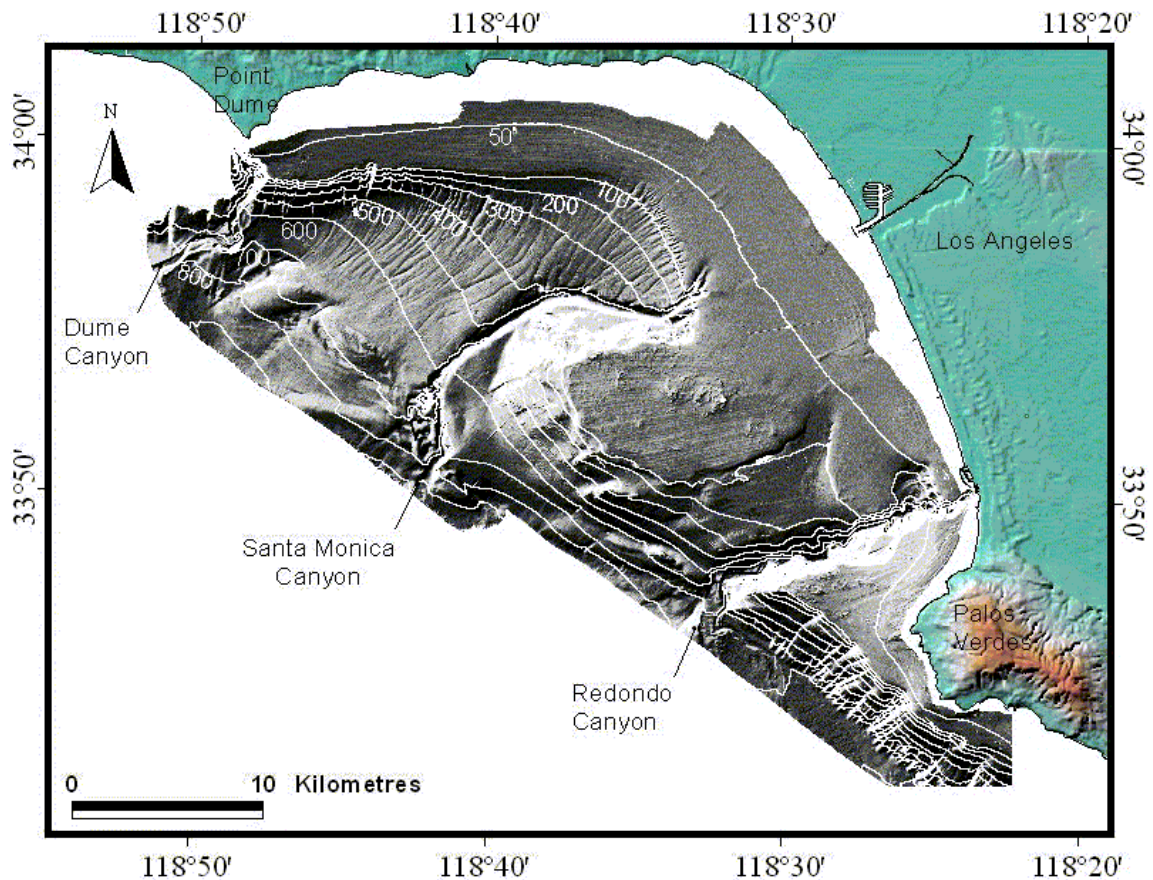
Figure 5.2. Sun-illuminated bathymetric DEM for Santa Monica Bay.

5.1.1 Description of Seafloor Morphology.

The Santa Monica Bay is characterized by the presence of three submarine canyons scouring the almost featureless shelf platform into the Santa Monica Basin down to about 800-m depth. Two canyons, Dume and Redondo, have origins localized close to the coastline in very shallow water, while the head of Santa Monica Canyon is at a depth of about 100 metres. The continental shelf is remarkably flat with a smooth gradient

towards a generalized slope at a depth of about 200 metres. The depth of the foot of the slope is variable but is recognizable in large extensions at about 500 metres. The central region on the shelf presents the largest bottom relief features with outcrops of sedimentary rock, that is part of the Santa Monica plateau [Gardner et al., 1997]. Similar features are observed on the east and south-east portions of the bay. The Los Angeles sewage outfall pipe was clearly depicted from near-shoreline to the vicinity of the head of the Santa Monica Canyon.

5.1.2 Data Transfer to GIS Packages

Bathymetric base maps and details of the observed bathymetric features were exported to a raster ASCII format where the cell values corresponded to the center of the cell (nodes). The ASCII files were formatted into a Arc/INFO GRID format compatible with ArcView GIS software. No interpolation or resampling of the original base maps was necessary, thus no detail was lost in the data format translation. These digital map products were the base for the subsequent spatial analysis procedures described in the section 5.2.

5.2 Spatial Analysis of Bathymetric DEM

In addition to the elemental depth thematic coverage, three other information layers were created from the bathymetric DEM. The first one corresponds to the elevation gradient or slope; calculation of the slope was performed using the function available in ArcView's Spatial Analyst extension. The second thematic layer involved the extraction

of topographic amplitude information (TAI). The TAI was the absolute value of the substraction of the original surface by the LPF surface (5x5 pixel window and average operation).

The third layer describing the topographic variability (TVI) was derived by separating the extreme data of the HPF using a threshold. A histogram showing the normal distribution of relative amplitudes helped to set the threshold values (see Figure 4.6). Data inside the limits were considered invariable and reclassified to zero value; data outside the limits were considered variable and reclassified to one hundred. A new layer with zero and one-hundred values was average-filtered with a 5x5 pixel window to obtain the final TVI. Each cell value in the TVI layer indicates the percentage of cells within the neighborhood that are outside the threshold and thus have a high elevation variability.

Appendix A contains maps (Plates A-2, A-3, and A-4) produced from the analysis of the bathymetric DEM described above. The full-coverage maps were generated by merging the regional base maps at the coarser resolution (16-m). Figure 5.3 presents a schematic example of these results. The illustrations represent a sampled bottom area of 100 x 100 cells at 8-m resolution. In (a) the seafloor elevation shows rock outcrops with altitudes above the base to about 20 m. In particular, this piece of seafloor was selected because it contains diverse surface features like a flat seafloor disrupted by high amplitude topography and significant slope. The percent of slope for the same sample is seen in (b) with ratios up to 25-30%. The surface in (c) corresponds to the topographic amplitude (TAI) with values up to 4.5 metres. Note that the surfaces's depth gradient has

been removed by the filtering procedure thus enhancing only the local elevation amplitudes.
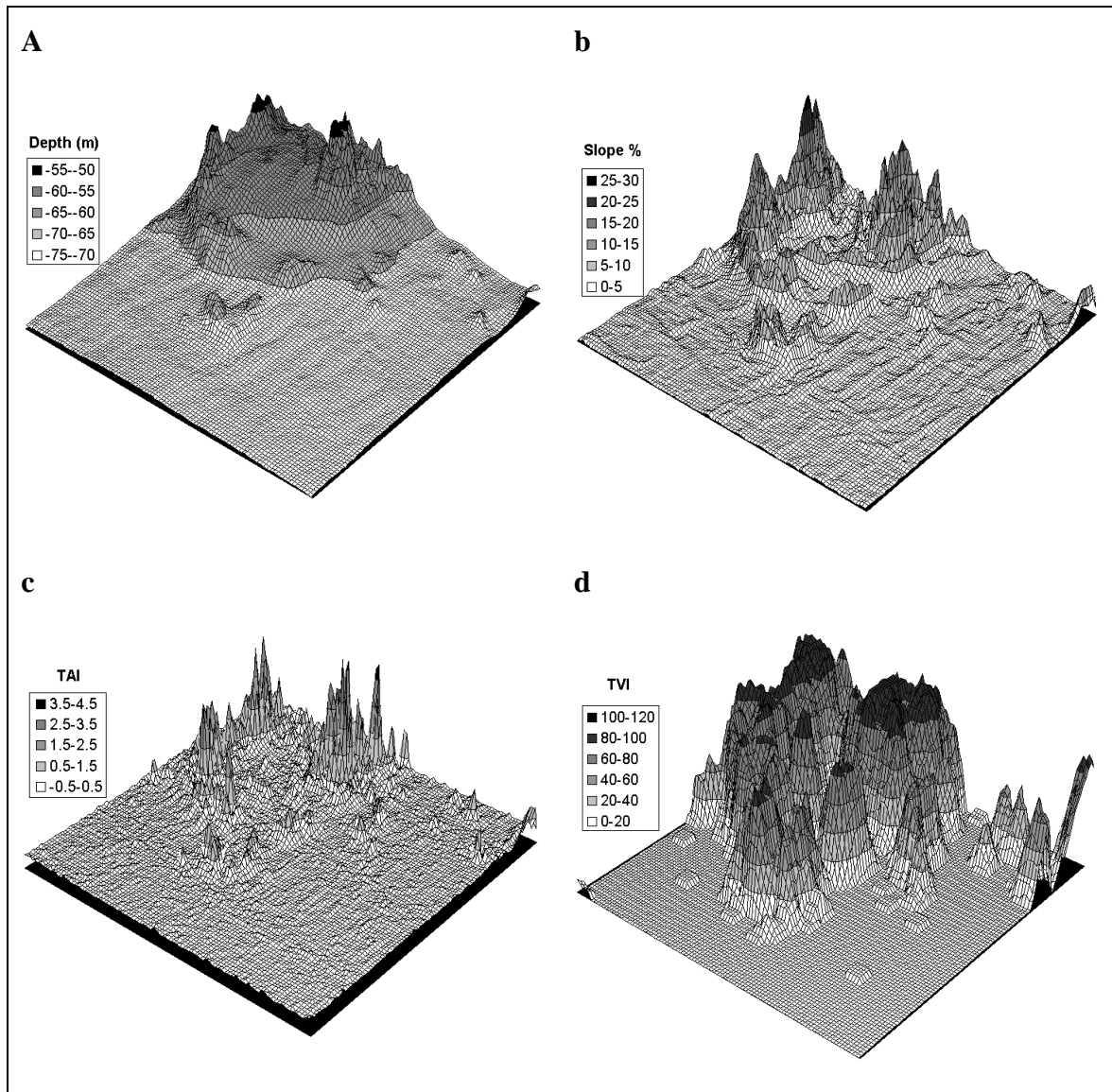
Figure 5.3. Samples of bathymetric derivatives of an 800-m^2 area. The elevation model is showed in (a), slope in (b), topographic amplitude (TAI) in (c); and topographic variability (TVI) in (d).

Illustration in Figure 5.3d shows the topographic variability index (TVI) with ranges going from 0 to 100 percent. Zero means that the whole neighborhood showed a

minimal of null variability, and one-hundred percent indicates that all cell values in the vicinity presented high variability.

Although bathymetric derivatives provided quantitative measures of the bottom surface characteristics, 3-D modeling using the interactive visualization software Fledermaus (IVS, Fredericton, Canada) helped to visualize and understand the relationships between the original DEM and the derived attributes. Figure 5.4 shows samples of 3-D views with slope and TVI draped over the bathymetric model. Three-dimensional visualization facilitates the association of the surface's attributes presented in Figure 5.3.

a   b
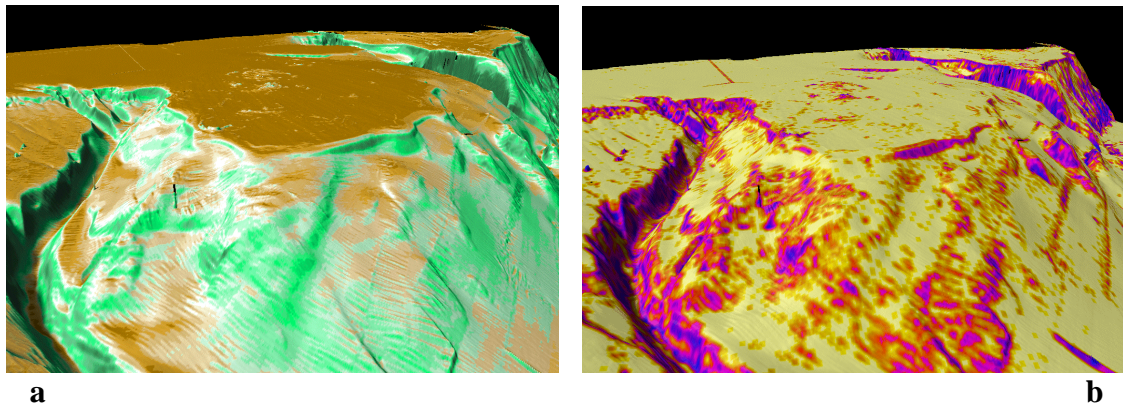
Figure 5.4 Detail showing the 3-D bathymetric model of the central region of Santa Monica Bay with draped derivatives: slope (a) and TVI (b).

The example presented in Figure 5.3 was for a surface gridded at 8-m node spacing. Having base maps created at other resolutions, it is likely to suppose that the same surface gridded at different cell spacing will show features that will appear smoother in the coarser resolution, in other words, a map resolution dependency. Since this speculation has a direct implication in the ability of DEM maps to describe surface

relief, a simple statistical analysis was performed to assess the hypothesis of map resolution dependency.

5.2.1 Map Resolution Analysis for Bathymetric DEM

Bathymetric base maps were gridded at various resolutions because the capability of MBSS to resolve the seafloor relief is mainly a function of depth. Considering this fact, it is assumed that the ability to describe surface attributes would be dependent on the resolution of the bathymetric DEM. However, it is also presupposed that the variability of the terrain model could remain invariant from changes in grid spacing. To test this assumption, analysis of variance (ANOVA) was used for each of the DEM derivatives.

Surface samples of depth, slope, TAI, and TVI were analyzed (separately) at two map resolutions (8 and 16 m cell-size). Five randomly selected surface areas of 320 m^2 were sampled. Values of the entire surfaces were assumed to follow a normal distribution due to the large number of cells. The total variance was broken in two-fold: variance within samples and variance between map resolutions. The ANOVA table appropriate to this problem is shown below:

Source of variation	Sum of Squares	Degrees of freedom	Mean Squares	F Test
Between map resolutions	SS_m	$m-1$	MS_m	MS_m / MS_s
Within samples	SS_s	$N-m$	MS_s	
Total variation	SS_t	$N-1$		

N= number of degrees of freedom in the total data set
m= number of degrees of freedom among map resolutions

The equivalency of map resolutions was formulated with the following hypotheses:

$$H_0: \sigma_1^2 = \sigma_2^2, \text{ against } H_1: \sigma_1^2 \neq \sigma_2^2.$$

The null hypothesis H_0 stated that the seafloor has equal variance for two map resolutions (σ_1^2 and σ_2^2); the alternative hypothesis H_1 stated the opposite. The critical value for F at the 5% level of significance was 1.46 [Davis, 1986 p.70]. Table 5.1 summarizes the results of the ANOVA tests and the acceptability of the H_0.

Table 5.1 Results of ANOVA test for the different bathymetric products, indicating the F test and the acceptability of H_0.

Layer	F test	H_0
Depth	1.0044	Accepted
Slope	1.6184	Failed
TAI	2.8070	Failed
TVI	1.1511	Accepted

The significance of the ANOVA test indicates that thematic layers representing attribute properties based on amplitudes of the terrain showed variance differences at distinct resolutions. As presupposed, the test means that the attributes of slope and TAI derivatives are dependent on the grid spacing. If no special considerations are taken to retain bottom feature details (e.g., shoal biasing, inflection retention), topographic amplitudes (crest and valleys) will be "smoothed" when downsized to a coarser resolution. On the other hand, one can say that there is no statistical evidence to suggest variance differences in depth and TVI attributes at the grid sizes tested. In the case of TVI, this may be explained by the index itself which is calculated from the relative variation of TAI rather than absolute differences. Independent of the amplitude ranges of TAI, the variability is preserved through the percentage calculation. The outcome of the above is that the terrain variability may be used as a surface descriptor unaffected by the map resolution.

5.3 Backscatter Analysis

A general backscatter imagery map for the complete area coverage was created at 16-m pixel-size. The objectives of this investigation were to generate a backscatter imagery map and to generalize the acoustic response for a potential bottom classification analysis, thus the full potential of imagery resolution was not employed. However, the map resolution used was already judged small enough considering the extent of areal coverage and the large depth ranges (down to 800 metres). In any case, the 16-m cell-size depicted very well the variations in backscatter strength represented as grey level tones. In this regard, conversion of backscatter strength to 8-bit grey scale was applied using a standard linear look-up table in terms of dB, where 0 dB =255 and –128 dB =0. The map showing the spatial backscatter variations in Santa Monica Bay is presented in Figure 5.5

5.3.1 General Backscatter Features

From the map presented in Figure 5.5 and Appendix B (Plate B-1), one can easily identify various classes of grey-level tones representing the strength of acoustic returns; lighter tones mean high backscatter and darker tones mean low backscatter. In general, the area of study is dominated by homogeneous low backscatter assumed to represent smooth fine sediments. This continuum is contrasted in the middle region of the bay where the outcrop of the Santa Monica plateau is located. This high backscatter area corresponds to a sedimentary rock element and presumably other coarse sediment types..
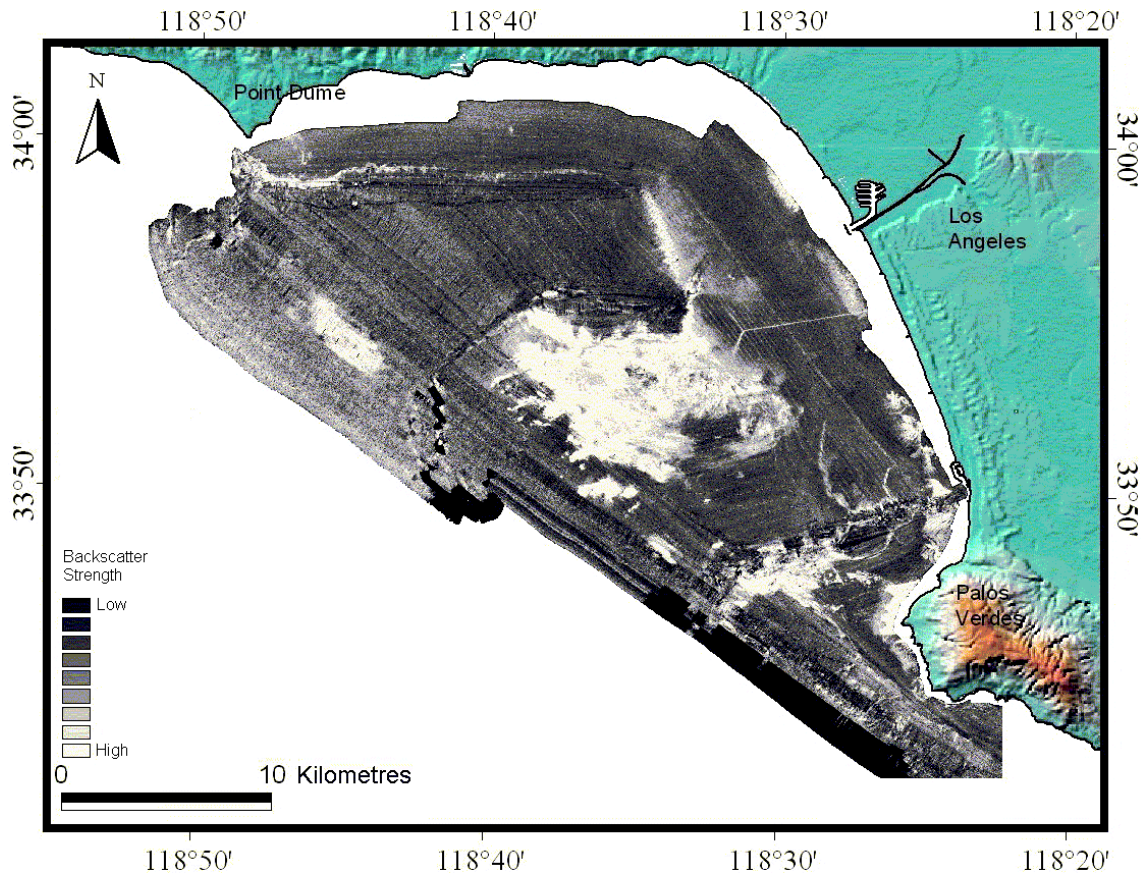
Figure 5.5. Backscatter imagery for Santa Monica Bay. Grey-level is equivalent to backscatter strength (dB); light tone mean high backscatter strength and dark tone means low.

The same lithology can be distinguished to the east and south east of the bay near the Palos Verdes peninsula. Other high backscatter zones are coincident with the edges of abrupt depth changes where consolidated material is exposed. The major sewage outfall pipe of the Los Angeles area is clearly visible within a low backscatter background. Areas of very dark grey-level represent data where the sonar could not resolve valid backscatter measurements due to various causes [Gardner, 1996]. These spurious cell values were removed for further analysis.

67

5.3.2 Texture Analysis

Texture analysis using grey-level co-occurrence matrices (GLCM) and unsupervised classification were calculated using EASI/PACE image processing software on a Windows NT workstation. After assessing the distribution of the pixel values of the backscatter imagery using a histogram, the scale was adjusted to the range of useful data (DN between 155-230). This was a simple way to eliminate the vast majority of bad data mentioned in section 5.3.1.

Texture measures of the image were derived from GLCM computed for a local rectangular window of 5x5 pixels. Measures were calculated for invariant directionality averaging $\theta=\{0°, 45°, 90°, 135°\}$, and distance length 1 (lag). The different texture measures estimated included:

- Mean (MEA)
- Homogeneity (HOM)
- Contrast (CON)
- Dissimilarity (DIS)
- Variance (VAR)
- Entropy (ENT)
- Angular Second Moment (ASM)
- Correlation (COR)
- GLDV Angular Second Moment (G-ASM)
- GLDV Entropy (G-ENT).

Descriptions of these texture measures are included in Appendix B-1.

Principal component analysis (PCA) provided the means to reduce the number of feature vector dimensions and to consolidate the textures with higher component weight.

The results of PCA included in Appendix B-2 showed that two eigenvalues accounted for 98% of the variance (85.18% and 12.87%, respectively); a third component contributed 1.7% of the variance, and the rest of the eigenvalues accounted for only 0.25%. Plots of variable loading showed that the first component is essentially represented by the MEA feature (average grey-level in the local window) with a relative proportion of G-ENT (all elements in the window having similar value). The second component represented the CON measure (large pixel value variation) and a relationship between DIS (similar meaning to CON) and ENT (pixels with relatively equal values).

The PCA helped to reduce the number of the texture measures to be used in unsupervised classification. Considering the contributions of the above texture features, from the 10 original measures only MEA, G-ENT, and CON were used as dimensions in the feature vector space. Using the unsupervised classification algorithm ISODATA, these three texture features were clustered into 5 classes; basically, this classification delineates the boundaries of high backscatter areas from the homogeneous low backscatter background with a couple of classes representing intermediate ranges. A map with backscatter texture classification can be found in Appendix B (Plate B-2).

Physical properties from core data provided by the USGS [Lee et al., 1998] were used for ground-truth comparison. For each core location, the textural class value was extracted and compared against surficial mean grain size. From these observations, frequency histograms were plotted showing the distribution of mean grain size within each class (Figure 5.6). The plots show that textural information barely describes two textural ranges with mean grain size values well separated. However, basic statistics also indicated that the ranges of mean grain size are too spread to really consider a true

association between the composite backscatter image based on principal texture elements, and sediment's grain size.
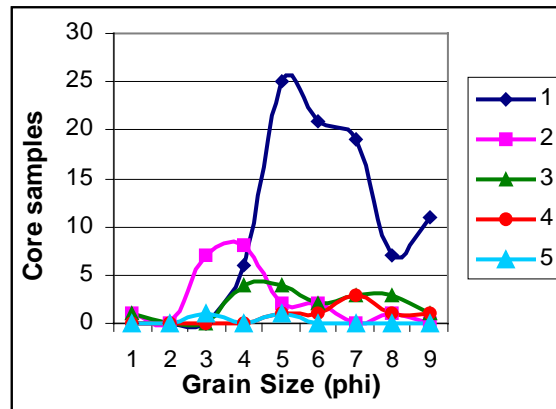
Figure 5.6. Frequency of core samples falling on a given textural class plotted against grain size. Only classes 1 and 2 have significant peaks for grain size but note how spread are the distributions.

Another approach was to compare individual texture features against sediment properties based on the hypothesis that grain size might be related to a particular texture measure rather than a multi-dimensional vector. The textural features MEA, G-ENT, and CON were plotted against grain size; graphics can be seen in Figure 5.7. From the three statistical features, only MEA showed a significant correlation with grain size (r=0.6854), while r for CON and G-ENT were less than 0.01 or close to undefined. The fourth chart (d) in Figure 5.7 is the correlation analysis of mean backscatter strength against grain size. It clearly shows a relationship similar to the MEA texture, indicating that little or no information is revealed from texture analysis other than that already known from mean backscatter strength.
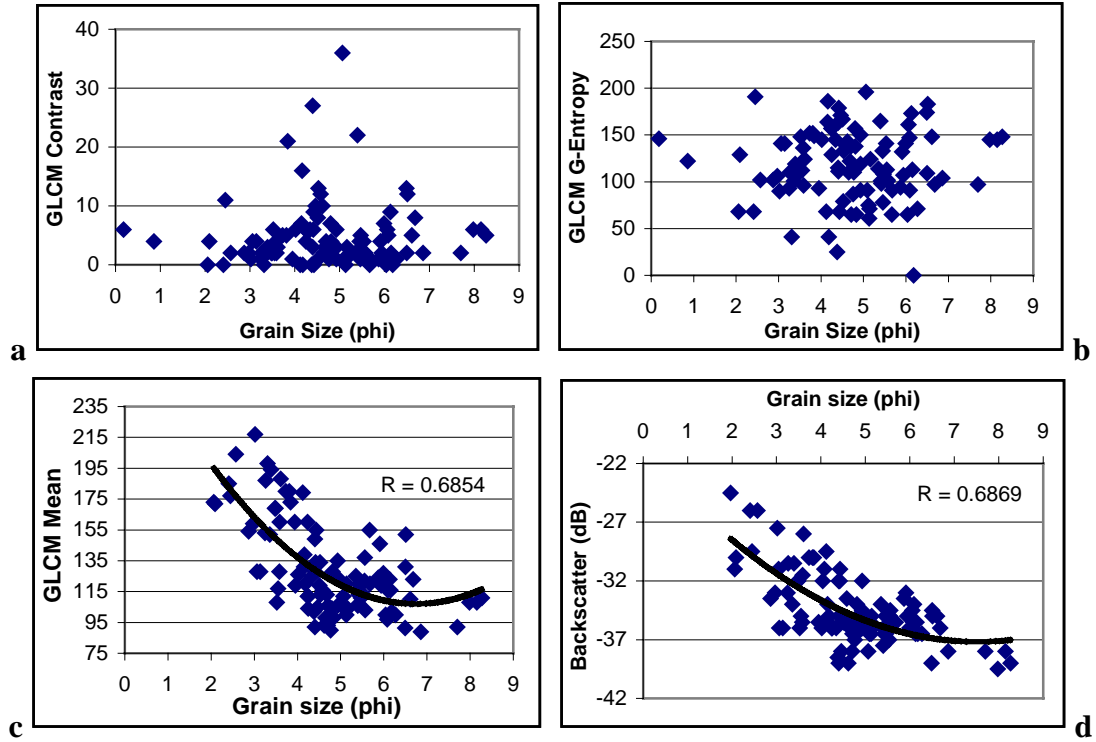
Figure 5.7. Charts of grain size plotted against principal textural features of the backscatter imagery: contrast (a), G-entropy (b) and mean (c). Chart (d) displays a plot of grain size and backscatter strength. Note the similar pattern of (c) and (d).

5.3.3 Angular Response Analysis

The angular response (AR) of backscatter strength was extracted and analyzed as a way to identify the acoustic signatures that could lead to bottom classification. These measurements were accomplished with the AR software tools developed by John Hughes Clarke at the University of New Brunswick specifically for EM-1000 systems[4]. A review of seafloor classification using the AR was presented in section 2.5.2; further details can be found in Hughes Clarke et al. [1997a].

---

[4] In principle, the tools have been applied to EM-1000 data but there is no indication that they could not be used for other Kongsberg-Simrad sonar types.

To obtain an averaged measure of the AR over a small piece of seafloor, stacks of 50 pings were sampled and mean AR curves estimated. Averaging over heterogeneous seafloor types was prevented by the algorithm that rejects those stacks presenting variations in the along-track direction; only stacks with backscatter strength varying in the across-track direction (the AR itself) were retained. AR curves were classified according the backscatter measures for the three main domains (Figure 5.8).
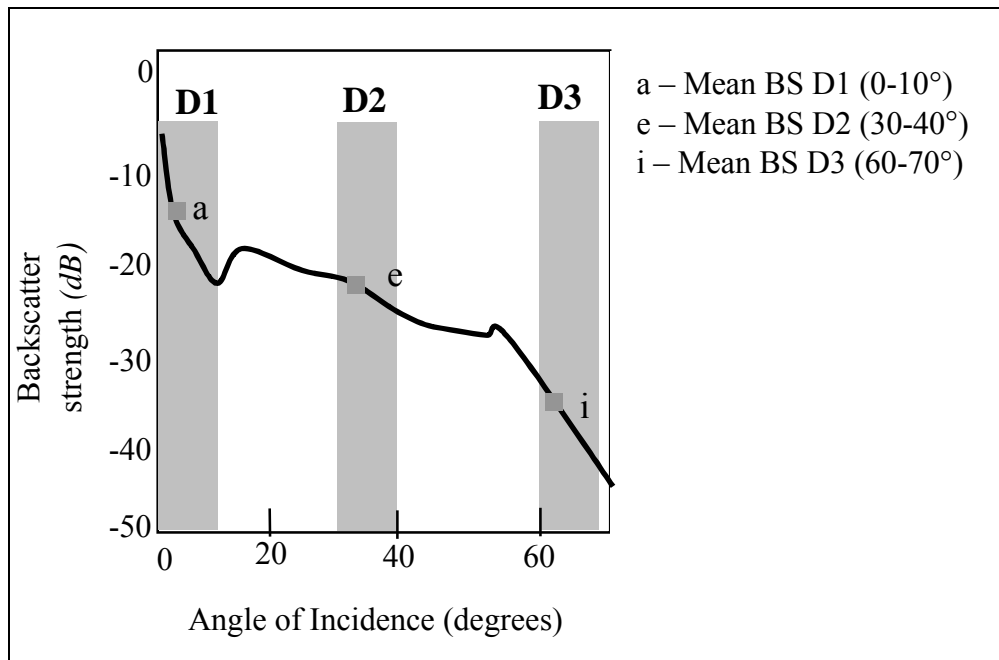
Figure 5.8. Location of backscatter measurements for three domains.

From the twelve available parameters, only three (the domains) were used to characterize bottom types. The idea behind this was that combinations of mean backscatter strength for each domain (a, e, i) would separate distinctive bottom type signatures. For this purpose, a multi-dimensional image was generated gridding each of the domains with the *weigh_grid* program. The average backscatter of custom angle

ranges (domains) was specified narrowing the gridding to only that interval, for instance, D1= 0°-10°, D2= 30°-40°, and D3= 60°-70°. Each gridded domain represented a layer in an image database (Plate B-3, Appendix B). This image was classified using a supervised classification (minimum distance) in EASI/PACE.

An important step in the classification procedure was the definition of signatures for each probable bottom type. To obtain the signatures, core data were used as ground-truth comparing the grain size statistics versus representative AR curves extracted from the geographic vicinities of core locations. The *AR viewer* was used to plot the average of all the AR curves lying within a buffer zone created for selected core locations (Figure 5.9). The general backscatter imagery map was used as background to visually identify regions of changing intensity.

AR curve averages were plotted and mean backscatter strength values for each domain were empirically extracted. A look-up table was created for a discrete number of bottom classes and corresponding domain ranges (Table 5.2). This look-up table was input to a supervised classification algorithm as class signatures. The classification results are presented in Figure 5.10. Class 1 does not have a mean grain size assigned because there was no core data sampling this bottom type; this AR curve was included in the classification because it highlights the highest backscatter signature.
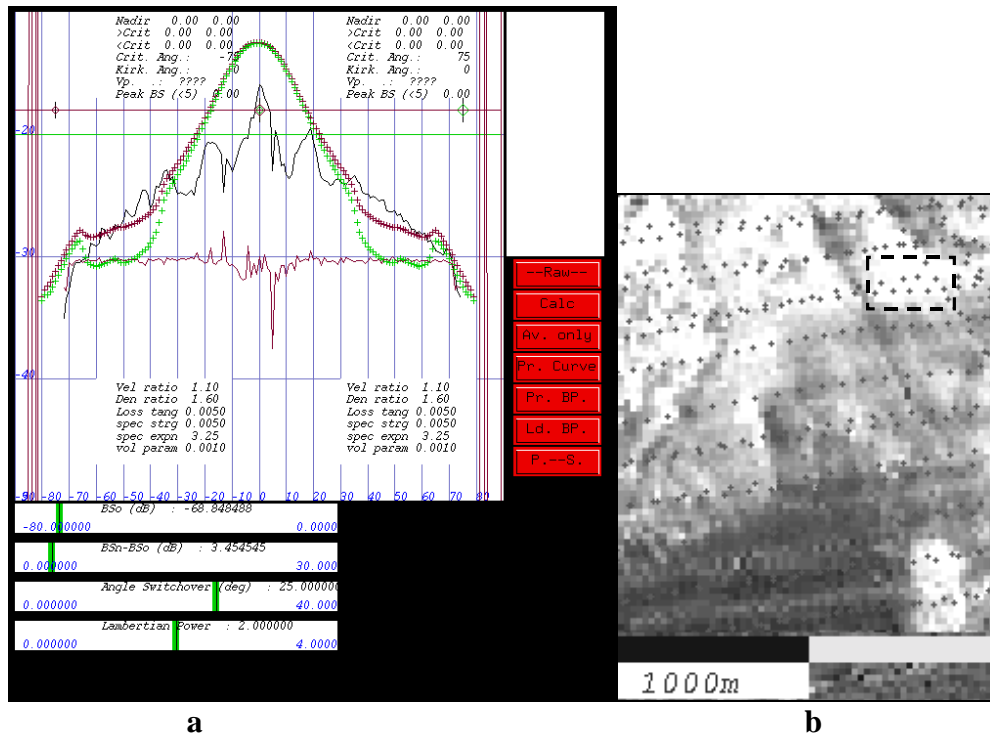
Figure 5.9. AR viewer tool used to plot distinctive AR shapes (a). Box at right shows dots representing the spatial distribution of 50-ping stacks averaged AR over backscatter imagery as background.

Table 5.2. Mean backscatter strength for each domain for each representative AR curve.

AR Curve	Mean Grain Size (phi)	Domain 1	Domain 2	Domain 3
Class 1	n.s.	-13.38	-17.49	---
Class 2	3.00	-18.95	-25.19	-30.97
Class 3	4.58	-19.86	-34.07	-40.17
Class 4	5.67	-23.92	-30.62	-36.30
Class 5	6.49	-32.83	-36.98	-43.16

Domain values in backscatter strength (dB)

74
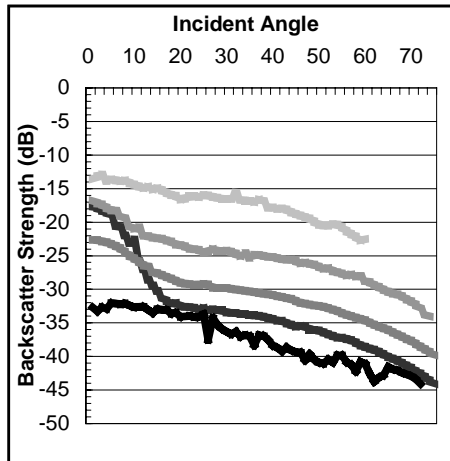
Figure 5.10. Chart showing representative angular response curves extracted (only one port to simplify).

Unfortunately, it was necessary to narrow the backscatter classification to areas above the 200-m isobath. Around this depth the EM-1000 operational mode changed from 150° angular sector (75° per side) to 120° (60° per side). This change in operational mode was required to adjust the data collection when surveying in deeper waters. The result of this adjustment is that no data were collected in deep water (about >200-m) for low grazing angles where the domain 3 is represented. Another factor restricting the utilization of AR analysis was the difficulties in acquiring valid data in the deeper areas [Gardner, 1996]. Nevertheless, it is expected that this coverage reduction should not affect the shelf region where the variation of backscatter classes is representative of various bottom types.

Figure 5.11 presents the results of the supervised classification to backscatter AR classes (also see Plate B-4, Appendix B). At least five classes showed significant association to mean grain size (except class 1). Averaged AR for 50-ping stacks exceeding the boundary detection threshold were rejected. This means that the AR for

seafloor showing a heterogeneous response in the along-track direction was not computed. The gaps produced for this reason were filled with interpolated values. Three backscatter classes were separated from the central high-backscatter area, two of them associated to grain size classes; another two classes were distinguished from the generalized low backscatter.
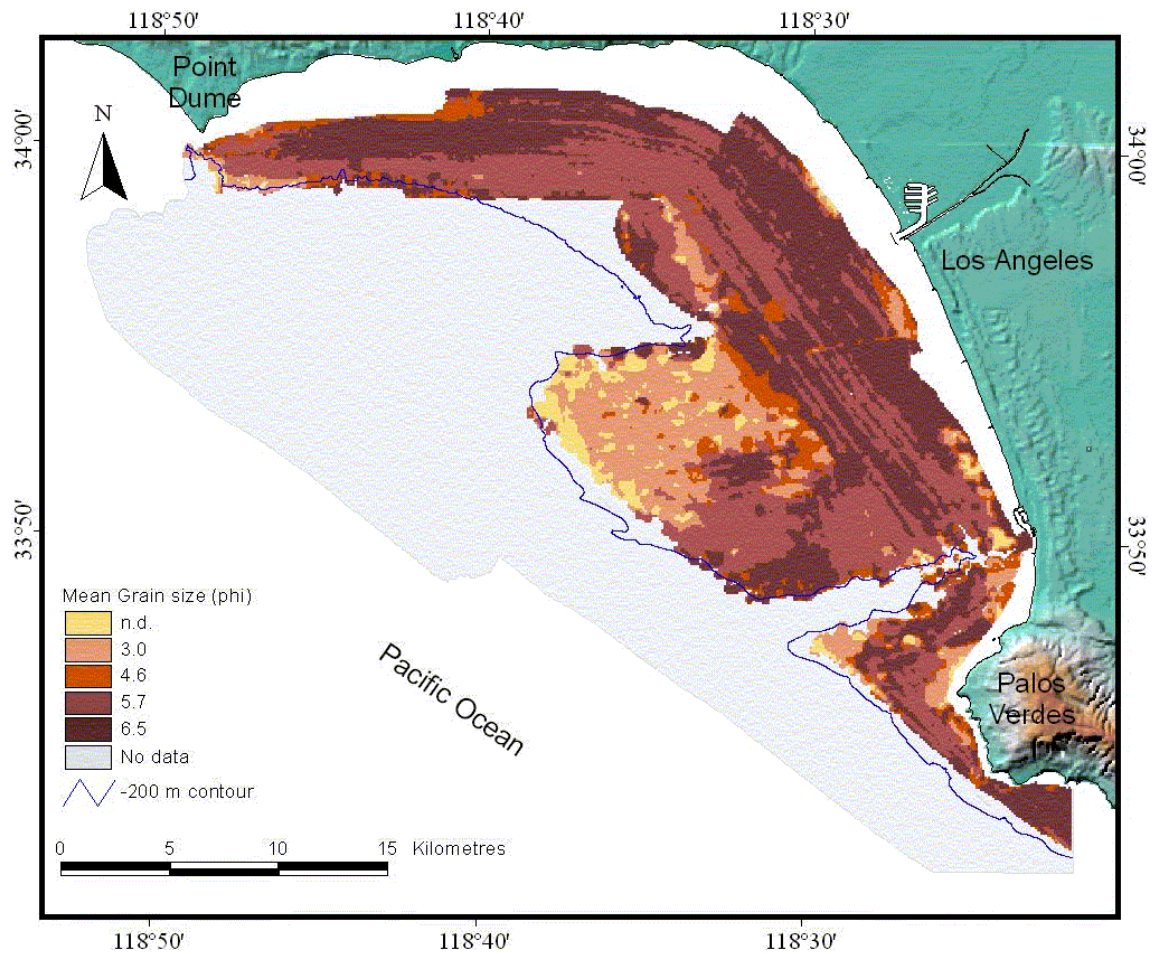
Figure 5.11. Results of backscatter classification using the angular response domains in supervised classification. The area classified was limited to above the 200-m isobath.

5.4 Summary of Results

The creation and analysis of multibeam data maps has resulted in a series of thematic layers whose attributes can be combined in attempts to model environmental conditions that influence the occurrence and distribution of ground fish and other organisms. From the basic multibeam sonar data products —bathymetric DEM and backscatter imagery— other information layers have been derived: percent of slope, topographic amplitude, topographic variability, backscatter textural classes, and backscatter angular response classification.

Some attributes have revealed a map resolution dependency (slope, TAI), while others (depth, TVI) retained their description capability despite different map resolutions. The utility of both groups should be discussed depending on the extent of their application.

In an effort to interpret backscatter imagery as a way to define bottom types, two approaches have been tested and results evaluated. Textural analysis has shown constraints as a refined classification procedure, while AR analysis showed more promising results but also possessed a geographic coverage limitation associated with sonar operational modes. Again, the utility of these results should be debated according to the initial objectives in this research.

The next step in this investigation is the analysis of the discrete entities (layers) created so as to generalize them into useful groups or classes. Attributes may be combined through spatial Boolean operations, simple arithmetical operations, and

statistical analysis. The layers to be used in map modeling will be selected after

discussing their significance in Chapter 6.

Chapter 6

DISCUSSION

This research has addressed an important topic that is common to many of the diverse branches of marine science. The topic is the utilization of acoustic remote sensing techniques and derived data products to support research in several fields (geological, biological, ocean engineering, and so on). The advances in digital data acquisition, processing, and handling are contributing to the use of existing bathymetry and imagery databases to perform specific analyses dealing with seafloor mapping. This fact has challenged the methods and procedures by which we analyze massive data sets, extract valuable information, and communicate the findings through map products (either traditional hard-copy or electronic versions).

In particular, the proposal described herein tried to depict some seafloor physical conditions relevant to benthic habitats with information extracted from multibeam sonar data. Perhaps the immediate question to answer is *What can we "see" with sonar data that may help to study bottom habitats?* The answer can be formulated depending on what one would like to "see". Sonar techniques are being used to study patterns directly related to a biological presence, like benthic activity (bioturbation) [Jumars et al., 1996], and mid-water fish schooling [Mayer et al., 1998; Gerlotto et al., 1999]. Nevertheless, this report has focused on the high-resolution full-bottom coverage capability of multibeam sonar to depict the continuous seafloor surface and classify three main variables: depth, relief, and bottom type. Chapter 3 reviewed why these components may

be important to the distribution of benthic environments, and presented specific processing techniques to map their spatial variability and correlate their magnitude against biological observations. The qualitative approach presented may be useful not only to relate seafloor information to habitat patterns, but —as proposed by Mayer et al. [1997a]— it may help to improve dramatically sampling and planning, to monitor trawling fishing activities, and to refine long-term fishing models through comparisons with archival data.

In this chapter, the significance of the results for each analytical stage are discussed.

6.1 Production of Reliable Mapping Products

During this investigation, base maps from a multibeam survey data set were produced and analyzed with a combination of research and well-proven spatial analysis tools. This assessment required the understanding of several concepts involved in the creation of digital maps such as acoustic ensonification (resolution, coverage) and the gridding and mosaicing of high-density data.

Various works cited in Chapter 3 have applied acoustic remote sensing for the characterization of sea-bottoms, most of them in a qualitative sense. In this research, the effort has focused on analyzing acoustic data in quantitative terms using standard techniques and simplifying the analytical methods. A key process in the success of these goals was the production of digital products from the sonar records.

The availability of suitable software tools to properly process multibeam sonar data is probably the most sensitive part in the production of digital maps. Within the OMG, the development of processing tools has been a major concern because of the special considerations that must be taken for reliable data production. In this regard, the present investigation has been fortunate to cover this part using the OMG's *SwathEd* family of processing tools. Although SwathEd capabilities include data acquisition and editing, the investigation focused on the utilization of modules regarding gridding and mosaicing. From Hughes Clarke [1998b], the most important implementations in these modules can be summarized as follows:

Gridding Module (*weigh_grid*)

- Depth values of regularly-spaced nodes are estimated by the weighted contributions of soundings in a predetermined search radius (w_r).

- Search radius w_r scales with angle of incidence and depth to account for the effect of beam footprint dimensions.

- Inter-swath overlap is controlled by another weighting function w_b, which justifies the effect of growing uncertainty of the soundings as grazing angle decreases.

- Because the weighted solutions are preserved, data can be gridded as data acquisition progresses instead of waiting until the total survey has been completed. Most important, erroneous data can be removed, corrected, and regridded without having to reprocess the complete data set.

<u>Mosaicing module</u>

- Accounts for differences in the across-track and along-track resolutions by averaging the across-track time traces to along-track footprint equivalents.

- Interpolates sets of neighbor pixels to fill inter-ping gaps; rules are implemented to prevent the filling of large areas that have not been ensonified.

- Unlike bathymetric gridding, inter-swath overlap is resolved by applying a priority function. This accounts for backscatter intensity variations as a function of geometry of ensonification.

Users of multibeam data must be aware of the above or similar considerations in order to control and understand the quality of produced digital maps. Presumably, other swath processing software available from research institutions (Lamont-Doherty Earth Observatory [Caress and Chayes, 1998]) or from commercial distributors can provide similar results to those obtained with the OMG tools.

As mentioned in section 4.1.3, bathymetric and imagery base maps were produced from data already edited for blunder removal and artifact compensation. Although the Santa Monica data set was cleaned in near real-time, reprocessing of sonar data could be performed in order to build a more robust confidence in the resulting measurements. In this project, no additional reprocessing was performed and the maps were produced directly from the source's data cleaning standards at the risk of finding unsuspected errors.

The bathymetric DEM showed some clear examples of uncompensated errors in the multibeam data. They were more noticeable after applying spatial analysis procedures

like sun-illumination and filtering, especially because these analyses were designed to resolve small details in amplitude and variability in the DEM (Figure 6.1). The errors are probably due to refraction, uncompensated motion attitude, or both, and are largely accentuated in the outer parts of the swath.

a   b
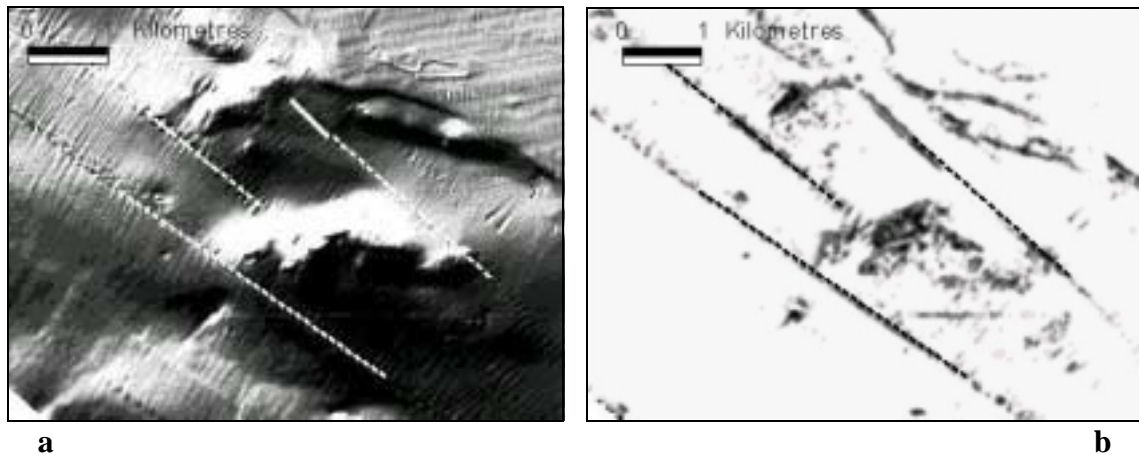
Figure 6.1. Errors in bathymetric swaths were noticeable after spatial analysis. Lines over surfaces show the inter-swath overlap where sounding solutions were noisier. Note that these errors are visible in the DEM sun-illuminated surface (a), and in the TVI surface (dark tones mean high variability) (b).

The ability to differentiate artifacts from real bottom features depends on the knowledge of the survey parameters like the geometry of measurements, line orientation, and problems encountered during acquisition, among others. If the errors cannot be completely eliminated, at least one should try to recognize the imaging geometry in order to avoid loss of true information and generation of false figures [Hughes Clarke, 1998b]. Despite the presence of artifacts in the final map products, they are not suspected of having significant consequences in the attribute quality of DEM-derived maps.

Notwithstanding, errors in the backscatter imagery are more difficult to correct since assumptions and models are applied to backscatter strengths (BS) during acquisition (gains, beam patterns, attenuation model) and sometimes small changes in system parameters remain unnoticed even upon careful post-processing. Figure 6.2 shows an example of the BS problem caused by changes in some of the acquisition parameters (which are not identified).

a   b
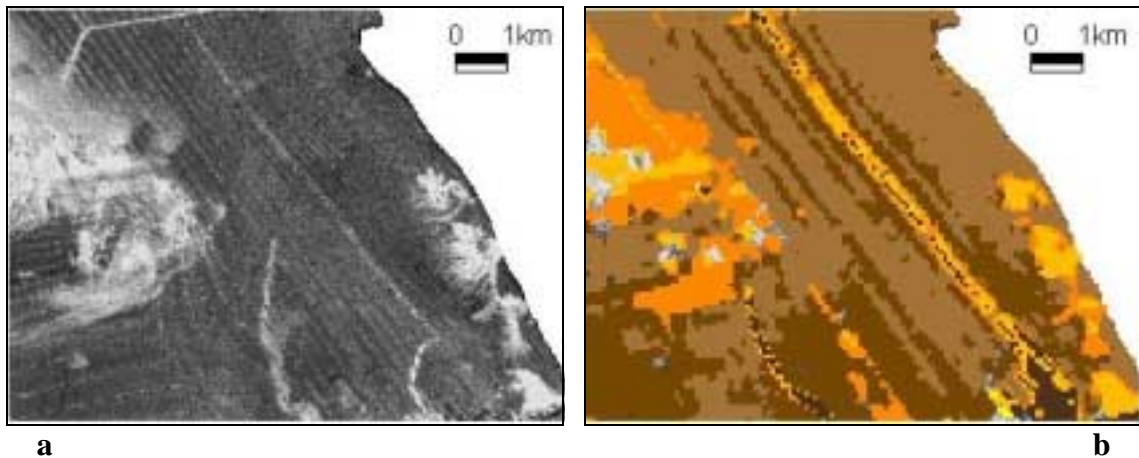
Figure 6.2. Errors in backscatter imagery were noticeable (nadir striping) in the gray-level image (a). However errors caused by changes in acquisition parameters are enhanced when classification routines (AR) are applied (b).

The picture at left shows the backscatter strength of a particular area and some striping effect caused by the difficulties in collecting data at nadir. It also displays a survey line with a slight variation in intensity that is grouped as a totally different bottom type after a classification procedure (AR) has been applied (Figure 6.2b). This also can be seen in Plate B-3 (Appendix B) where the bad striping problem is caused mainly in high incidence angles (domain 3) with components in the near-nadir region (domain 1). Therefore, in the parameterization of AR curves it would be useful to

identify sources of error and take remedial action through the use of filters or other processing techniques.

Because errors in the backscatter imagery are enhanced by classification methods (in particular the AR method), they will have a direct consequence in the reliability of the bottom type estimation. Therefore, in the absence of better ways to compensate for errors in the BS data one should look to methods to generalize the imagery, like noise removal, smoothing, segmentation, edge detect, etc., in order to minimize these undesirable contributions.

6.2 Analysis of DEM Derivatives

Depth estimates have been traditionally measured efficiently and economically with vertical single-beam echosounders. Commercially available seafloor classification systems have been developed based on the data collected with vertical incidence measurements. However, a prohibitively large number of vertical incidence survey lines would be required to roughly match the descriptive capability of swath sonar systems. With MBSS not only depth measurements are made, but the spatial variability of seafloor elevations can be modeled as additional information.

The spatial variability of the bathymetric DEM was used to quantify the topographic roughness or relief as may be related to the distribution of habitats. Carr [1991] observed that vertical relief was a source of non-random distribution of fish species. Similarly, Stein et al. [1992] found that particular bottom types had the most distinct fish

assemblages; some of these bottom types are characterized by their relief variation, such as mud, rocky ridges, and boulders.

A version of the methodology described by Chavez and Gardner [1994] was used to characterize amplitude and variability of seafloor morphology in ecological terms. Basically, two surface indices were developed to describe bottom relief in simple terms at the local scale. This method can be easily implemented in common raster GIS and image processing packages without expensive computations and in a form easy to portray. The only assumptions that affect the objectiveness of the procedure are the definition of the threshold limits to separate the variance of the data. Chavez and Gardner [1994] proposed to select around 15% of the data at both extremes of the normal distribution. In this research, the standard deviation at the point of maximum curvature at both sides of the Gaussian curve (see Figure 4.5) was used as a more appropriate criterion to set the threshold. It was evident that the limits selected this way might vary depending on how homogeneous the surface was. In this case, the relatively featureless surface of the area of study allowed a clear separation between variable and non variable data.

Only the local variability (5x5 pixel window) was investigated, but the method can extract spatial indices at the intermediate and regional scales by enlarging the filter window size. The relevance of regional scale morphology for ecological applications is matter of discussion among specialists.

Although no direct reference was found making a relationship between degree of slope of bathymetric DEM and fish or habitat distribution, slope may provide an

estimate of the bottom stability. Large slopes may be considered unfavorable for well-structured sediment-based habitat because terrain could be subject to instabilities (e.g. slides). However, sloped terrain may offer favorable conditions for upwelling or enhanced turbulence and the consequent distribution of nutrients, which are closely related to the food chain. The study of the upwelling process and primary organic productivity (linked to fisheries) may well benefit from the spatial analysis of high-resolution seafloor surface models.

6.3 Spatial Resolution Issues

The merits of the raster model to produce digital maps results in the availability of a large collection of spatial analysis and filtering tools. This is because the data structure is easy to manipulate and display, and the modeling is simple due to the spatial homogeneity of cells. However, in the case of multibeam data one must deal with the issues of static spatial resolution grids whose cell dimension and interpolation process are dependent on the acquisition geometry. To grid and mosaic the whole Santa Monica Bay survey area at appropriate resolutions a discretional base map design was required. Some basic rules were used to locate the extension of each map box, like mean water depth, surface feature extraction, manageable image size, and so forth. However, this created the inconvenience of managing multiple base maps at different resolutions.

In order to solve the inconvenience of numerous base maps, they were combined in a single general map sheet at the lowest resolution of the original base maps. Using large

grid cells to downsize higher resolution maps may result in the loss of information truly resolved by the sonar. Consequently, all associated DEM derivatives will reflect this fact. To assess the grid resolution degradation and evaluate its implications on the capability to describe seafloor attributes, a simple ANOVA test was performed using data samples from the same seafloor at two typical resolutions. The results indicated that attributes related to amplitudes of the terrain are grid-size dependent and thus unable to describe the same piece of seafloor at different resolutions. Attributes based in DEM amplitude like percent of slope and TAI were useful to describe bottom patterns at a local scale (for a given base map at certain resolution), still they have limitations in depicting large regions, for instance, the complete shelf map was a combination of different grid sizes. On the other hand, attributes representing spatial variability (depth and TVI) showed no statistical differences at the resolution tested.

The significance of these results is that the spatial variability of the bathymetric DEM can be used as attributes independent of map resolution and thus as local and regional parameters to classify the seafloor surface. This is very important from the ecological point of view since most studies dealing with the characterization of bottom environments need to formulate models for regional scales, for example, Heceta Bank (Oregon) [Stein et al., 1992]; Georges Bank (NE Atlantic) [Valentine, 1992]; Stellwagen Bank (Massachusetts) [Baker et al., 1998]; and Monterey Bay, (California) [Green et al., 1995]; just to mention a few.

6.4 Classification of Backscatter

One of the goals defined at the beginning of this investigation was the classification of acoustic backscatter response in terms of the sedimentary and lithologic structure of the sea-bottom. For example, it is more meaningful and tangible to think of the species-habitat relationship between a fish and sediment grain size than acoustic backscatter strength (BS). However, it could be useful to develop a complete study of fish-habitat associations based in BS, since this phenomena is closely related to the sea-bottom structure. Two methods were used for the purpose of classifying the seafloor composition: 1) texture analysis and, 2) angular response analysis.

6.4.1 Texture Analysis

The first approach made use to the textural information contained in a backscatter image without trying to model the bottom response from any theoretical or empirical foundation. The primary idea of using co-occurrence matrices is the segmentation of the imagery into discrete entities based on the contribution of several statistical parameters. These parameters may be thought of as the response of acoustic energy to the statistical roughness of the surface, which should be a function of different seafloor types. The number of feature vector dimensions created with GLCM was reduced through principal component analysis. Three statistical features classified in the unsupervised mode with the ISODATA method resulted in the segmentation of two main distinctive backscatter classes (see Plate B-2). The outcome of the texture analysis was not enough to confidently assign grain size classes to the derived texture classes. Even though the two

distinctive classes were correlated to single mean grain sizes (see Figure 5.6), the accuracy of this estimation was doubtful because of the large standard deviations and considerable overlap between samples.

Reed and Hussong [1989] worked with GLCM for side scan sonar imagery segmentation and obtained moderate results. However, they classified a variety of geologic environments characterized by lithologies with a large range of backscatter strength (e.g. basaltic outcrops and sedimentary deposits). In contrast, Santa Monica Bay is dominated by unconsolidated material, few areas of sedimentary rock outcrops, and presumably no other rock lithologies. From the Plate B-1 included in Appendix B, one can appreciate that the highest BS values range about −19 dB (lighter tones), which according to available generic models at 100 kHz [Applied Physics Laboratory, 1994] corresponds to sandy gravel materials.

The above scenario explains why the textural information from the backscatter imagery was not as useful as on studies in regions with notable differences in seafloor types [Reed and Hussong, 1989]. Apparently, the closeness of backscatter values between sediment types (mainly fine sand, silt and silty muds) makes the GLCM texture backscatter classification difficult to implement. In addition, it is important to remember that the textural information contained in backscatter maps is the result of a transformation process. First, pixels created from time series traces are averaged to an along-track footprint equivalent (section 4.2.2), and second, pixels are transformed from a swath-oriented representation to a rectilinear grid. It is expected that these transformations would affect the textural information of the final backscatter imagery.

6.4.2 Angular Response Analysis

The method of angular response (AR) for seafloor classification resulted in a better discrimination of sediment regions compared to textural analysis. The number of classes defined agreed to some extent with the number of probable bottom types separated with visual interpretative methods. However, these classes might not be completely related to one specific sediment property, e.g. grain size, because the parameterization of curve shapes is based on several sediment properties (density, wave velocity, volume parameter, etc.). The above consideration was tested by plotting mean grain size data from core analysis against the classified AR layer. Correlation coefficients were determined for AR classes against mean grain size (Figure 6.3).

a   b
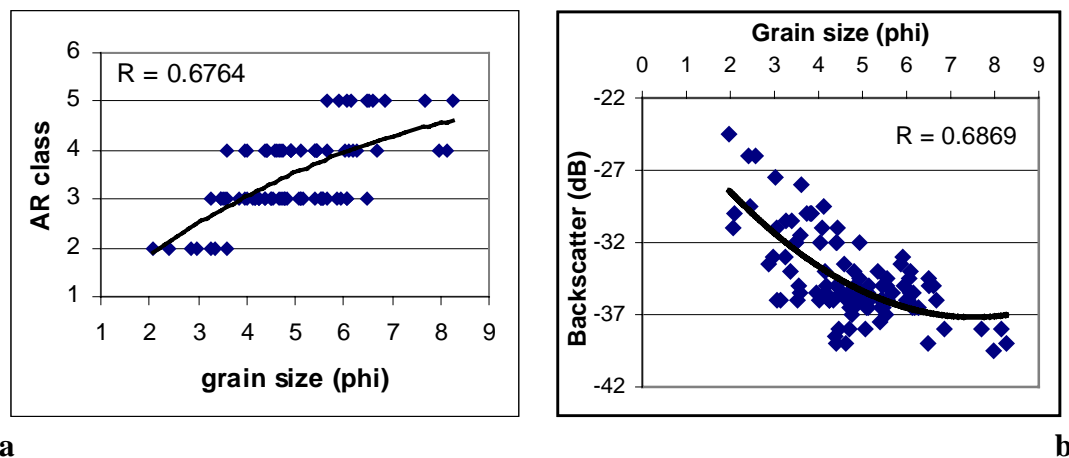
Figure 6.3. Grain size from core samples plotted against AR classes (a) and backscatter strength (b).

The correlation coefficient between grain size and AR classes is moderated (*r*=0.6764) and the relationship is very similar to that found between grain size and backscatter strength (*r*=0.6869) (Figure 6.3). Similar findings are observed by Borgeld et

al. [1999] for an EM-1000 data set collected in northern California, regarding the correlation between backscatter and sediment properties.

A major constraint in the capability of the AR method for seafloor classification is the effect of angular sector reduction in the EM-1000 when changing operating modes from 150° to 120°. This automatically prevents the acquisition of data for low grazing angles. Certainly, the variation of the other 10 or 11 parameters extracted can be used for sediment boundary discrimination, however, no further methodology was reviewed to ascertain this probability. As mentioned by Artilheiro [1998], if the best separation among sediment types occurs for intermediate incidence angles (between 20° and 60°), then the probability of correlating BS to bottom types based on data from such angular sector might be higher. These assumption can be seen in Figure 6.4 where grain size is plotted with BS from different angle intervals. The correlation coefficient for angles of incidence between 30°-40° (dm2) is higher than for angles of incidence between 0°-10° (dm1) and 60°-70° (dm3).
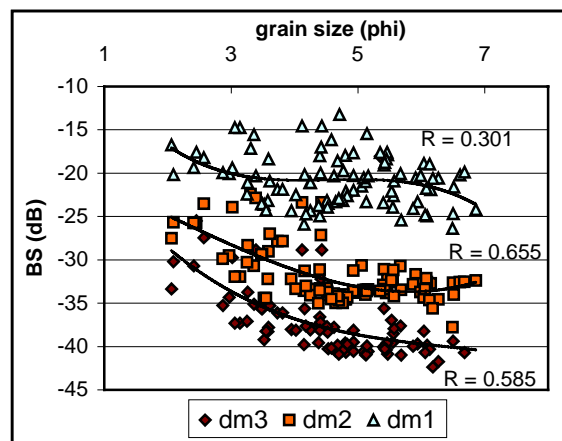
Figure 6.4. Grain size plotted with BS for three angle of incidence intervals (domains).

As discussed in this chapter, confident backscatter classification is a complex task still far from being an automated procedure. Thinking in terms of investigators from several disciplines who may be eager to utilize backscatter imagery for seafloor discrimination, it could be interesting to analyze the mean backscatter strength as a direct variable for environmental scrutiny without implementing further classification models. It would not be like the traditional interpretation of side scan sonar records but a semi-quantitative approach taking advantage of calibrated multibeam sonar measurements, digital map generation, and popular spatial analysis tools.

6.5 Map Modeling

After deriving a series of thematic maps from the analysis of multibeam data, the next issue is how to use these data to provide information to answer questions about the seafloor conditions. There is a wide range of methods available to manipulate spatial data and obtain new information that in most cases is easier to represent and ergo to understand. In the same way that the landscape can be divided into basic entities or *mapping units* to evaluate qualitative land properties [Borrough and McDonnell, 1998], mapped seafloor properties can be reclassified into basic spatial entities and their attributes evaluated in terms of their suitability to identify bottom environments. Here is where ecological modeling should play an important role because it is necessary to

define some rules or physical models to build equivalencies between the existing information layers and the units that can be used for the specific purpose.

The definition of physical models requires the input of a certain degree of knowledge of the desired application. Particularly if we want to know the distribution of a specific ground fish species, it is necessary to have some parameters that will create new mapping units showing the potential distribution of that species. For example, to find appropriate food and shelter, a certain fish species *X* requires a shallow bottom in a reef community structure (Figure 6.5).
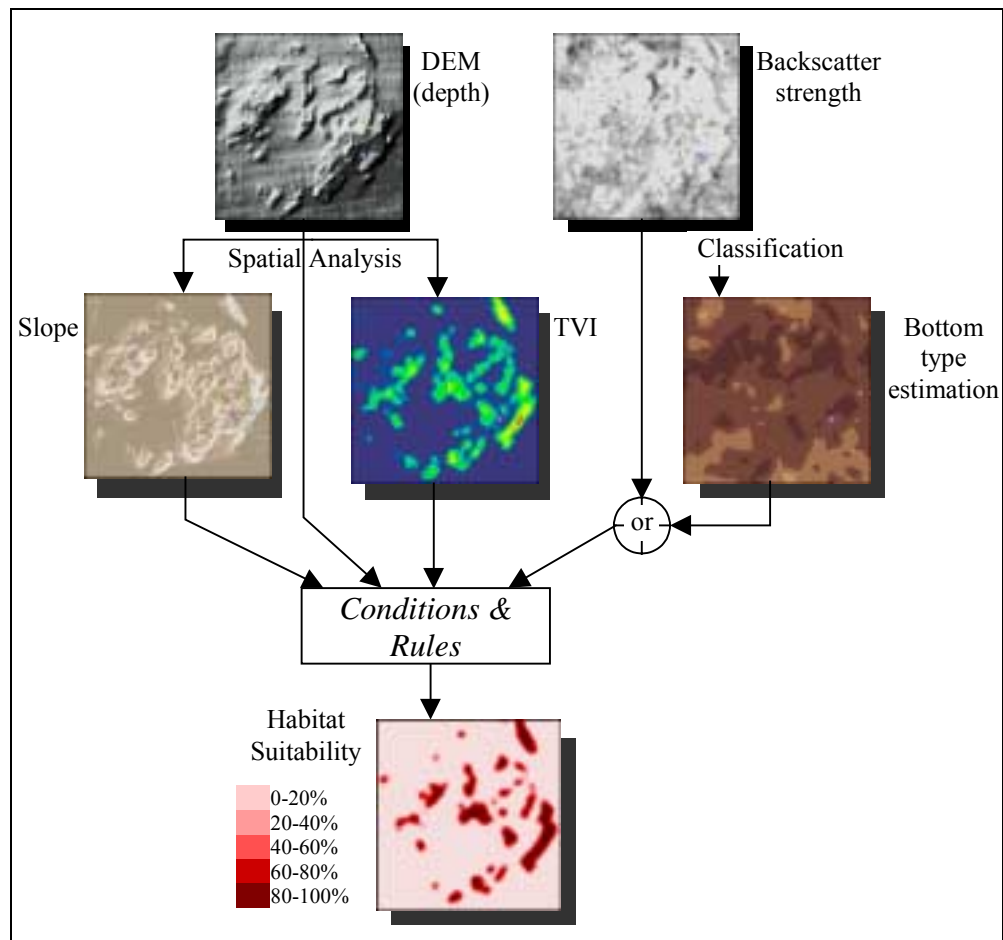
Figure 6.5. Flow diagram for determining the hypothetical suitable bottom habitat for fish species *X* (after Borrough and McDonnell [1998]).

Three bottom surface parameters are the input to model the regions that fulfill these conditions: depth, rough relief identified by high topography variability, and bottom type represented by rock or other consolidated exposed material approximated with mean backscatter strength.

The values of the continuous surfaces must be limited to discrete entities to reduce the number of resulting mapping units. For example, depth can be classified based on vertical zoning criteria; the same can be applied to slope, TAI, TVI, and backscatter classes. Table 6.1 shows the reduction of a continuous seafloor surface into discrete entities.

Table 6.1. Creation of discrete entities or classes from each bathymetric DEM derivative and inclusion of backscatter classification.

Depth range (m)	Depth classes	TVI (%)	TVI classes
<30	Shallow	0-10	Null
30-100	Mid- Shallow	10-40	Low
100-200	Intermediate	40-70	Intermediate
>200	Deep	70-100	High

Slope range (%)	Slope classes	TAI (m)	TAI classes
0-5	Flat	0.0-0.5	Very Low
5-10	Low	0.5-1.5	Low
10-20	Intermediate	1.5-2.5	Intermediate
20-30	Steep	2.5-3.5	High
>30	Very steep	>4.5	Very High

Backscatter Strength	Bottom Type Estim.
Very High	Rock
High	Gravel/Coarse Sand
Intermediate	Medium Sand
Low	Fine Sand/Silt
Very Low	Mud

The seafloor qualities or suitability classes are determined by the habitat conditions of depth, relief (TVI), and bottom type, and ranked with assigned classes. Suitable areas are not merely the result of a Boolean union AND between thematic classes, which may result in sharp and unrealistic boundaries. Seafloor suitability qualities can be assigned from the variance of surrounding neighborhoods as a spatial variability index. Certain areas can be 100% suitable only if attributes from neighbor cells are also 100% suitable, otherwise they will be assigned a value indicating the suitability variation within that neighborhood. In this way suitability classes are created to signify a more realistic scenario.

The modeling of potential habitat identification cannot be complete without the input of other important habitat conditions like salinity, temperature, dissolved oxygen content, marine flora, etc. This requires a comprehensive data compilation and contribution of expertise from fisheries biologists, oceanographers, geographic engineers, hydrographers, marine geologists, and resource managers. Marine habitat modeling has been implemented for the development of suitability indices and benthic characterization in various instances [Coyne and Christensen, 1997; Yoklavich et al., 1997]. These works have used various levels of habitat modeling in which the seafloor structure has been identified as an important set of the environmental parameters used to generate suitability indices and benthic habitats. Undoubtedly, multibeam sonar map products and derivatives would be essential information input to quantitative analyses for seafloor and coastal system modeling. In an effort to develop a partial habitat modeling with multibeam map products, the last part of this report is dedicated to establishing relationships between ground fish observations and map attributes.

Chapter 7

DEVELOPING RELATIONSHIPS WITH BIOLOGICAL OBSERVATIONS

In this chapter, the attributes from maps created with the methodology described in previous chapters are compared against observations of benthic fish. The main goal is an attempt to develop relationships between diverse information layers derived from multibeam data and the biological response. There is no intention to make an exhaustive and definitive study of factors affecting the distribution of organisms and habitats, but rather to identify environmental variables (topography, backscatter strength, bottom type) that may help to populate specific environmental modeling studies with relevant information.

7.1 Source of Biological Data

The biological data used in this report comes from a regional monitoring program planned and implemented by the Southern California Coastal Water Research Project (SCCWRP). The SCCWRP is a joint inter-government agency effort focusing on marine environmental research where the common mission is to gather the scientific information necessary for effective, and cost-efficient, protection of the southern California marine environment [Southern California Coastal Water Research Project, 1998]. To reach this main objective coordinated monitoring projects have been conducted, including a large regional program known as the Southern California Bight

Pilot Project (SCBPP). The SCBPP was implemented in 1994 to "...develop and demonstrate and integrated, coordinated, regional environmental monitoring program based on existing compliance monitoring programs" [Cross and Weisberg, 1995].

The geographic extent of the project included the continental shelf to the 200-metre isobath from Point Conception to the U.S.-Mexico international border with specific and extensive sampling in Santa Monica Bay (Figure 7.1). The SCBPP monitoring framework established a standardized measurement of biological response, contaminant exposure, habitat condition, and human impact over the geographic extent of the project. Data produced by this monitoring program was accessed and retrieved via the Internet. Main factors making these data valuable for the purpose of this report are: 1) the coverage extent of the sampling; 2) the high number of physical and biological parameters measured; and 3) the data set reliability based on the standardized methods and procedures used to analyze the data [Cross and Weisberg, 1995].

7.2 Sampling Data

Sampling stations were distributed in three depth zones: shallow (10-25 m), intermediate (25-100 m), and deep (100-200 m). Parameters measured included benthic invertebrates and ground fish, sediment characteristics (grain size, total organic carbon and nitrogen, trace metals, among others), water quality (dissolved oxygen, temperature, salinity), sediment toxicity, PCB and DDT in fish tissue, and marine debris.
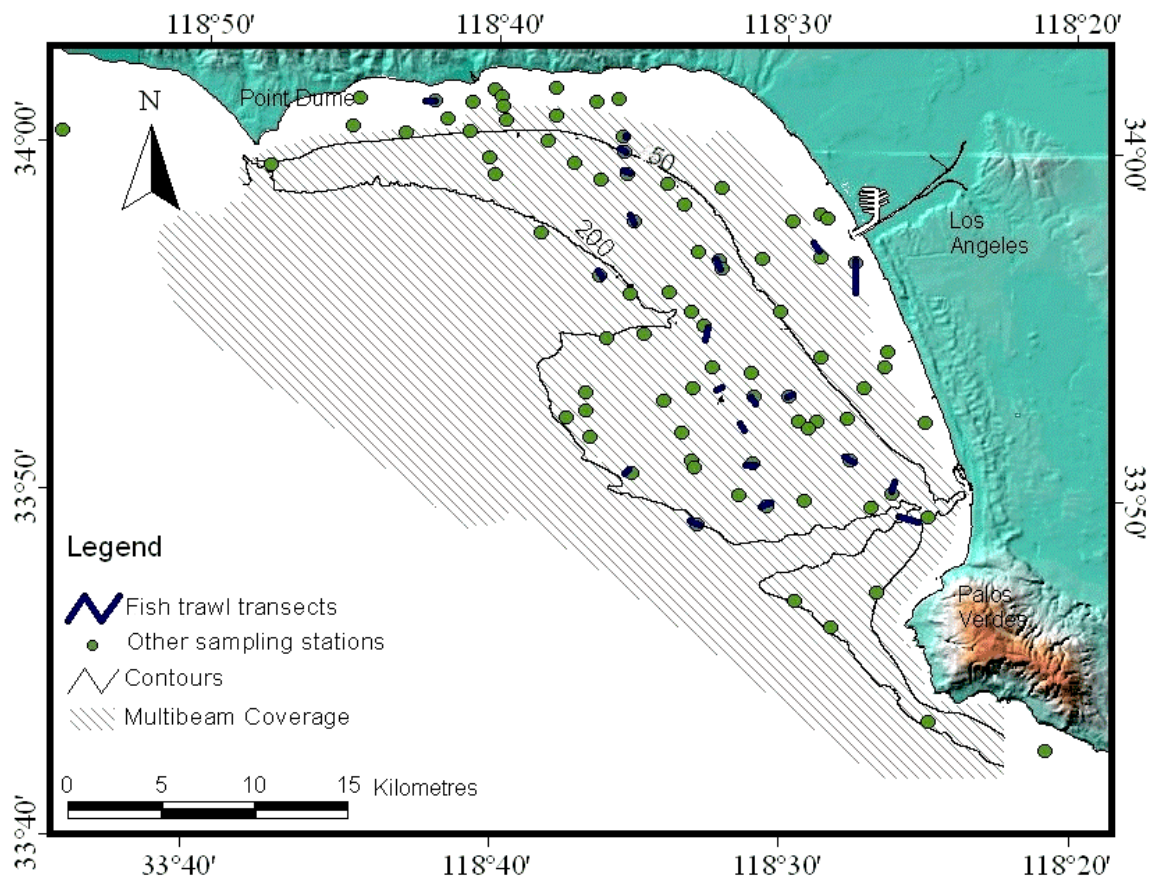
Figure 7.1. The SCBPP sampling stations coverage in Santa Monica Bay.

This report focused on the data collected by trawling catches from which fish abundance, diversity, and biomass were estimated. Further details of the sampling design can be found on-line at the Southern California Coastal Water Research Project web site at http://www.sccwrp.org/tools/methods.htm. Ground fish samples were collected by trawling hauls of regular time duration and vessel speed and transects coordinates at the start and end of trawls were collected with GPS. Organisms collected were identified as to species, individuals were counted, and individuals/species were weighed to the nearest 0.1 kg. In addition, the Shannon-Wiener diversity index was calculated for each station. This index measures the number of species and/or the

99

number of individuals in each species within a sample. It questions how difficult it would be to correctly predict the species of the next individual collected. The higher the index the harder the chances of knowing the next individual's species (higher diversity). Although the study project covered the overall continental shelf extension some problems were associated with the retrieval of acceptable trawl samples, presumably caused by bottom roughness. Consequently, a sample bias towards soft-bottom habitats is expected.

7.3 Data Analysis Procedures

Ground fish data were input in a GIS environment along with the derived multibeam map products. Trawling data were geographically represented as line vectors standing for the haul transects. The following records were included in the attribute table of the added feature layer: abundance (number of individuals), biomass (weight of individuals), number of species, and Shannon-Wiener diversity measures.

Buffer zones of 100 m were generated around each transect line to intersect a discrete extension of each thematic layer separately. Grid cell values from each layer were extracted by overlay operation, averaged, and added to the attribute table (Table C.1, Appendix C). Relationships between fish parameters, depth, TVI, slope, AR classes (bottom type), and backscatter strength were investigated by regression analysis as well as partial correlation to evaluate the relative importance of each seafloor variable [Coleman et al., 1997]. Principal component analysis (PCA) among seafloor attributes was estimated to establish the variables to keep in control during partial correlation analysis.

7.4 Results of the Correlation Analysis

A total of 21 trawling samples were located within the geographic extent of the Santa Monica Bay. From these stations, three were discarded because they contained no data or fell outside the multibeam area coverage. Abundance per trawl ranged from 52 to 383 individuals (mean 183.4); number of species from 5 to 23 (mean 13.3); biomass from 1.0 to 12.1 kg (mean 5.9); diversity H' from 0.7 to 3.7 (mean 2.3); and eveness J' from 0.3 to 0.9 (mean 0.6). The seafloor variables in the areas of sampling had depths from 19.6 to 217.2 metres (mean 97.8); slopes from 0.3 to 10.9 percent (mean 1.7); TVI values from 0 to 42.3 percent (mean 3.2); AR classes included 3, 4, 5, 6 (dominant 4); and BS values from −37.5 to −29.5 dB (mean −34.9).

The PCA identified depth as the seafloor's principal component among the other derivatives. Consequently, depth was used as a control variable in the partial correlation analysis. Each fish variable was compared against seafloor variables where correlation coefficients were estimated at variable confidence levels. The complete correlation matrices are included in Appendix C (Tables C.2 to C.4). From Table C.4 it can be observed that in general, the best correlation coefficients for all comparisons are below $r=0.6$, which could be considered moderately low, however, the significance level for these cases are $p<0.05$. Correlation analysis with $r≈0.5$ and $p<0.05$ are listed in Table 7.1; associations between other variable pairs were very low or undefined and are not presented.

Table 7.1. Significant associations between fish observations and seafloor variables after partial correlation analysis.

Fish parameter	Seafloor variable	Correlation coefficient r	Level of significance p
Abundance	Depth	0.5112	0.03
Number of species	TVI	0.4619	0.05
Biomass	AR classes	0.5592	0.02
Biomass	BS	0.5607	0.02
Diversity H'	BS	0.5531	0.04
Diversity H'	AR classes	0.4815	0.04
Eveness J'	BS	0.5943	0.01
Eveness J'	AR classes	0.4628	0.05

Visualization methods (either 2-D or 3-D) can help in the understanding of these correlations. Figure 7.2 presents 2-D views of the spatial distribution of fish abundance overlaid on the seafloor properties. Three-dimensional representations may offer more spatial reasoning and information extraction because any of the seafloor properties (e.g. backscatter) can be draped over the bathymetric relief (thus adding another dimension to the analysis), and trawling transects and sampling stations can be added to the scene with the appropriate symbology (see Plates D.1 to D.5, Appendix D).

7.5 Summary and Discussion

A wide range of statistical analysis methods can be used to compare fish assemblages among transects and specific associations among fish abundance, individual species, and seafloor characteristics [Carr, 1991; Stein et al., 1992, Perry et al., 1994; Collie et al., 1997]. The approach presented in this work was chosen, considering the objectives of this report, for its simplicity and its fit to the nature of the data.

Depth

Slope

Fish Abundance (num. ind. per trawl)

⊕ 68 - 110   ⊕ 111 - 164   ⊕ 165 - 262   ● 263 - 308   ● 309 - 500

0   5   10   Kilometres

Topographic Variability

Backscatter strength
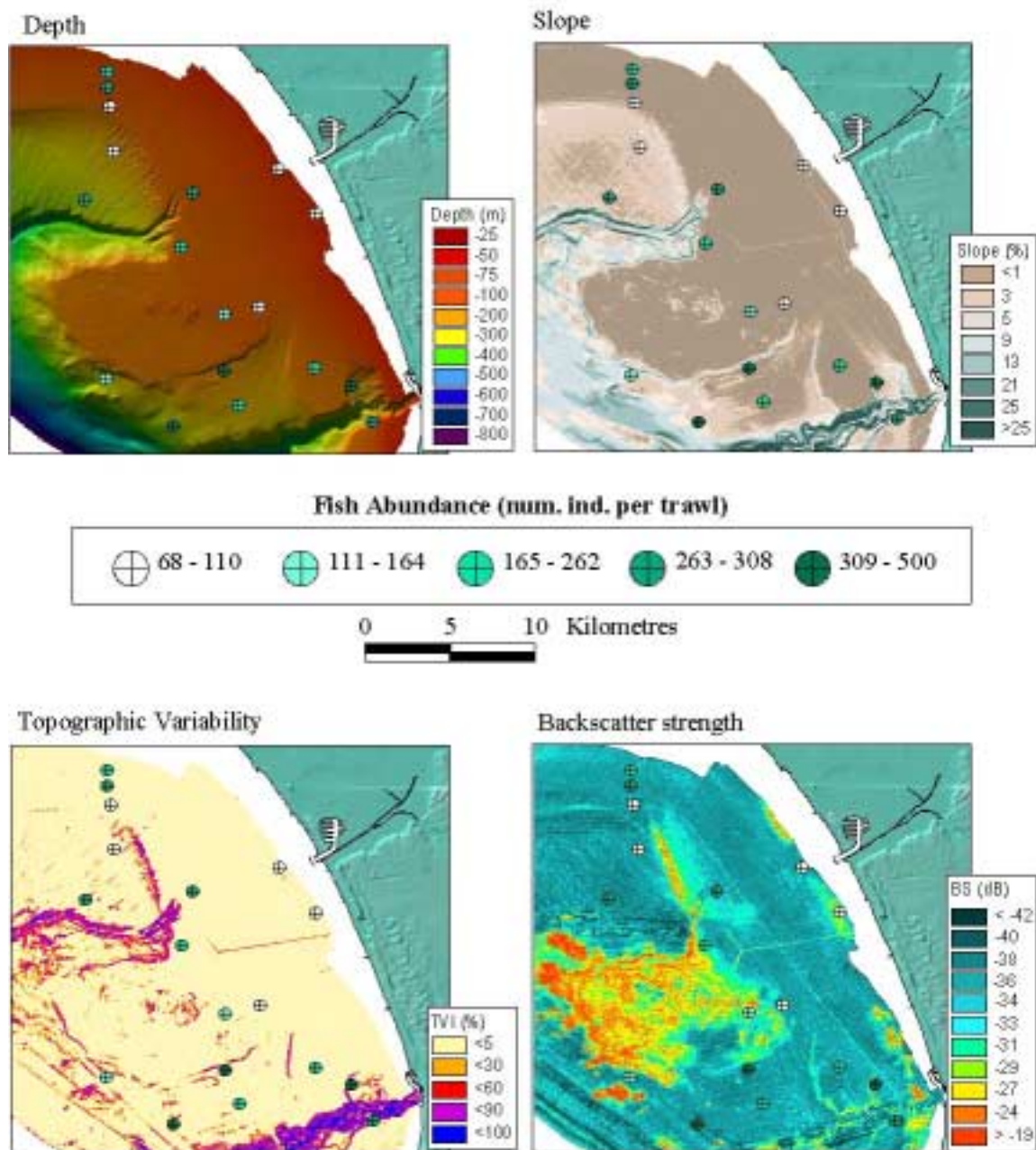
Figure 7.2. Distribution of fish abundance variability and seafloor variables.

The PCA tests were performed on samples of map values from the buffer extraction to find a main variable among the variety (depth, slope, TAI, TVI, BS). The significance of this test is not equivalent to a multivariate analysis of the complete grid images as it was solely used to identify a dominant component within samples.

Grid attribute samples corresponded to the distribution of trawling stations which are biased towards shallow to intermediate depths (0-200 m) and soft-bottoms. Since trawling sampling was designed to collect depth and regional sub-populations in a random fashion from a systematic grid design [Allen and Moore, 1995], it was intended to portrait all the seafloor environments. Despite this consideration, it was observed that sampling capability was limited in areas where rough relief caused problems in the retrieval of an acceptable sample.

From the above, it would be proper to say that benthic sampling would have greatly benefited if multibeam sonar data had been used to design the survey. Sampling methods and apparatus might have been better chosen to increase the rate of sampling success and diminish the risk to equipment damage or loss if the morphology of the seafloor configuration could be integrated in monitoring designs.

Despite the above, fish abundance correlated significantly with depth. The same pattern has been previously observed with the same data set [Allen and Moore, 1995] and for other studies in various regions [Perry et al., 1994; Coleman et al., 1997; Greenstreet, et al., 1997]. Topographic variability presented only a weak correlation with the number of species, although it should be stated that sampling over rather rough relief was affected by problems with retrieving acceptable samples.

Biomass and diversity measures showed a similar relationship with AR classes. Since AR classes were comparable to bottom types based on grain size, the result can confirm a traditional association between fish assemblages and sediment type. Nevertheless, more interesting to see was a similar affinity between fish catch parameters and BS; this could reveal a potential indicator associating BS measures and fish distribution in environmental modeling.

Spatial analysis and statistical methods provided the quantitative information presented in the different thematic maps along with biological and geological data. Nevertheless, to facilitate the interpretation of these rather complex associations 3-D modeling, sun-illumination, and color-coded attributes can offer a natural looking, easily interpretable seafloor [Mayer et al., 1997b]. Terrain derivatives (like slope, TAI and TVI) as well as backscatter products can be draped over the bathymetric DEM; a less common but equally intuitive way to explore the data is the utilization of, for instance, the TVI data as a 3-D landscape with backscatter draped over it (Plate D.5).

Chapter 8

CONCLUSION

This investigation has described a methodology aimed at the application of high-resolution multibeam sonar data for the remote sensing of seafloor variables relevant to the spatial distribution of bottom environments. Emphasis has been on the creation of digital map products capable of retaining the information produced by millions of individual soundings in their interaction with the sea-bottom interface.

A critical topic in the creation of digital models from multibeam data is the understanding of the geometry of the measurements and the ability to determine the acoustic system parameters of particular sonars. Independent of data quality assurance during acquisition, it is necessary to consider those quality issues during post-processing that will affect the reliability of the measurements. The issues referred to can be identified as map resolution, interpolation filters (transformations), and geometry of measurements (depth, angle of incidence, footprint).

Seafloor conditions in terms relevant to benthic habitats were described based on the geomorphology and the geology. Thematic maps for both were generated; geomorphology was described in terms of amplitude and variability of surface features (TAI and TVI, respectively) as well as basic surface derivatives (slope). Attempts to describe the geology were made with the analysis of backscatter strength.

A method to depict geomorphologic amplitudes and variability was developed from the digital image analysis literature as the advantages of the raster model were exploited.

106

The methodology uses principles and tools that no longer pertain to research fields but that are currently commonly used in industry, research, and academic entities.

The same cannot be said regarding geologic depictions using backscatter strength. Of two methodologies used to classify the acoustic scattered response from the seafloor, neither of them showed high confidence levels. AR analysis presented a closer look at bottom type classification when compared to sediment properties, but there were strong sonar operational issues that limited the area coverage capability. The results of bottom type classification were not significantly better than the direct utilization of backscatter strength measures, meaning that mean BS is a good predictor of seafloor type.

Because the map resolution is dependent on the depth of the area surveyed, concerns were addressed regarding the description capability of thematic maps at different resolutions. It was found that attributes based on the amplitude of features showed a map resolution dependency (TAI, slope), while those based on surface variability described the surface independent of the grid size used (TVI).

Synoptic digital maps were created showing the quantitative measures of information derived from the analysis of multibeam data. Visualization methods helped to understand the relationships between the bathymetry and derivatives as well as backscatter. The spatial modeling of attributes from each thematic map can provide information to identify suitable bottom habitats. Emphasis was made regarding the capability to manipulate and generate new information with map modeling tools available in common GIS packages.

Finally, moderate to low relationships were observed between seafloor attributes and fish parameters. Perhaps the major utility of the analysis performed was the potential use of highly descriptive multibeam map products to address the sampling design and improve the methods and sampling devices.

8.1 Recommendations for Future Work

Based on results and discussion regarding sea-bottom classification using backscatter strength, it is recommended to extend the research about the potential associations between calibrated mean backscatter strength and seafloor environments in order to determine habitat attributes which affect population and community dynamics.

In this report, only three AR parameters were explored in an attempt to classify the seafloor in sedimentary terms. Therefore, the natural step would be the extension of these analyses to explore other relationships between AR parameters and measurable seafloor properties.

It would be important to evaluate, from the scientific and managerial points of view, the classification methods and terminology used in the completion of this research, as it has been pointed out that there is a need to unify these issues with respect to research completed by different people and organizations. It is also suggested that standardized techniques and procedures using multibeam sonar specifically designed for planning sampling surveys be developed.

Another useful direction would be to promote the mining and incorporation into GIS environments of the existing data that have been collected, processed, and archived (multibeam, side scan, core data, fisheries data, etc.), and implement database architectures that facilitate accessibility by potential users.

REFERENCES

Allen, M.J. and S.L. Moore (1995). "Spatial variability in southern California demersal fish and invertebrate catch parameters in 1994." SCCWRP Annual Report 94-95. Westminster, Cal. http://www.sccwrp.org/pubs/annrpt/94-95/art-14.htm February 8, 1999.

Applied Physics Laboratory (1994). "High Frequency Ocean Environmental Acoustic Models Handbook." University of Washington. TR 9407-AEAS 9501. IV-22 – IV 25.

Artilheiro, F.M.F. (1998). *Analysis and Procedures of Multibeam Data Cleaning for Bathymetric Charting.* M.Eng. report, Department of Geodesy and Geomatics Engineering Technical Report No. 192, University of New Brunswick, Fredericton, New Brunswick, Canada, 186 pp.

Auster, P.J., R.J. Malatesta, R.W. Langton, L. Watling, P.C. Valentine, C.S. Donaldson, E.W. Langton, A.N. Shepard, I.G. Babb (1996). "The impacts of mobile fishing gear on low topography benthic habitats in the gulf of Maine (northwest Atlantic): Implications for conservation of fish populations." *Review Fish Science,* **4**(2):185-202.

Baker, J.L., T.S. Unger, and P.C. Valentine (1998). "Mapping the sea floor of the Stellwagen National Marine Sanctuary, Massachusetts Bay using GIS." *EOS, Trans*. A.G.U., **79**(45):F460.

Bonsdorff, E., R.J. Diaz, R. Rosenberg, A. Norkko, and G.R. Cutter Jr (1996). "Characterization of soft-bottom benthic habitats of the Åland Island, northern Baltic Sea." *Mar. Ecol. Prog. Ser.,* **142**:235-245.

Borgeld, J.C., J.E. Hughes Clarke, J.A. Goff, L.A. Mayer, and J.A. Curtis (1999). "Acoustic backscatter of the 1995 flood deposit on the Eel shelf." *Marine Geology,* **154**:197-210.

Borrough, P.A. and R.A. McDonnell (1998). *Principles of Geographic Information Systems*. Oxford University Press, New York.

Caress, D.W. and D.N. Chayes (1998). "Mapping the seafloor: Software for the processing and display of swath sonar data." Lamont-Doherty Earth Observatory, Columbia University, Palisades, N.Y. http://www.ldeo.columbia.edu/MB-System/html/mbsystem_home.html. August 18, 1999.

Carr, M.H. (1991). "Habitat selection and recruitment of an assemblage of temperate zone reef fishes." *J. Exp. Mar. Biol. Ecol.*, **146**:113-137.

Chavez, P.S., Jr. and J.V. Gardner (1994). "Extraction of spatial information from remotely sensed image data —an example: GLORIA side scan sonar images." *Canadian Journal of Remote Sensing,* **20**(4):443-453.

Chavez, P.S., Jr. and H.A. Karl (1995). "Detection of barrels and waste disposal sites on the seafloor using spatial variability analysis on side scan sonar and bathymetry images." *Marine Geodesy,* **18**:197-211.

Chivers, R.C., N. Emerson, and D.R. Burns (1990). "New acoustic processing for underway surveying." *The Hydrographic Journal,* (56):9-17.

Coleman, N., A.S.H. Gason, and G.C.B. Poore (1997). "High species richness in the shallow marine waters of south-east Australia." *Mar. Ecol. Prog. Ser.,* **154**:17-26.

Collie, J.S., G.A. Escanero, and P.C. Valentine (1997). "Effects of bottom fishing on the benthic megafauna of Georges Bank." *Mar. Ecol. Prog. Ser.,* **155**:159-172.

Collins, W.T. and R.A. McConnaughey (1998). "Acoustic classification of the sea floor to address essential fish habitat and marine protected area requirements." *Proceedings of the Canadian Hydrographic Conference '98*, Victoria, B.C., 10-12 March, pp. 369-377.

Collins, W.T., R. Gregory, and J. Anderson (1996). "A Digital Approach to Seabed Classification." *Sea Technology* **37**(8):83-87.

Coyne M.S. and J.D. Christensen (1997). "Biogeography program: Habitat suitability index modeling." Technical guidelines, NOAA, NOS, Ocean Resources Conservation and Assessment, Biogeography Characterization Branch, Silver Spring, Maryland.

Cross, J.N. and S.B. Weisberg (1995). "The Southern California Bight Pilot Project: An overview." SCCWRP 1994-95 Annual Report, SCCWRP, Westminster, Cal. http://www.sccwrp.org/ pubs/annrpt/94-95/art-12.htm. February 1999.

Cusson, M. and E. Bourget (1997). "The influence of topographic heterogeneity and spatial scales on the structure of the neighboring intertidal endobenthic macrofaunal community." *Mar. Ecol. Prog. Ser.*, **150**:180-193.

Davies, J., R. Foster-Smith, I. Sotheran, and R. Walton (1998). "Post-processing acoustic ground discrimination data for detailed biological resource mapping." *Proceedings of the Canadian Hydrographic Conference '98,* Victoria, B.C., 10-12 March 10-12, pp. 432-444.

Davis, J.C. (1986). *Statistics and Data Analysis in Geology*. 2nd ed., John Wiley & Sons, Toronto.

de Moustier, C. (1988). "State of the art in swath bathymetry survey systems." *International Hydrographic Review*, **LXV**(2):25-54.

de Moustier, C. (1998a). "Fundamentals of echo-sounding II." 1998 Coastal Multibeam Sonar Training Course, Darmouth, N. S., April 20-24. Lecture Notes #4. Ocean Mapping Group, Department of Geodesy and Geomatics Engineering, University of New Brunswick, Fredericton, N.B.

de Moustier, C. (1998b). "Acoustic seabed interaction theory." 1998 Coastal Multibeam Sonar Training Course, Darmouth, N. S., April 20-24. Lecture Notes #21. Ocean Mapping Group, Department of Geodesy and Geomatics Engineering, University of New Brunswick, Fredericton, N.B.

de Moustier, C. (1998c). "Oblique incidence classification methods." 1998 Coastal Multibeam Sonar Training Course, Darmouth, N. S., April 20-24. Lecture Notes #23. Ocean Mapping Group, Department of Geodesy and Geomatics Engineering, University of New Brunswick, Fredericton, N.B.

de Moustier, C. and D. Alexandrou (1991). "Angular dependence of 12-kHz seafloor acoustic backscatter." *J. Acoust. Soc. Am.,* **90**(1):522-531.

de Moustier, C. and H. Matsumoto (1993). "Seafloor acoustic remote sensing with multibeam echo-sounders and bathymetric side scan sonar systems." *Marine Geophysical Researches*. **15**:27-42

Fader, G., J. Shaw, R. Miller, B. Todd, R. Courtney, and R. Parrott (1998). "Multibeam bathymetry in coastal resource, habitat and hazard assessment." *Proceedings Fifth International Conference on Remote Sensing for Marine and Coastal Environments*, San Diego, Cal. October 5-7. ERIM International, Inc., Ann Harbor, Michigan.

Farr, H.K. (1980). "Multibeam bathymetric sonar: SEA BEAM and HYDRO CHART." *Marine Geodesy*, **4**(2):77-93.

Gardner, J.V. (1996). "Cruise report Coastal Surveyor CS1-96 Santa Monica Shelf. September 25 to October 29, 1996." U.S. Geological Survey Misc. Report, Menlo Park, Cal.

Gardner, J.V. and L. Mayer (1998). "Cruise report RV Ocean Alert Cruise A2-98-SC Mapping the Southern California Continental Margin." USGS Open-File Report 98-475, Menlo Park, Cal.

Gardner, J.V., P. Dartnell, L.A. Mayer, and J.E. Hughes Clarke (1997). "The physiography of the Santa Monica continental margin from multibeam mapping." *EOS Trans.* A.G.U., **78**:F350.

Gardner, J.V., M.E. Field, H. Lee, B.E. Edwards, D.G. Masson, N. Kenyon, and R. Kidd (1991). "Ground-truthing 6.5 kHz side scan sonographs: What are we really imaging?" *Journal of Geophysical Research,* **96**(B4):5955-5974.

Gerlotto, F., M. Soria, and P. Fréon (1999). "From two dimensions to three: The use of multibeam sonar for a new approach in fisheries acoustics." *Can. J. Fish Aquat. Sci.,* **56**(1):6-12.

Greene, H.G., M.M. Yoklavich, D. Sullivan, and G.M. Cailliet (1995). "A geophysical approach to classifying marine benthic habitats: Monterey Bay as a model." Alaska Department of Fish and Game, Commercial Fisheries Management and Development Division, Special Publication No. 9.

Greenstreet, S.P.R., I.D. Tuck, G.N. Grewar, E. Armstrong, D.G. Reid, and P.J. Wright (1997). "An assessment of the acoustic survey technique, RoxAnn, as a means of mapping seabed habitat." *ICES Journal of Marine Science,* **54**(5):939-959.

Grémare, A., J.M. Amoroux, and G. Vétion (1998). "Long-term comparison of macrobenthos within the soft bottoms of the bay of Banylus-sur-mer (northwestern Mediterranean Sea)." *Journal of Sea Research,* **40**:281-302.

Guichard, F. and E. Bourget (1998). "Topographic heterogeneity, hydrodynamics, and benthic community structure: A scale-dependent cascade." *Mar. Ecol. Prog. Ser.*, **171**:59-70.

Hammerstad, E., F. Pøhner, F. Parthiot, and J. Bennett (1991). "Field testing of a new deep water multibeam echo sounder." *Proceedings IEEE Oceans '91 Conference,* Honolulu, Hawaii. **2**:743-749.

Hughes Clarke, J.E., L.A. Mayer and D.E. Wells (1996). "Shallow-water imaging multibeam sonars: A new tool for investigating seafloor processes in the coastal zone and on the continental shelf." *Marine Geophysical Researches,* **18**:607-629.

Hughes Clarke, J.E. (1997). "Are you getting 'full bottom coverage'?" Ocean Mapping Group, Department of Geodesy and Geomatics Engineering, University of New Brunswick. http://www.omg.unb.ca/~jhc/coverage_paper.html. July 7, 1998.

Hughes Clarke, J.E. (1998a). "Multibeam sonar imaging." 1998 Coastal Multibeam Sonar Course, Darmouth, N. S., April 20-24. Lecture Notes #10. Ocean Mapping Group, Department of Geodesy and Geomatics Engineering, University of New Brunswick, Fredericton, N.B., Canada.

Hughes Clarke, J.E. (1998b). "Use and abuse of raster DTM." 1998 Coastal Multibeam Sonar Course, Darmouth, N. S., April 20-24. Lecture Notes #28. Ocean Mapping Group, Department of Geodesy and Geomatics Engineering, University of New Brunswick, Fredericton, N.B., Canada.

Hughes Clarke, J.E. (1998c). "SwathEd software toolkit overview." Ocean Mapping Group, Department of Geodesy and Geomatics Engineering, University of New Brunswick, Fredericton, N.B., Canada. http://www.omg.unb.ca/~jhc/SwatEd.html. March 19, 1999.

Hughes Clarke, J.E., B.W. Danforth and P. Valentine (1997a). "Areal seabed classification using backscatter angular response at 95 kHz." In *High Frequency Acoustics in Shallow Water*, Eds. N.G. Pace, E. Pouliquer, O. Bergen, and A. Lyons. Proceedings of SACLANT Conference, Lerici, Italy, 30 June to 4 July, SACLANT CP-45, 5 pp.

Hughes Clarke, J.E., A. Roy, and C. Reed (1997b). "Bay d'Espoir, aquaculture surveys: Overview and highlights." Ocean Mapping Group, Department of Geodesy and Geomatics Engineering, University of New Brunswick, Fredericton, N.B., Canada. http://www.omg.unb.ca/~jhc/bdespoir/HighLights.html. July 7, 1998.

Jackson, D.R., D.P. Winebrenner, and A. Ishimaru (1986). "Application of the composite roughness model to high-frequency bottom scattering." *J. Acoust. Soc. Amer.,* **79**:1410-1422.

Jumars, P.A., D.R. Jackson, T.F. Gross, and C. Sherwood (1996). "Acoustic remote sensing of benthic activity: A statistical approach." *Limnol. Oceanogr.,* **41**(6):1220-1241.

Lee, H.J., S. Weisberg, S. Bay, C. Alexander, B. Edwards, E. Zeng, and M. Dojiri (1998). "Evaluating Changing Sediment Contamination Conditions, Santa Monica Bay, Cal." *EOS, Trans.* A.G.U., **79**(45):312.

Matsumoto, H., R.P. Dziak, and C.G. Fox (1993). "Estimation of seafloor microtopographic roughness through modeling of acoustic backscatter data recorded by multibeam sonar systems." *J. Acoust. Soc. Amer.,* **94**(5):2776-2787.

Mayer, L., J. E. Hughes Clarke and S. Dijkstra (1997a). "Multibeam sonar: potential applications for fisheries research." In *Changing Oceans and Changing Fisheries: Environmental Data for Fisheries Research and Management,* Eds. G.W. Boehlert and J.D. Schumacher. NOAA Technical Memorandum NOAA-TM-NMFS-SWFSC-239, pp. 79-92.

Mayer, L., J. E. Hughes Clarke and S. Dijkstra (1999). "Multibeam sonar: potential applications for fisheries research." *Journal of Shellfish Research,* **17**(5):1463-1467.

Mayer, L., Y. Li, G. Melvin, and C. Ware (1998). "The application of 3-D visualization technology to pelagic fisheries assessment and research." ICES Conference Meeting 1998/S:2.

Mayer, L., S. Dijkstra, J.E. Hughes Clarke, M. Paton and C. Ware (1997b). "Interactive tools for the exploration and analysis of multibeam and other seafloor data." In *High Frequency Acoustics in Shallow Water*. Eds. N.G. Pace, E. Pouliquer, O. Bergen and A. Lyons. Proceedings of SACLANT Conference, Lerici, Italy, 30 June to 4 July, SACLANT CP-45, pp. 355-362.

McCormick, M.I. (1994). "Comparison of field methods for measuring surface topography and their association with a tropical reef fish assemblage." *Mar. Ecol. Prog. Ser.,* **112**:87-96.

Mills, G.B. and R.B. Perry (1992). "EEZ bathymetric mapping for ocean resource management." *Sea Technology,* **33**(6):27-34.

Mitchell, N.C. and J.E. Hughes Clarke (1994). "Classification of seafloor geology using multibeam sonar data from the Scotian Shelf." *Marine Geology,* (121):143-160.

Mourad, P.D. and D.R. Jackson (1989). "High frequency sonar equation models for bottom backscatter and forward loss." *Proceedings IEEE Oceans '89 Conference,* **4**:1168-1175.

Nishimura, C. E. (1997). "Fundamentals of acoustic backscatter imagery." Naval Research Laboratory, Marine Geoscience Division NRL/FR/7420-97-9848, U.S. Navy, Washington, D.C.

Novarini, J.C. and J. W. Caruthers (1998). "A Simplified approach to backscatter from a rough seafloor with sediment inhomogeneities." *IEEE Journal of Oceanic Engineering*, **23**(3):157-166.

PCI (1997). "TEX - Texture analysis algorithm." EASI/PACE v. 6.2.2 Help, PCI, Richmond Hill, Ontario, Canada.

Perry, R.I., M. Stocker, and J. Fargo (1994). "Environmental effects on the distribution of groundfish in Hecate Strait, British Columbia." *Can. J. Fish. Aquat. Sci.*, **51**:1401-1409.

Poppel, L.J., R.S. Lewis, R. Zajac, D.C. Twichell, and H.J. Knebel (1995). "Sidescan-sonar surveys of critical habitats in Long Island Sound, Connecticut." USGS Woods Hole Field Center. http://woodshole.er.usgs.gov/epubs/abstracts/msg00014.html. May 20, 1998.

Reed IV, T. B. and D. Hussong (1989). "Digital image processing techniques for enhancement and classification of SeaMARC II side scan sonar imagery." *Journal of Geophysical Research,* **94**(B6):7469-7490.

Renard, V. and J.P. Allenou (1979). "SeaBEAM, multi-beam echosounding in "Jean Charcot". Description, evaluation and first results." *International Hydrographic Review,* **LVI**(1):35-67.

Rhoads, D.C., J.A. Muramoto, and R.Ward (1996). "A review of sensors appropriate for efficient assessment of submerged coastal habitats and biological resources." Technical Report EL-96-10, U.S. Army Engineer Waterways Experiment Station, Vicksburg, Massachusetts.

Rukavina, N. (1998). "Experience with a single-beam seabed-classification system in environmental surveys of river and lake sediments." *Proceedings of the Canadian Hydrographic Conference '98,* Victoria, B.C., March 10-12,pp. 446-455.

Scanlon, K.M., C.C. Koening, G.R. Fitzhugh, C.B. Grimes, and F.C. Coleman (1998). "Surficial geology of benthic habitats at the shelf edge, northeastern Gulf of Mexico." *EOS, Trans.* A.G.U., **79**(1):OS3.

Scott, J.S. (1982). "Selection of bottom type by groundfishes of the Scotian shelf." *Can. J. Fish. Aquat. Sci.*, **39**:943-947.

Southern California Coastal Water Research Project (1998). "Southern California Coastal Water Research Project: A public agency for marine environmental research." SCCWRP, Westminster, Cal. http://www.sccwrp.org/. February 1999.

Stein, D.L., B.N. Tissot, M.A. Hixon, and W. Barss (1992). "Fish-habitat associations on a deep reef at the edge of the Oregon continental shelf." *Fishery Bulletin*, **90**(3):540-551.

United States Geological Survey (1998). "Relating geology of benthic habitats to biological resources." Report of a joint USGS and NOAA scientific workshop, May 5-7, Reston, Virginia. U.S. Geological Survey, National Coastal and Marine Geology Program.

Valentine, P. (1992). "Geology and the fishery of Georges Bank." U.S. Geological Survey, Marine and Coastal Geology Program. http://marine.usgs.gov/fact-sheets/georges-bank/title.html. May 27, 1999.

Ware, C., W. Knight, and D. Wells (1991). "Memory intensive statistical algorithms for multibeam bathymetric data." *Computers & Geosciences*, **17**(7):985-993.

Wells, D.E. (1997). "Underwater Acoustics." Hydrographic Surveying I Lecture Notes . Department of Geodesy and Geomatics Engineering, University of New Brunswick, Fredericton, N.B.

Wood, J. (1996). *The Geomorphological Characterisation of Digital Elevation Models*. Ph. D. dissertation. Department of Geography, University of Leicester, Leicester, U.K. http://www.geog.le.ac.uk/jwo/research/dem_char/thesis/. June 3, 1999.

Yoklavich, M.M. (1997). "Applications of side-scan sonar and *in situ* submersible survey techniques to marine fisheries habitat research." *In* Boehlert, G.W. and J.D. Schumacher, (Eds.). *Changing Oceans and Changing Fisheries: Environmental*

Data for Fisheries Research and Management. NOAA Technical Memorandum NOAA-TM-NMFS-SWFSC-239. U.S. Department of Commerce. pp. 140-141.

Yoklavich, M.M., G.M. Cailliet, H.G. Greene, and D. Sullivan (1995). "Interpretation of side-scan sonar records from rockfish habitat analysis: Examples from Monterey Bay." Alaska Department of Fish and Game, Commercial Fisheries Management and Development Division, Special Publication No. 9.

Yoklavich, M., R. Starr, J. Steger, H.G. Greene, F. Schwing, and C. Malzone (1997). "Mapping benthic habitats and ocean currents in the vicinity of central California's Big Creek ecological reserve." NOAA Technical Memorandum NOAA-TM-NMFS-SWFSC-245, U.S. Department of Commerce. 52 pp.

APPENDIX A

General bathymetric map and derivatives from multibeam sonar data for Santa Monica Bay.

Plate A-1   Color-coded 2-D relief bathymetric DEM

Plate A-2   Slope of bathymetric DEM

Plate A-3   Topographic amplitudes of bathymetric DEM

Plate A-4   Topographic variability of bathymetric DEM

All maps projected in UTM zone 11, unit metres, and Datum NAD 83.

APPENDIX B

General backscatter strength map for Santa Monica Bay and maps resulting from texture and AR analyses.

APPENDIX B-1

The following are brief explanations of the grey level co-occurrence matrices (GLCM) texture features available in EASI/PACE v. 6.2.2 [PCI, 1997].

Angular Second Moment. It is high when the GLCM has few entries of large magnitude; low when all entries are almost equal. This is a measure of local homogeneity.

Contrast. It is a measure of the amount of local variation in the image. It is high when the local region has a high contrast in the grey level scale.

Correlation. Measures the linear dependency of grey levels of neighboring pixels. When the scale of the local texture is much larger than the distance of the grey scale, correlation is typically high. When the local texture has a scale similar to or smaller than the grey scale, there will be low correlation between pairs of pixels.

Dissimilarity. Similar to contrast. High when the local region has a high contrast.

Entropy. This is the opposite of angular second moment. It is high when the elements of GLCM have relatively equal values. Low when the elements are close to either 0 or 1 (i.e. when the image is uniform in the window).

GLDV§ Angular Second Moment. High when some elements are large and the remaining ones are small. Similar to angular second moment, it measures the local homogeneity.

GLDV§ Contrast. It is mathematically equivalent to the contrast measure. It is left here for compatibility reasons.

GLDV[§] Entropy. High when all elements have similar values. This is the opposite of GLDV angular second moment.

GLDV[§] Mean. It is mathematically equivalent to the dissimilarity measure above. It is left here for compatibility reasons.

Homogeneity. This is the opposite of contrast. It is high when GLCM concentrates along the diagonal. This occurs when the image is locally homogeneous in the scale of the grey level range.

Mean. Average grey level in the local window.

Variance. Grey level variance in the local window. High when there is a large grey level variation in the local region.

[§]Gray level difference vector (GLDV) is derived from the GLCM by adding the matrix elements in lines parallel to the main diagonal. It counts the occurrence of reference neighbor pixel absolute differences. Element 0 of the GLDV is the number of times the difference is 0 (e.g., the neighbor pixel value equals the reference pixel value). Element 1 is the number of times the absolute difference is 1 (e.g., the reference minus neighbor pixel value is −1 or +1), and so forth.

APPENDIX B-2

Principal component analysis of textural measures derived from GLCM.

Table B.1. Basic statistics of input channels

Channel	Feature	Mean	Dev.
3	HOM	0.9052	0.1127
4	CON	0.6904	1.6956
5	DIS	0.2597	0.3638
6	VAR	0.4624	0.6237
7	ENT	0.7532	0.841
8	ASM	1.3432	0.7072
9	COR	0.1939	0.2293
10	G-ASM	0.7866	0.2326
11	G-ENT	0.3783	0.424
16	MEA	3.9182	4.2068

Table B.2. Covariance matrix for input channel

	3	4	5	6	7	8	9	10	11	16
3	0.013									
4	-0.118	2.875								
5	-0.038	0.527	0.132							
6	-0.062	0.897	0.218	0.389						
7	-0.091	0.740	0.260	0.440	0.707					
8	0.075	-0.572	-0.208	-0.360	-0.587	0.500				
9	-0.018	0.131	0.048	0.100	0.155	-0.139	0.053			
10	0.026	-0.202	-0.072	-0.119	-0.193	0.162	-0.041	0.054		
11	-0.047	0.405	0.137	0.226	0.352	-0.290	0.072	-0.098	0.180	
16	-0.345	2.126	0.901	1.603	2.791	-2.452	0.731	-0.794	1.394	17.698

Table B.3. Percentage of total variance contributed by each eigenchannel

Eigen-channel	Eigen-value	Dev.	%Var.
1	19.2513	4.3876	85.18%
2	2.9097	1.7058	12.87%
3	0.3848	0.6203	1.70%
4	0.0294	0.1716	0.13%
5	0.0173	0.1314	0.08%
6	0.0043	0.0657	0.02%
7	0.0021	0.0457	0.01%
8	0.0015	0.0393	0.01%
9	0.0002	0.0136	0.00%
10	0	0.0062	0.00%

Table B.4. Eigenvectors of covariance matrix (arranged by rows)

|	1	2	3	4	5	6	7	8	9	10
3	0.020	-0.146	-0.055	-0.097	-0.159	0.139	-0.041	0.045	-0.080	-0.955
4	-0.027	0.913	0.147	0.246	0.138	-0.091	0.012	-0.036	0.081	-0.219
5	0.076	0.308	-0.135	-0.200	-0.643	0.511	-0.117	0.162	-0.294	0.201
6	0.096	-0.093	-0.172	0.624	-0.217	-0.100	0.631	0.153	-0.291	-0.011
7	0.119	0.196	-0.413	-0.628	0.092	-0.427	0.370	0.025	-0.232	-0.013
8	0.137	0.029	-0.294	-0.003	0.633	0.637	0.166	0.243	-0.001	0.007
9	-0.084	0.010	0.270	-0.251	-0.206	0.253	0.617	-0.176	0.582	-0.006
10	-0.200	-0.033	0.711	-0.204	0.185	0.053	0.191	0.223	-0.538	0.005
11	-0.360	0.008	-0.153	0.043	0.088	0.211	0.073	-0.816	-0.348	-0.001
16	-0.880	0.020	-0.262	0.008	-0.034	-0.041	0.001	0.374	0.116	0.000
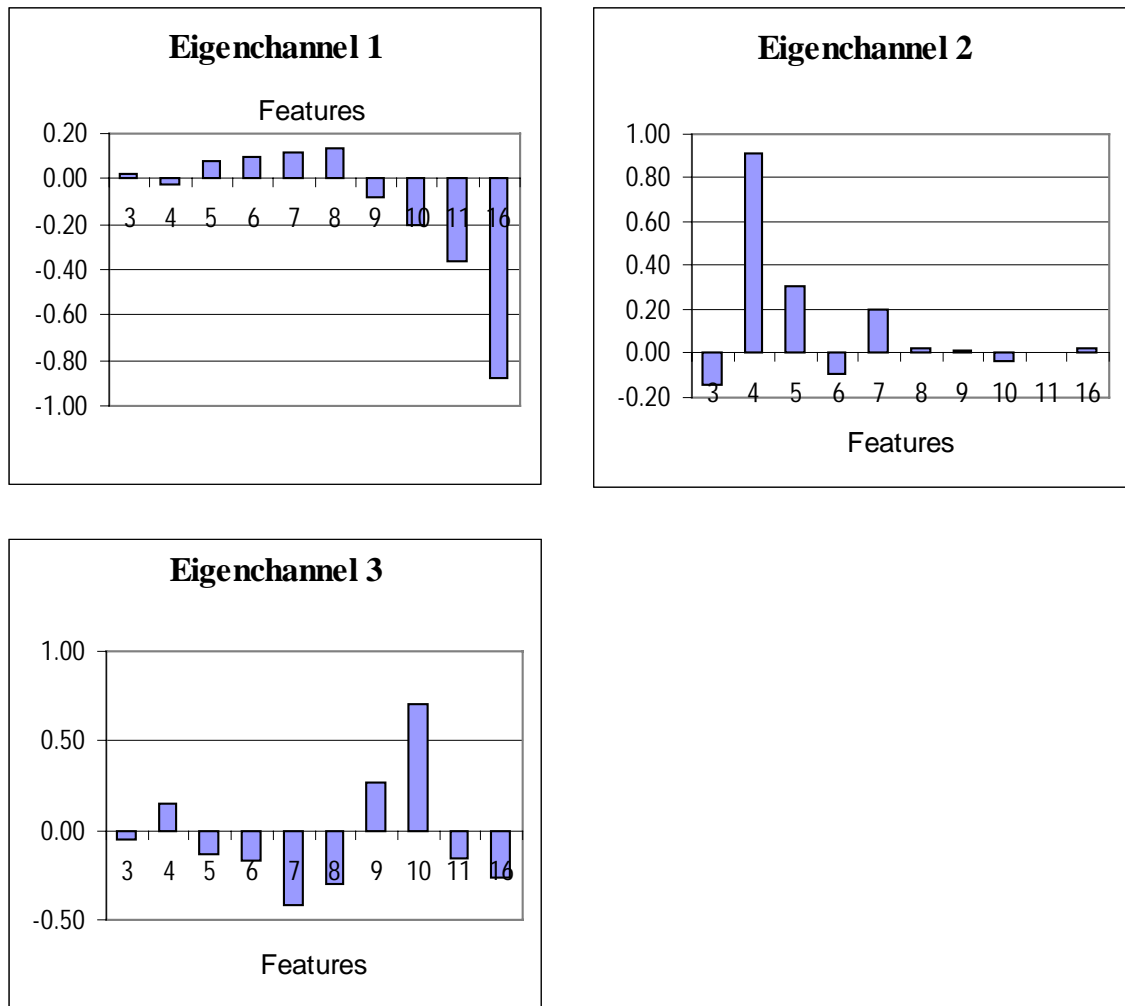
Figure B.1. Plots of principal component loading for the three first components.

Correlation analysis results among fish catch parameters and map attributes from multibeam data products.

Appendix C-1. Relation of fish parameters and map attributes

Appendix C-2. Partial correlation analysis results

Table C.1. Relation of fish catch parameters from SCBPP data and map attributes
from derived multibeam sonar data for Santa Monica Bay.

Fish _Abun	Fish_ NoSp	Fish_ Biom	Trawl_ Range	H'[a]	H'max[a]	N[a]	J'[a]	Eveness[a]	Depth	TVI	Slope	AR_ class	BS
195	13	7.9	555.6	2.42	3.70	5.35	0.65	0.41	-44.1	0.0	0.5	3	-35.5
231	14	4.2	463.0	2.30	3.81	4.92	0.60	0.35	-49.6	0.0	0.5	4	-35.5
84	14	2.0	463.0	2.11	3.81	4.31	0.55	0.31	-59.6	0.0	1.0	4	-37.0
73	11	1.4	493.9	2.56	3.46	5.89	0.74	0.54	-123.9	0.0	1.8	4	-36.0
76	5	3.4	493.9	1.15	2.32	2.22	0.50	0.44	-22.9	1.2	1.7	3	-36.0
55	6	10.4	463.0	2.27	2.58	4.82	0.88	0.80	-19.6	0.0	0.4	2	-31.5
218	16	5.4	463.0	2.82	4.00	6.97	0.70	0.44	-55.8	0.0	0.5	3	-34.5
236	6	4.0	555.6	0.73	2.58	1.66	0.28	0.28	-217.2	0.4	0.5	4	-37.5
201	15	9.1	493.9	2.81	3.91	7.02	0.72	0.47	-67.0	0.0	0.5	2	-30.5
52	14	1.0	463.0	2.90	3.81	7.46	0.76	0.57	-59.3	0.0	0.4	3	-36.5
126	21	5.6	524.7	3.70	4.39	12.97	0.84	0.62	-58.5	0.0	0.3	2	-29.5
166	14	3.2	555.6	2.28	3.81	4.85	0.60	0.35	-75.6	0.0	3.1	4	-35.5
323	13	5.6	524.7	1.32	3.70	2.50	0.38	0.19	-100.6	0.0	3.4	4	-35.0
96	7	3.6	463.0	2.01	2.81	4.04	0.72	0.58	-165.7	5.5	1.2	5	-36.0
358	17	10.6	586.5	2.03	4.09	4.08	0.50	0.24	-130.5	8.9	0.6	3	-35.0
193	16	12.1	555.6	2.93	4.00	7.64	0.73	0.48	-133.2	0.0	0.5	3	-34.5
235	23	4.2	555.6	2.45	4.52	5.48	0.54	0.24	-168.1	42.3	2.3	3	-37.0
383	16	12.0	555.6	2.38	4.00	5.20	0.59	0.32	-209.5	0.0	10.9	4	-36.0

[a]Shannon-Wiener diversity measures

APPENDIX C-2

Partial correlation analysis of fish catch parameters and seafloor properties.

Table C.2. Basic statistics for data in Table C.1

Variable	Mean	Standard Dev.	Cases
MEAN_DEP	-97.8167	61.3193	18
AR CLASSES	4.3333	0.8402	18
BS	-34.9444	2.2287	18
TVI	3.2389	10.0338	18
FISHABUN	183.3889	102.2782	18
FISHNOSP	13.3889	4.9365	18
FISHBIOM	5.8722	3.6001	18
H' diversity	2.2864	0.6972	18
J' evenness	0.6261	0.1561	18

Table C.3. Zero order partials for MEAN_DEPTH

FISHABUN	FISHNOSP	FISHBIOM	H' diversity	J' evenness
-0.5112	-0.0927	-0.1533	0.2679	0.4250
p=0.030	p=0.714	p=0.544	p=0.282	p=0.079

Degrees of freedom= 16; p= 2-tailed level of confidence.

Table C.4. Partial correlation coefficients controlling for MEAN_DEPTH

	AR CLASSES	BS	TVI
FISHABUN	-0.1520	0.1463	0.0059
	p=0.560	p=0.575	p=0.982
FISHNOSP	-0.3872	0.2657	0.4619
	p=0.125	p=0.303	p=0.052
FISHBIOM	-0.5592	0.5607	-0.1355
	p=0.020	p=0.019	p=0.604
H' diversity	-0.4815	0.5531	0.1141
	p=0.043	p= 0.039	p= 0.663
J' evenness	-0.4628	0.5943	-0.0262
	p=0.050	p=0.010	p=0.921

Degrees of freedom= 15; p= 2-tailed level of confidence.

APPENDIX D

The plates in this appendix are 3-D views from the Santa Monica Bay's continental shelf (about -200 m). The images show color-coded attributes of terrain derivatives or backscatter draped over the bathymetric DEM. Also, a fish parameter (e.g. abundance) from sampling stations is overlaid on top of the surface. Stations are represented as circles of 300 m radius and the color saturation (either warm or cool tones for better contrast) indicate number of individuals.

Plate D-1. Color-coded bathymetry

Plate D-2. Topographic variability index draped over bathymetry

Plate D-3. Slope draped over bathymetry

Plate D-4. Backscatter strength draped over bathymetry

Plate D-5. Backscatter strength draped over topographic variability DEM
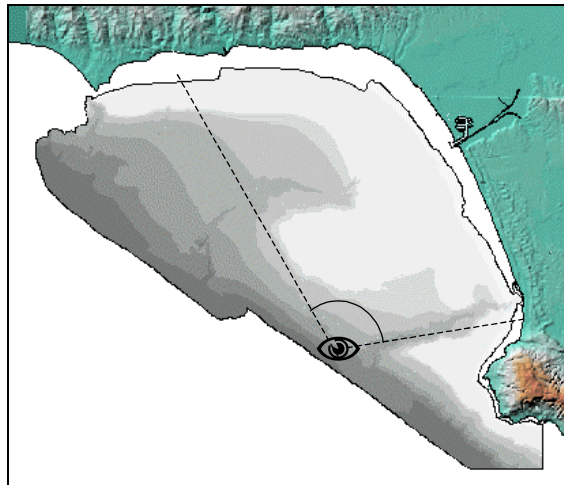
Figure D.1. Perspective of plates' view.

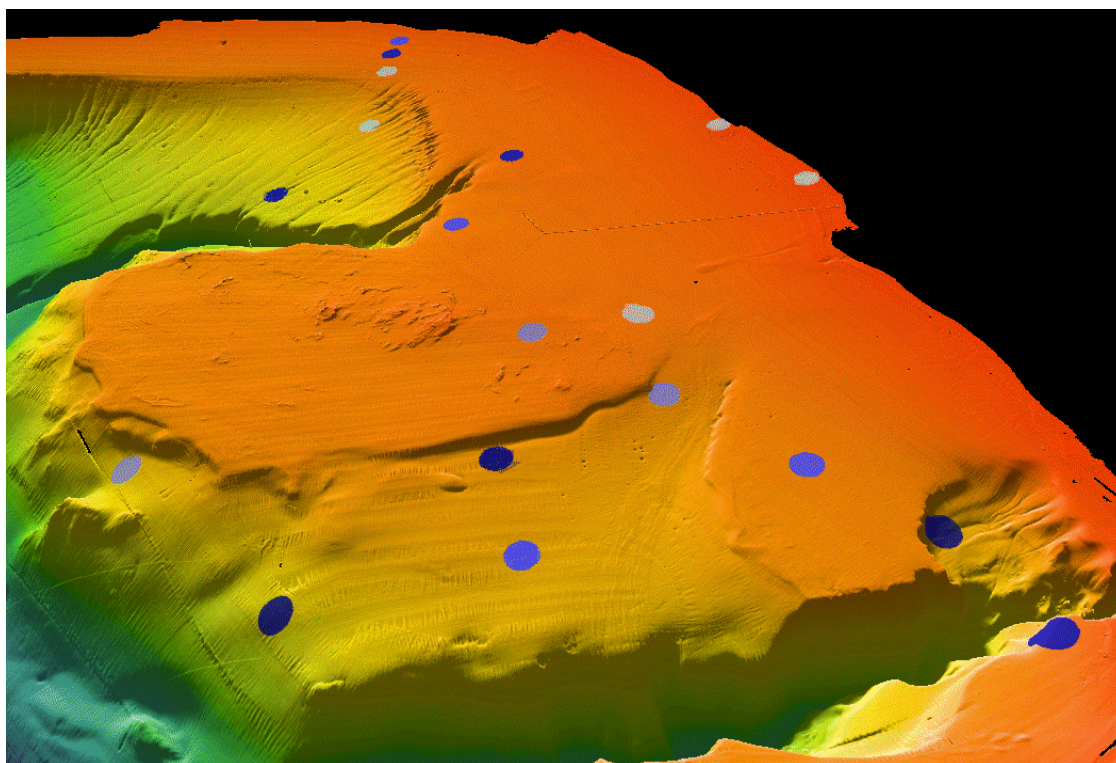Plate D-1 Color-coded 3-D bathymetry
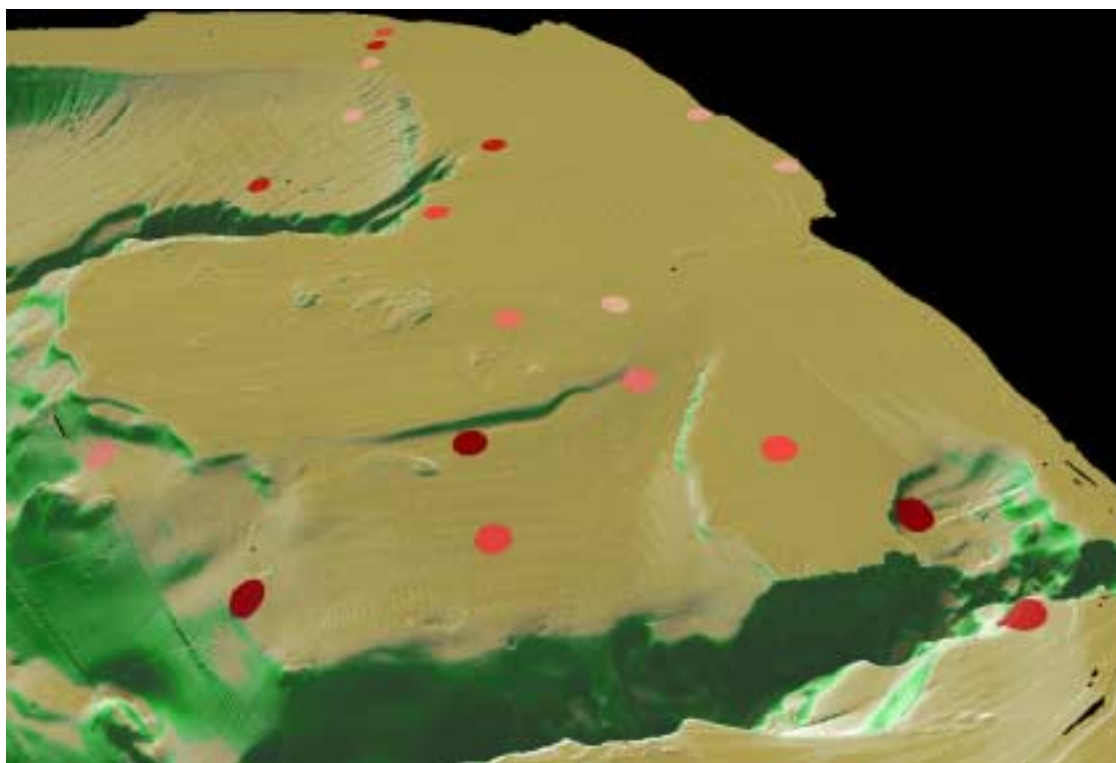

Plate D-2. Slope draped over bathymetry
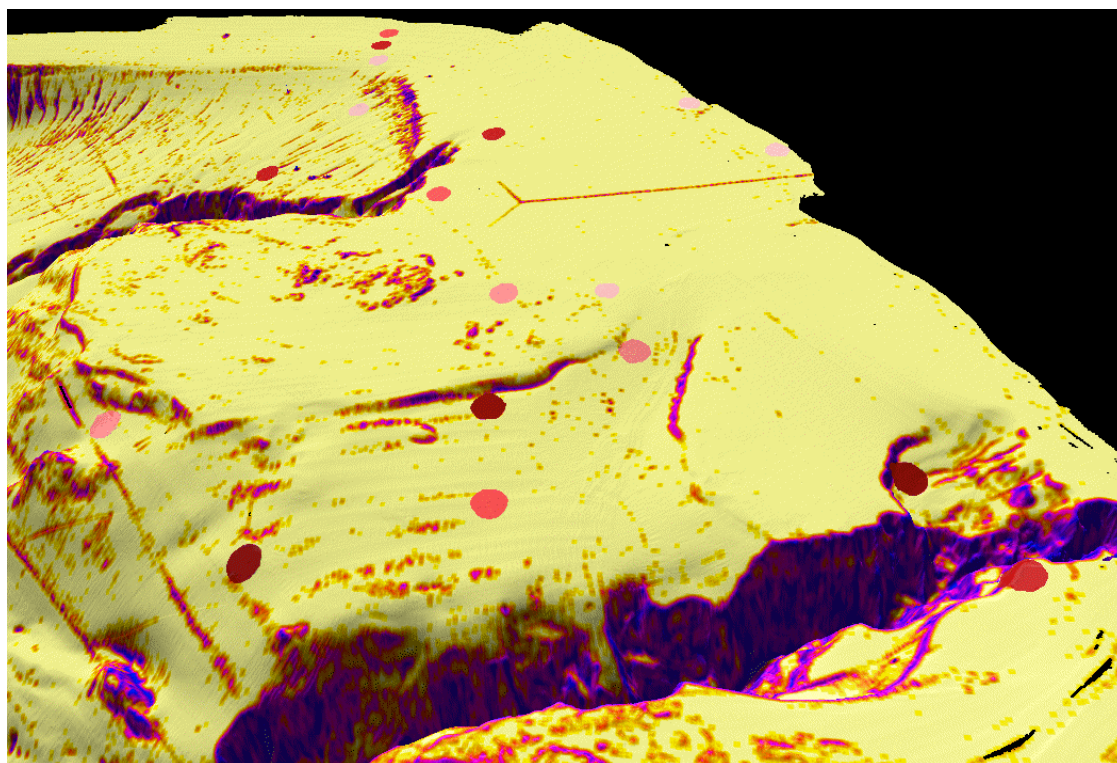
Plate D-3 TVI draped over bathymetry

Plate D-4 Backscatter draped over bathymetry

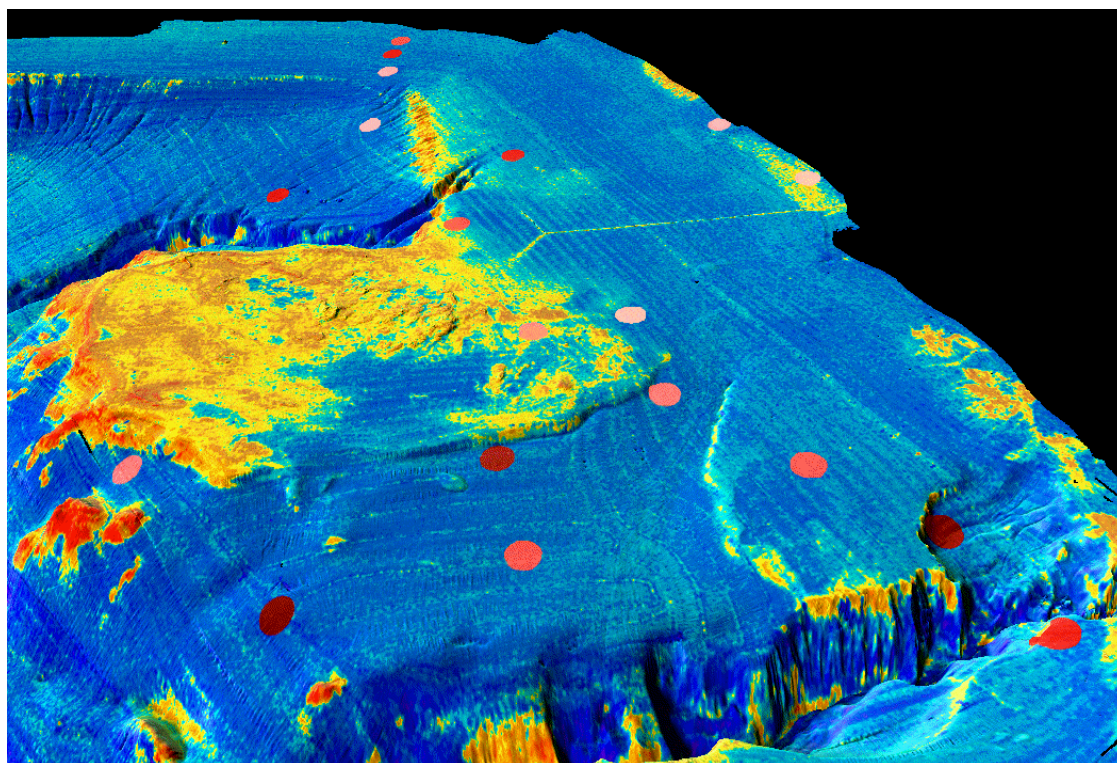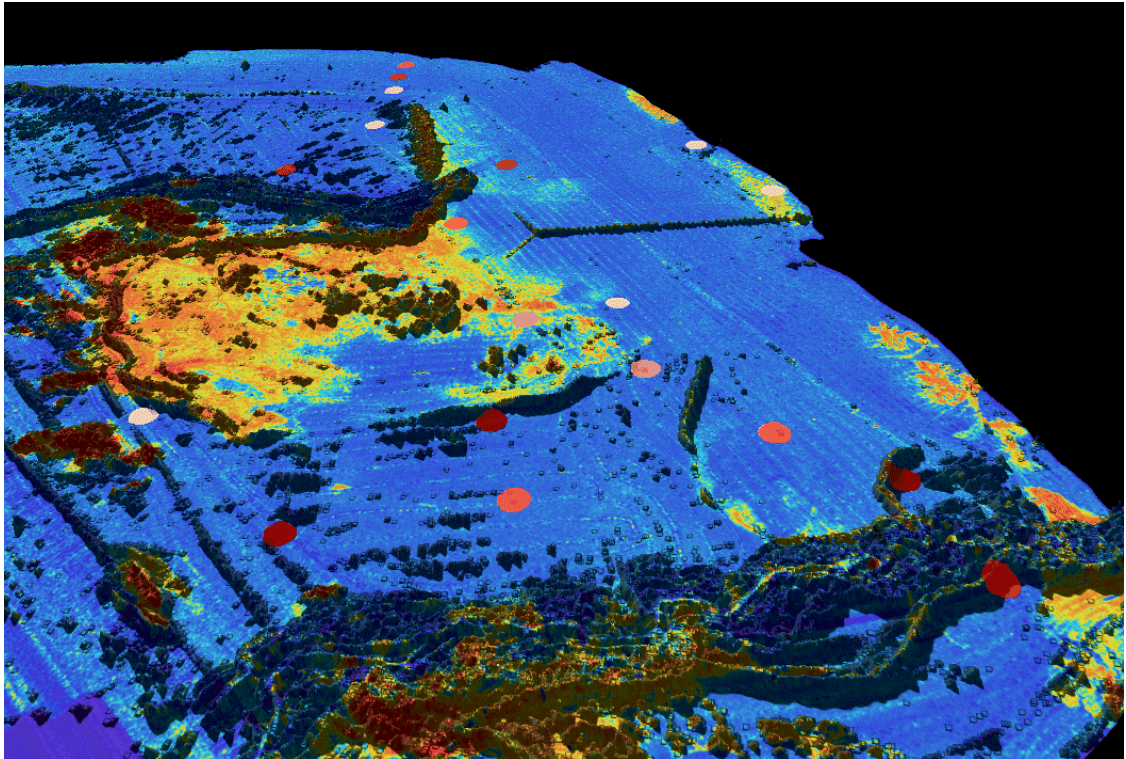Plate D-5 Backscatter draped over TVI DEM

VITA

Candidate's full name:	José Vicente Martínez Díaz
Place and date of birth:	México City, D.F., México March 19, 1968
Permanent address:	Poussin 16 Int. 3 México City, D.F. 03920 México
Schools attended:	Instituto Superior de Estudios Comerciales México City, D.F., México. 1983-1986
Universities attended:	Universidad Autónoma de Baja California Facultad de Ciencias Marinas Ensenada, Baja California, México. Bachelor of Science in Oceanology 1986-1991 University of New Brunswick Department of Geodesy and Geomatics Engineering Fredericton, New Brunswick, Canada Master of Engineering candidate 1997-1999